MULTI-PHYSICS MODELING AND SIMULATIONS OF THERMALLY-ASSISTED COMPACTION OF GRANULAR MATERIALS

BY GÜLŞAD KÜÇÜK

A dissertation submitted to the

Graduate School—New Brunswick

Rutgers, The State University of New Jersey

in partial fulfillment of the requirements

for the degree of

Doctor of Philosophy

Graduate Program in Mechanical And Aerospace Engineering

Written under the direction of

Alberto M. Cuitino

and approved by

New Brunswick, New Jersey

January, 2015

ABSTRACT OF THE DISSERTATION

Multi-Physics Modeling and Simulations of Thermally-Assisted Compaction of Granular Materials

by Gülşad Küçük

Dissertation Director: Alberto M. Cuitino

Having characteristics that differ from those associated with solids, liquids, and gases, granular materials require miscellaneous multi-physics approaches that integrate theories at different scales. The abstract behavior of granular material provides limitless arrangements in terms of microscopic and macroscopic properties, specifically concerning the thermally-assisted compaction process. However the uniqueness of particulate systems reduces significantly the effectiveness of conventional compaction models based on continuum mechanics description. Thus the current study engages with the problem at both discrete and continuum levels, and bridges the gap between particle-mechanics and macro-scale theories.

A mathematical formulation that integrates the thermal and mechanical behavior of discrete system of particles is presented. It is worth noting that thermal expansion experienced by the compacted particles increases the nonlinearity in the thermo-elastic contact problem, which results in various interesting aspects unique to granular matter. Numerical analysis reveals the role of thermal expansion, the role applied thermal and mechanical loads during thermally-assisted compaction of spherical, perfectly conforming particles.

Modeling consolidated granular media by using continuum mechanics requires an additional concentration on defining the effective transport properties of the material. Taking advantage of the effective medium approximation, an equivalent continuum model for the state

of small-strain deformation under the applied thermal gradient is investigated. The discrepancy between discrete and continuum analysis underlines the importance of describing an effective thermal expansion parameter. Starting from the fundamental understanding of particle interactions, an effective thermal expansion coefficient is derived for the current problem statement.

Unlike the continuum media, granular materials host inhomogeneous distribution of contact networks, which results in uneven distribution of loads in the dense particulate assemblies. Moreover these structural arrangements play critical role in forming preferred paths of heat transport. In spite of the recent experimental and theoretical studies on the evolution of force chains, the formation of heat chains and the correlation between the heat and force chains still remain unclear. In this study two-dimensional numerical simulations are demonstrated to understand some of the fundamental concepts such as: (i) formation of force and heat chains (ii) formation of localized hot zones, (iii) cross-property relations between contact force distributions and heat transported at the contact surfaces, (iv) influence of system characteristics such as diverse size distribution of particles, binary material constituents and different boundary conditions.

Acknowledgements

I would like to thank all the faculty in the department of Mechanical and Aerospace Engineering with whom I have had the opportunity to take a class or to discuss a topic. I am very grateful to my dissertation committee members: Prof. Yogesh Jaluria, Prof. Assimina Pelegri, and Prof. Stephen Tse, and Prof. Marcial Gonzalez for spending part of their very valuable time inspecting this work and for providing me with suggestions on how to improve this dissertation. I would like to express sincere gratitude to the former graduate director Prof. Haim Baruh for accepting me into the department by providing me the opportunity to be with the brightest minds here in Rutgers University.

I owe a great deal of gratitude to my thesis supervisor Prof. Alberto M. Cuitiño for his guidance and endless goodwill during my study. I feel proud to be part of his team and I have the chance to benefit from his incredibly vast knowledge on contact mechanics. I will forever cherish what I learned from him, from a research perspective, as well as a life perspective.

I can not imagine a more welcoming environment than Rutgers for someone who has just left home at the age of 26. I will always remember Mechanical and Aerospace Department with lovely people. I am thankful for all the help and kindness of Aiesha, Carmen, Cynthia, John, and Shefali. There are also these individuals whom I always enjoyed their company in the department, who were my office mates, my colleagues, thanks Pam, Kellie, Feruza, Daisy, and Mona. I am also grateful to Dr. Yuriy Gulak for his support and willingness to help me any time when I was in need.

I would like to express my best feelings to all of my friends who were beside me, who helped me feel like at home even though we are far away from our land. I would like to thank my friends; Deniz, Aylin, Burçe, Gizem, Erhan, Selen, Ali, Sıddıka, Uğur who were always there for me. Special thanks go to Gökhan, Turgay for also helping me as my technical mentors.

Words are not enough to express my sincere gratitude and appreciation to my mother and father. They provided me with a wonderful childhood and they still take care of me. I feel blessed to be born in a family with limitless kindness, generosity and unconditional support. I am also grateful to my grandma Nimet Ersavaş, my aunt Zeynep Zümrüt Ersavaş, and my uncle Mustafa Sabri Ersavaş for their endless support and love.

Dedication

To my lovely mother, Ayşe Vedia Küçük

and my father, Çakır Ali Küçük

Table of Contents

List of Tables

List of Figures

Chapter 1

Introduction

1.1 Motivation

Designing materials based on the required properties of the end product, is a topic of great current interest. Consolidation of granular materials is important to vast array of engineering operations, some of which are construction, chemical, manufacturing, and mining. In addition to these, confined products are daily life essentials through pharmaceuticals, household powders, and cosmetics. Producing these materials with desired functionalities while avoiding the possible disadvantages of compaction processes is of interest to a large number of researchers in the field. Specifically computational mechanics is served to predict the material properties of the confined end products. In the remainder of this section two of the edge-cutting science-integrated technology applications of this crucial tool is explained through examples from different fields.

Defense and space industry provides a vast medium of research to challenge and improve computational mechanics applications. The leading edge of study is mainly focused to develop advance materials and coatings with improved mechanical properties and performance required for structural and functional forms, such as the energetic materials' applications on personnel or vehicular armor to sensor devises. Common ground is that the required mechanical, thermal, and electrical properties of the materials can be engineered by applying different production techniques starting from powder. There exists two main considerations in integration of advanced materials to military applications: (i) time needed at trial and error stage in development processes, (ii) extreme costs of physical experimentations. These two factors enhance the importance of numerical simulations done on modeling the consolidation process of powders through various manufacturing techniques. The robust demand on constitutive mathematical models that predict the macroscopic material properties in accordance with the microscopic structural characteristics stems from the need to achieve accuracy in these numerical simulations.

Pharmaceutical industry also takes advantage of computational mechanics at different stages of drug development. Most of the pharmaceutical drugs are initially produced as powders and consolidated to required dosages. This process is generally called as tableting. There exists ubiquitous problems associated with tablet manufacturing, such as chipping, picking, binding, punch sticking, mottling, capping, and laminating. The macroscopic failure in consolidation can be explained through continuum constitutive theory. For instance, punch sticking is the state of powders remaining on the punch surface after compaction. This is mostly due to excessive adhesion to the tooling material, and is highly undesired, particularly for the cases where the amount of active ingredient is crucial in dosage form. However it is well-known that this problem lays down the roots in atomistic and/or molecular level interactions.

Loh et al.'s study is a relevant application of science to improve technology by integration of materials' modeling at different scales. They aim to predict the macroscopic properties of the tablet starting from quantum mechanical methods to calculate the gas phase properties of the single molecule of interest and guide the parameterization used in molecular models, where the crystalline phase of the material is simulated and Young's moduli, yield stress and surface energies are predicted. This enabled them to model the tableting ability with excipient microcrystalline cellulose (MCC) and active ingredient [41].

The above mentioned fields are some of the active areas of research where computational mechanics plays critical role in modeling consolidated granular powders. During the process of consolidation, particles come into contact to form numerous arrangements which ultimately determine their macroscopic mechanical, thermal, and electrical properties. As a consequence they exhibit a spectacular variety of characteristics and they behave differently from conventional solid, liquid and gaseous matter [29]. Current study is aimed to investigate a subset of this class, which is comparatively visited less. In thermally-assisted consolidation processes elastic granular materials are driven to form contact with each other as a results of not only compaction force but also thermal expansion. Bundling the coupled physical processes in simulations while maintaining accuracy and robustness is particularly challenging. Predicting the micro structural arrangement of the granular bed and the macroscopic behavior of thermoelastically bonded particles in such situations is of considerable importance. This study is intended to bridge the gap between the fundamental understanding of particle-mechanics and the macro-scale applications.

1.2 Literature Review

In recognition of the ubiquity of granular materials, there has been considerable research focused on understanding fundamental concepts related to various multi-physics problems of contact mechanics. Since compaction of granular matter is of great importance for a wide array of manufacturing processes, theoretical modeling and numerical simulations serve as an important tool to forecast the mechanical, thermal and electrical behavior of materials , particularly at extreme conditions, where conducting experiments are infeasible.

We classify four main categories that contribute to modeling and simulation of granular media. These are: early analytical studies, experimental studies, continuum modeling of heterogeneous media, discrete modeling of heterogeneous media.

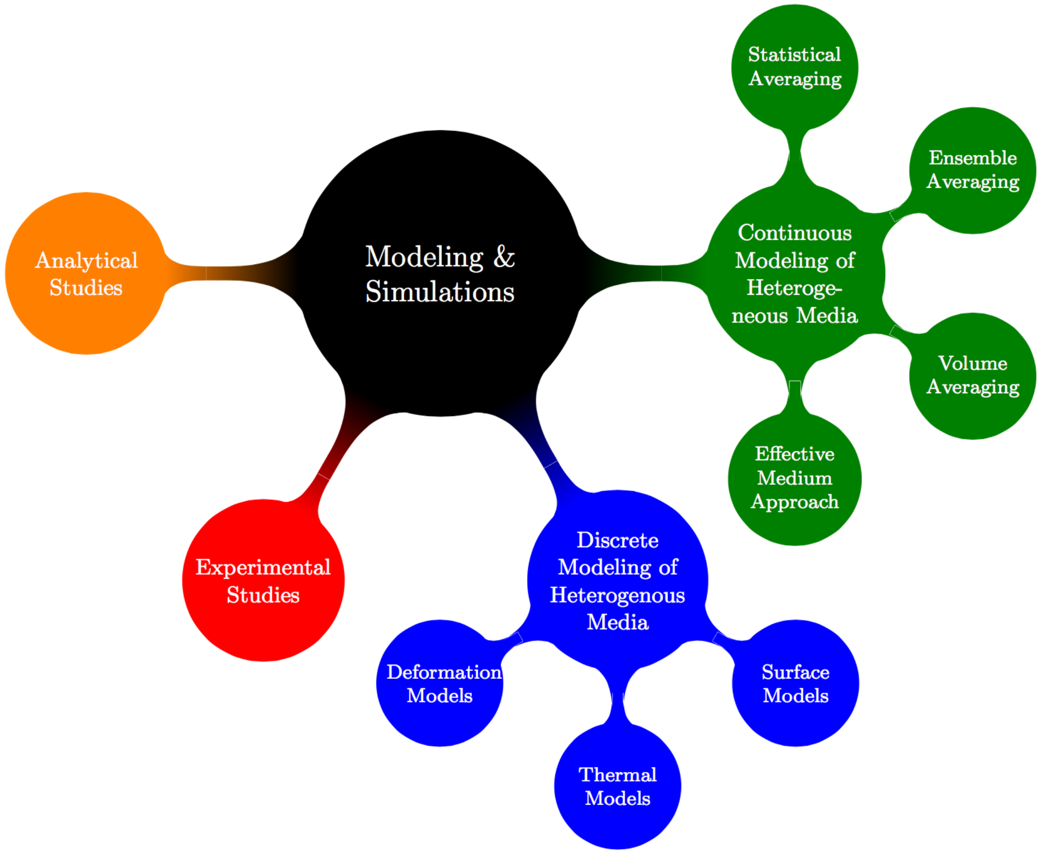

Figure 1.1: Outline of the granular materials research.

It is intuitive that the macroscopic behavior of granular materials depends on the phenomenological interactions that occur at the particle level. However the exact nature of this dependence is yet not well understood [71]. At present, one of the mostly implemented methodology to simulate granular matter is based on continuum mechanics description, which requires definitions of effective material properties of the overall granular assembly. Experimentation techniques are generally insufficient to determine these properties under different boundary conditions. Moreover homogenization methods that are introduced to estimate average of the overall characteristics can become irrelevant to express the altering nature of the discrete particle systems. Although there exists considerable amount of computational challenges to model a large number of particles system with discrete elements methods, improvements done in formalisms and new simulation techniques increase the achievability of calculations starting at particle level.

1.2.1 Analytical Studies

Granular materials research differs from continuum solid research mainly due to the change in the grounds for constitutive relations. Continuum mechanics approach is founded on molecular interactions whereas granular mechanics bases on particle interactions. This distinction enforces the definition of a new length scale to understand granular structural systems. Unlike the continuum solid, granular materials are explained through the perspective of contact mechanics approach where particle interactions at the mutual surface of contact are considered.

The pioneer of contact mechanics is Heinrich Hertz who is also very well known for his contributions to the field of electrodynamics. Analytical solutions of compaction of granular materials are rooted on his immense important work (1882) that elucidates the deformation mechanism taking place at the frictionless contact of two elastic bodies of ellipsoid profile [27]. Based on elasticity and continuum mechanics, he put forward the fundamentals of contact mechanics, which has inspired large number of researchers in the field of granular materials. Since then numerous analytical solutions are proposed that cover a wide range of problems regarding the variety of phenomenon involving granular materials.

Initial attempt to understand the macroscopic behavior of granular assemblies led researchers to focus on determining the descriptions of effective elastic properties of the body under external loads [65, 19, 47, 49]. Starting from the contact mechanics fundamental concepts, Walton solves the equation of equilibrium for a single sphere, which is under the action of gravity, fluid pressure and compressive forces of F_T and F_B for the appropriate boundary conditions [72].

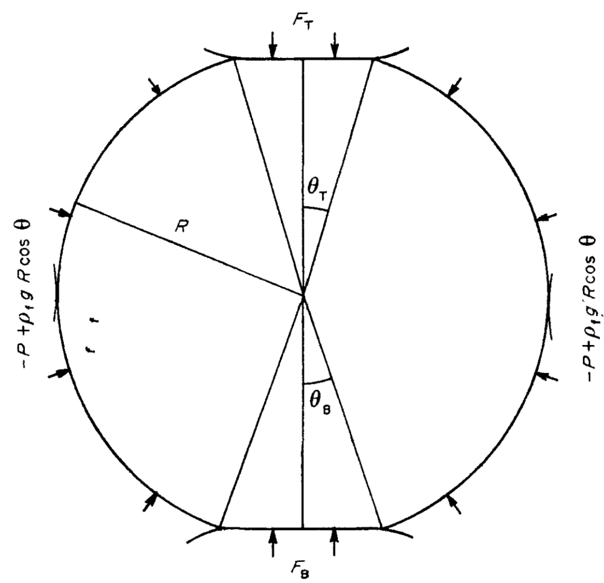

Figure 1.2: Single sphere under vertical compression sketch, adopted from Walton [1975].

Walton relates the incremental strain of single particle to an array of particles which are named as chain of particles, and derived the incremental stress to compress this system of particles incrementally. The correlation between incremental stress and incremental strain is basically the definition of the principal elastic moduli of the granular assembly [72].

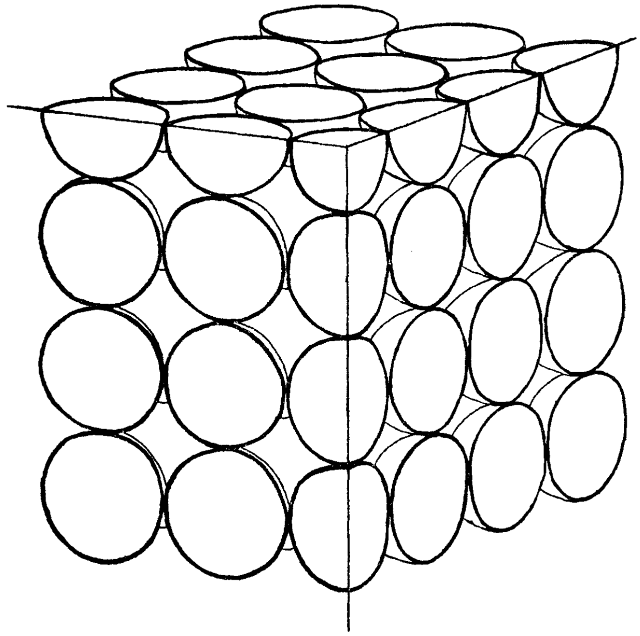

Figure 1.3: Cubic packing sketch, adopted from Walton [1975].

Later Walton derived the effective elastic moduli of a random packing under the particular cases of hydrostatic compression and uniaxial compression [73].

There has been considerable research focused on understanding the multi-physics of thermo-elastic deformation of spherical particles. This is the class of problems in which heat is transferred through the mutual surface of contact where elastic deformation develops the flat circle of contact area. The coupled physics of this problem is generally associated with thermal contact models which incorporate the Hertz law of deformation.

The major heat transfer mechanisms in compacted particle beds [68].

- Conduction through solid particle
- Conduction through the contact area between two touching particles
- Conduction to/from interstitial fluid
- Heat transfer via convection
- Radiation between particle surfaces
- Radiation between neighboring voids

For a system of granular media where the thermal conductivity of the solid particles is much larger than the interstitial medium, the driving mechanisms for the heat transfer are the first two. Concerning the problem of thermally-assisted compaction of spherical particles in vacuum, we focus on the thermal contact models that consider the conduction through solid particle and through the contact area between two touching particles.

In terms of contact surface geometry, the heat transfer phenomena at the mutual surface of contacting particles can be treated with two perspectives, assumption of perfectly conforming contacts of smooth particles, and conforming rough surface analysis based on generalization of asperity and surface roughness. Although we focus on perfectly smooth particles of conforming contacts, we give a brief definition and of the rough surface models.

The classical conforming rough contact models is developed for elastic, plastic, elasto-plastic particles of spherical, and elliptical shapes. Among these there exists studies which investigate the thermal conductance through the mutual surface of contacting particles, various theoretical models have been proposed to explain this phenomena. Sridhar and Yovanovich focused on rough surface analysis for conforming and nonconforming contact surfaces [62, 63]. In this study thermal contact conductance model is incorporated with an elastoplastic deformation model. Bahrami et al. developed a compact analytical model for predicting thermal contact resistance for different regimes of contact [2]. In this study they assumed a non-conforming macro-contact area exists of conforming rough micro-contacts, sum them up along this apparent radius of contact. The two limiting ends of the model is 1) two conforming rough surface 2) elasto-constriction limit (the Hertzian smooth contact with flat circular are of contact), and iii) transition region or general contact in which both R_L and R_S exist and have the same order of magnitude [3]. This is illustrated in Figure 1.4.

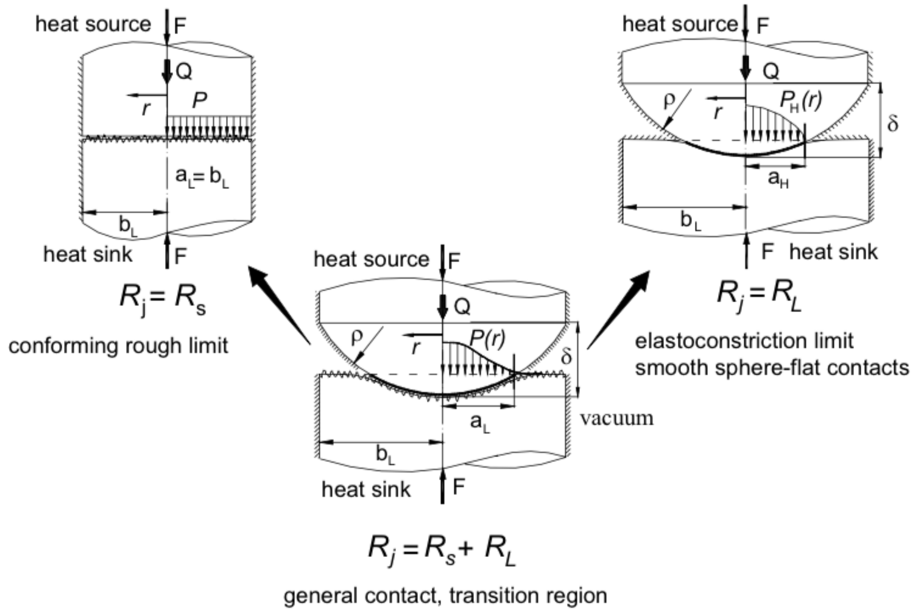

Figure 1.4: Thermal contact resistance for rough surface analysis, adopted from Bahrami [2004].

Analytic solution of the heat conduction through the solid phase of ordered spherical particles have been proposed by Chan and Tien[10] and Kaganer [32]. Chan and Tien established an explicit functional relationship between the thermal conductance of packed spheres and fundamental system parameters such as imposed thermal and load conditions, the geometric parameters (e.g., sphere thickness, shell thickness, packing configuration, etc), regarding thermal and mechanical properties of the particulate material [10]. They classify the mechanisms of heat conduction from one sphere to another: (i) Macroscopic constriction resistance due to the contraction of conduction passages, (ii) microscopic constriction resistance due to surface roughness at the contact area, film resistance due to surface contamination. Chan and Tien argued that macroscopic constriction resistance is dominant in the heat transfer and microscopic mechanism is negligible.

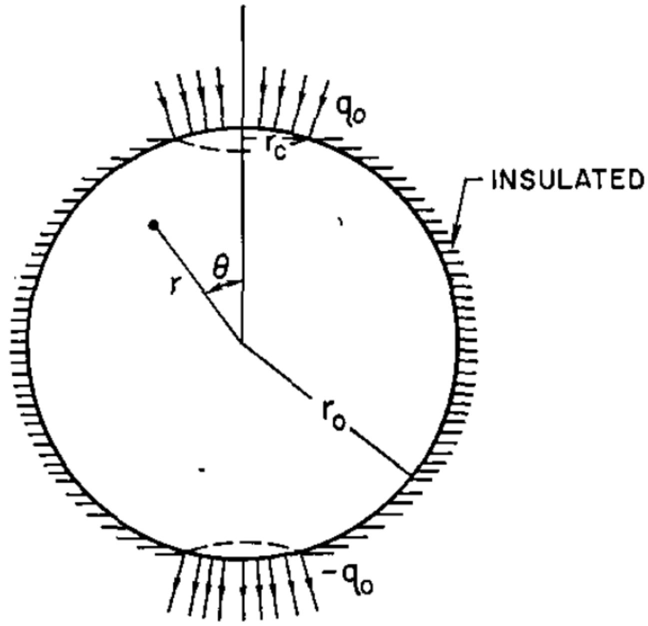

Figure 1.5: Single particle heat transfer model, adopted from Chan and Tien [1973].

The two main assumptions for the analytical model are the following:

- Radius of the circular contact is given by the Hertz relation for elastic contact of two smooth spheres.
- Contact surface has a uniform heat flux and the rest of the surface is insulated.

$$\frac{\partial}{\partial r}\left(r^2\frac{\partial T}{\partial r}\right)+\frac{1}{sin\theta}\frac{\partial}{\partial\theta}\left(sin\theta\frac{\partial T}{\partial\theta}\right) = 0 \tag{1.1}$$

Boundary conditions: for $0 \leq \theta \leq \theta_o$

$$k\left(\frac{\partial T}{\partial r}\right)_{r_o} = q_o \tag{1.2}$$

for $\theta_o < \theta < \pi - \theta_o$

$$k\left(\frac{\partial T}{\partial r}\right)_{r_o} = 0 \tag{1.3}$$

for $\pi - \theta_o < \theta < \pi$

$$k\left(\frac{\partial T}{\partial r}\right)_{r_o} = -q_o \tag{1.4}$$

By the method of separation of variables

$$T(r,\theta) = C_o + \sum_{n=1}^{\infty} C_1 r^n P_n cos(\theta) \tag{1.5}$$

P_n Legendre Polynomials

C_o arbitrary constant

C_1 constant determined by the outer BC's and the orthogonal properties of Legendre polynomials (non-zero only when n is odd)

$$C_1 = \frac{2n+1}{n}\left(\frac{q_o}{k_s r_o^{n-1}}\right)\int_{x_0}^{1} P_n(x)dx \tag{1.6}$$

$$x_o = cos\theta_o \tag{1.7}$$

$$\int_{x_o}^{1} = \frac{1}{2n+1}\Big(P_{n-1}(x_o) - P_{n+1}(x_o)\Big) \tag{1.8}$$

Definition of thermal resistance,TR, of the sphere with radius r_o

$$TR = \frac{\bar{T_a} - \bar{T_a'}}{Q} \tag{1.9}$$

$\bar{T_a}$ and $\bar{T_a'}$ are the respective mean temperatures of the diametrically opposing contact regions where heat is supplied and removed across the contact areas.

$$\bar{T} = \frac{\int_{A_c} T(r_o,\theta)dA}{\int_{A_c} dA} \tag{1.10}$$

Q is the total amount of heat passing through the sphere for $r_c \ll r_o$, $Q = q_o \pi r_c^2$.

$$\bar{T_a} = \frac{\int_0^{\theta_o} T(r_o,\theta)\pi r_o^2 sin2\theta d\theta}{\int_0^{\theta_o} \pi r_o^2 sin2\theta d\theta} \tag{1.11}$$

$$\bar{T_a'} = \frac{\int_{\pi-\theta_o}^{\pi} T(r_o,\theta) sin2\theta d\theta}{\int_{\pi-\theta_o}^{\pi} sin2\theta d\theta} \tag{1.12}$$

They investigated the conductance of packed spheres of uniform size and the basic regular arrangements, simple cubic, body-centered cubic and face-centered cubic.

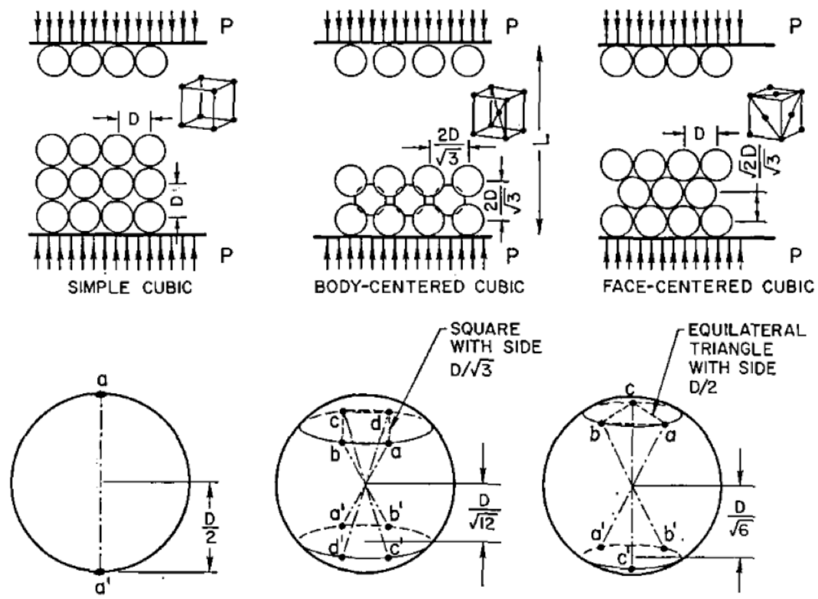

Figure 1.6: Thermal contact patterns of different regularly packed spheres, adopted from Chan and Tien [1973].

In our study we also consider simple cubic packing of spherical particles, in spirit to Chan and Tien's study we elucidate the assumptions and the proposed solution in our thermal contact model. Chan and Tien solves the constriction resistance of a solid sphere in simple cubic arrangement, for which the contact radius is much smaller than the particle radius :

$$TR = \frac{0.53}{ka} \tag{1.13}$$

where a is the contact radius.

In an attempt to find the approximate effective thermal conductivity of randomly packed granular beds, Batchelor and O'Brien focused on the heat flux across the flat circle of contact between smooth, conforming, and elastic particles [7]. In this study we adopt Batchelor and O'Brien's model for predicting the heat conductance, which is the ability of two touching surfaces to transmit heat through their mutual interface. This analogy has been used by several groups earlier [52], [58], [68], [71], [76].

In this aspect, theoretical studies on the formulation of thermo-elastic contacts of nearly in contact, point contact ,and a flat circle of contact has gained significance. Batchelor and O'Brien clearly discusses these three contact zones and provided the basis for many other mathematical models [7]. In this study it is aimed to derive the effective conductivity of a stationary granular material through which there is a steady transport of heat or electricity.

- Granular material is assumed to in a statistically homogeneous medium consisting of a uniform matrix and randomly arranged inclusions.

- Volume averaging formalism, which is prosed by Batchelor, is adopted to estimate the effective thermal conductivity of granular bed [6]. In this method an average volume is defined to be large compared to the small-scale deviations in volume fraction of each component, but also small enough such that the variation of field variable is slightly observed.

- Granular material is concerned to be in statistically isotropic structure in which case second-rank tensor effective thermal conductivity **k** is assumed to be a scalar.

- Since the thermal conductivity of the particle is relatively large with respect to the matrix, where the particle is embedded in, the temperature gradient within the particles are calculated to be relatively small. Therefore temperature within the one particle is assumed uniform and large temperature gradient between particles.

Based on the above assumptions Batchelor and O'Brien formulated the heat flux for nearly in contact, in contact cases which are shown in figures 1.7, 1.11 respectively. Once the particles are in contact, they deform slightly and develop a flat circle of contact whose dimensions may be related to the load by the Hertz Theory.

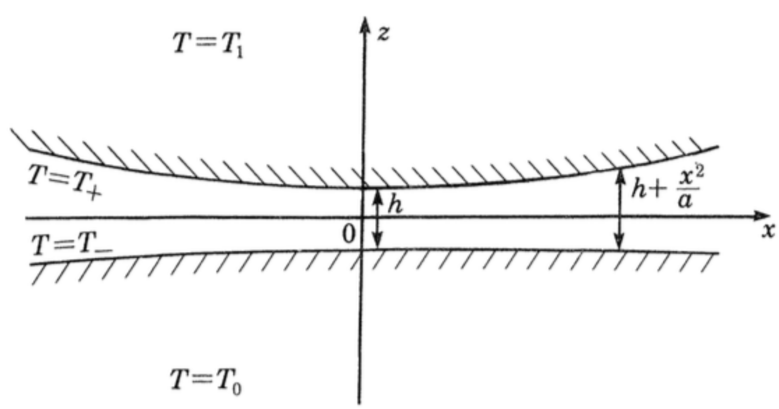

Figure 1.7: Particles nearly in contact case, adopted from Batchelor and O'Brien [1977].

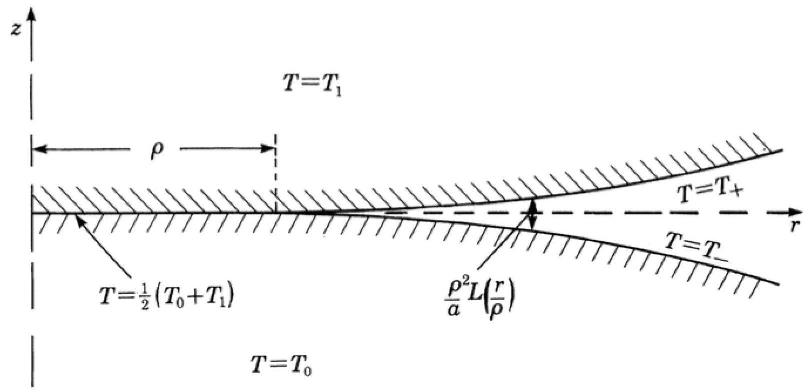

Figure 1.8: Particles at conforming flat circle of contact case, adopted from Batchelor and O'Brien [1977].

Since we have also adopted Batchelor and O'Brien's thermal contact model in this study, we elucidate their solution in detail in chapter 4. For the basic case of simple cubic packing of spherical particles bed, the proposed solution in this study is:

$$\tilde{k} = \frac{2k}{\pi} \frac{a}{R_{ref}} 1.57 \tag{1.14}$$

1.2.2 Experimental Studies

The field of granular matter research is highly visited by researcher in terms of experimental studies. However we focus our attention to studies that consider the effective material properties of the compacted particle systems and the force network generation within the granular assembly under external load.

There has been experimental studies that verifies Batchelor and O'Brien's study [26, 58]. Shonnard et al. aimed to check the inner expansion theory of Batchelor and O'Brien for a point-contact porous medium [58]. The effective thermal conductivity of unit cell of spatially periodic porous medium is measured. In this study two large metal hemispheres are kept under temperature gradient and constraint within two parallel plexiglass walls. They compared the test results with Batchelor and O'Brien's theoretical results and experimental study of Nozad et al. [52].

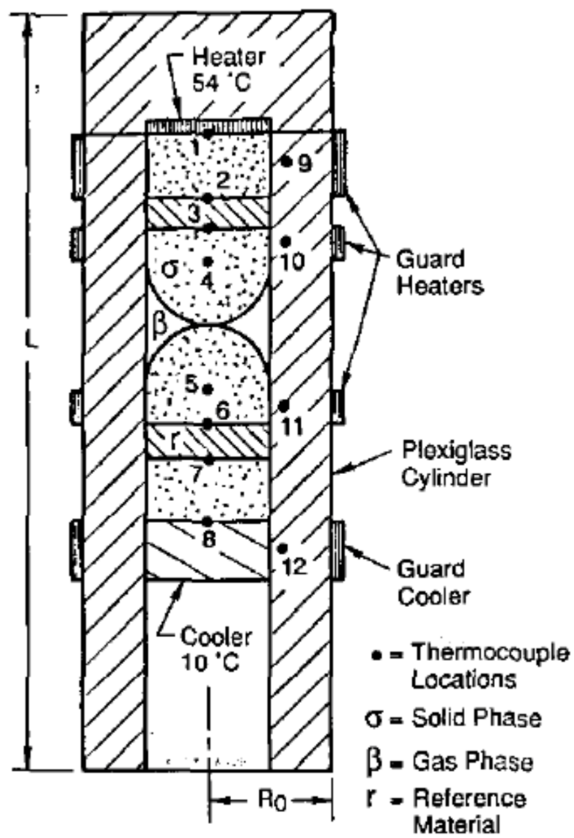

Figure 1.9: Experimental set-up to estimate the effective thermal conductivity of spherical particles, Shonnard and Whitaker [1989].

Experimental results show that for a compacted granular system under a uniaxial load, the distribution of contacts determine the distribution forces within the system of particles. Surprisingly even for homogenous systems, these forces are unevenly distributed such that particular structural paths supporting the most of the applied forces and the rest are lightly compacted or even carry no load at all. These preferred arrangements to deliver force are named as force chains or force networks in the literature [1, 23, 61, 8, 54]. We give two examples of the techniques used in meaning force network distributions within the particle beds.

Mueth et al. measured the distribution of normal forces exerted by granular material under uniaxial compression onto the interior surfaces of a confining vessel [50]. Randomly packed mono dispersed glass beads are compacted by the moving upper piston and the lower piston is fixed. Upon the application of external load on the system the beads press the carbon paper into white paper, leaving marks which are used to determine the contact forces [50]. After a systematic set of experiments, empirical functional form for the force distribution is proposed .

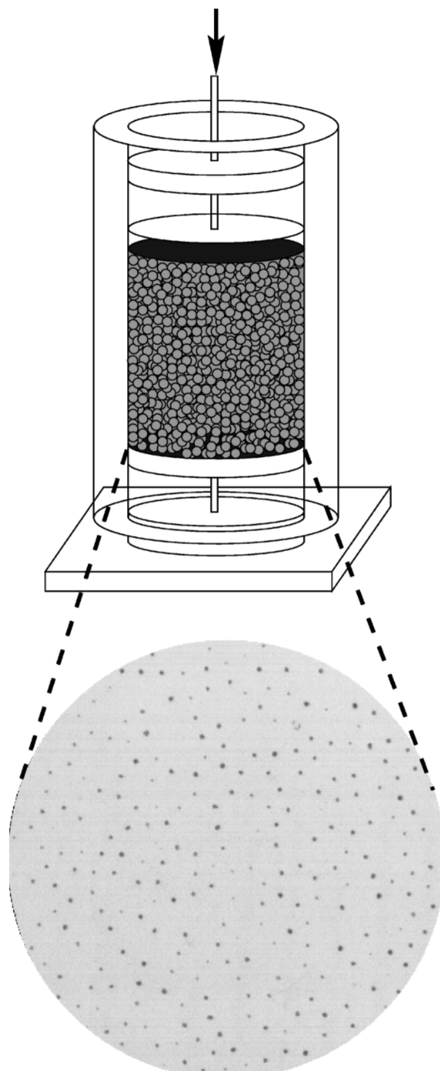

Figure 1.10: Experimental set-up using carbon paper to trace force distributions of a compacted granular bed, adopted from Mueth et al. [1998].

Photoelasticity is also widely used in investigating force networks for systems of particles (e.g: [43], [28], [23]). Taking advantage of birefringence property of some materials, light propagation though the granular assembly can traced during compaction and the evaluation of stress chains can be observed.

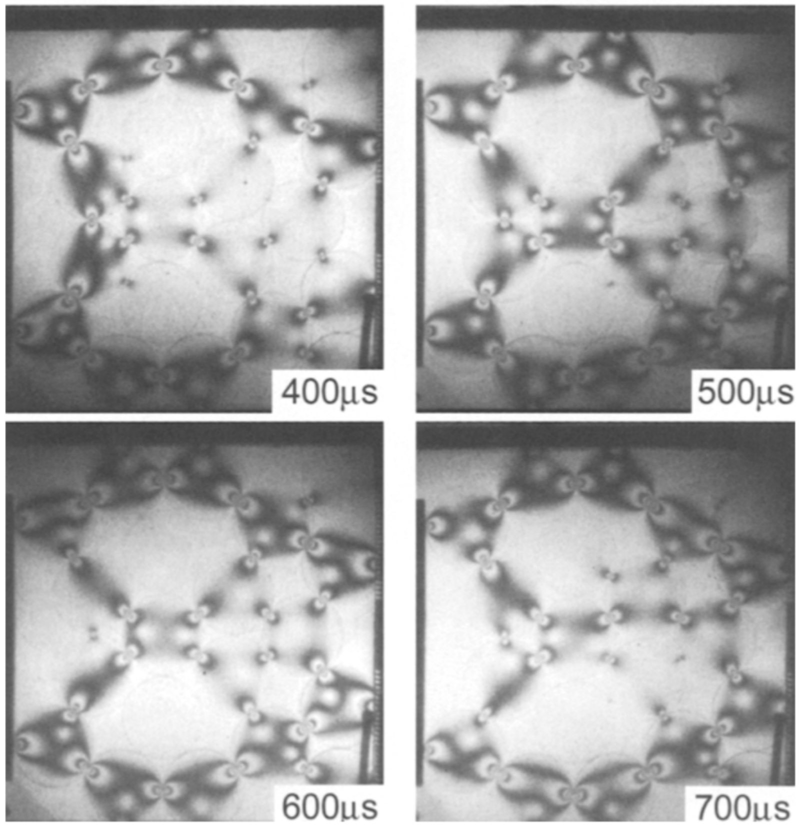

Figure 1.11: Dynamic stress chain formation in two dimensional polymethylmethacrylate (PMMA) discs, adopted from Foster et al. [2002].

Foster et al. examined the polymethylmethacrylate (PMMA) discs under transient load to trace the formation of stress chains by using photoelastic experiments [23]. The critical question in PMMA consolidation is the reason of the unexpected crystal failure, which is suspected to be caused by unevenly stress chain formations. The main advantage of this method is that it provides information about the microstructure of the compacted granular assembly without using destructive experimentation methods.

There has been two classes of approach proposed to undertake the heat transfer in granular materials. First approach considers the particle bed as porous medium, a 'smeared' continuum mechanics approach is adopted to unveil the effective properties and characteristics of particle bed which is assumed to be statistically homogeneous [22]. Second mostly known approach treats the particles as individual bodies such that the coupled effects of various multi-physical phenomena can be coupled for each particle. The integration of particle motion and energy to the macroscopic behavior of the assembly, provides the required understanding of overall behavior of the confined material. The common feature of these approaches is that the determination of the effective material and transport properties is based more on an ad hoc manner than on a rigorous theoretical foundation, which may introduce modeling errors that are difficult to quantify and control [22]. Thus the continuous research on improving the theoretical models and numerical simulation schemes stays as an active area of research in the study of granular matter,.

1.2.3 Continuum Modeling of Heterogenous Media

Continuum modeling of granular media is based on solving conservation equations of mass, energy and momentum, coupled with constitutive laws describing state of bulk material, and its interaction with the boundary conditions. Generally these models aim to determine the state of granular assembly in terms of average contact coordination number, porosity, and bulk material properties in relation with the applied loads on the system. Due to the ubiquitous fluctuation in microstructure formation of granular materials under compaction, heterogeneities are observed in various aspects such as formation of aggregates, force chains, hot zone localizations of chemical reactions, etc.

There has been excessive amount of research on continuum modeling of heterogenous particulate matter. Specifically in the subject of compaction process of granular media, the initial models known as Cam-Clay model and Drucker-Prager cap model are originated from soil mechanics by and and gained popularity in implementation to various fields [17, 57, 18, 40].

Analyzing large systems with high order heterogenous material introduces the complexity of establishing effective elastic, plastic and transport properties of the granular assembly depending on the constitutive laws required. Conservative research approached the problem by practicing homogenization techniques. Some of these are: statistical averaging, ensemble averaging, volume averaging and effective medium approach. In order to apply the well established continuum solid mechanics theorems, effective medium approach aims to replace the heterogenous with effective homogenous medium properties. In this method granular material is assumed to be statistically homogenous [71]. This is achieved by treating the system as units of ordered arrays, simulating disordered arrangements by statistical correlation functions or using empirical correlations.

Regarding thermal conductivity through granular assembly, the concept of estimating the overall transport property is based on Maxwell's expression for the effective conductivity of spherical inclusions [46]. Although a proper estimate of the effective properties is contingent upon the knowledge of unit controlling processes at particle level, there is remarkable effort to improve the averaging techniques that are used in homogenization. By using these techniques Torquato stated the upper bound on the effective conductivity of a heterogenous granular system by using Maxwell's correlation functions [66]. However it is critical that the statistical correlation functions and analytical solutions are constraint with the assumption done to evaluate the solutions [71].

Recently quasi-continuum approach has been developed and the formulation is used for simulation of inter-particle bonding in granular systems. Zheng and Cuitino implemented quasi-continuum approach to bridge the micro and meso scale through discrete-continuum formulation of elastic-inelastic deformations occurring in the post-rearrangement regime of consolidation of inhomogeneous granular beds [74]. Since this approach provides the flexibility of storing individual particle interactions in a FEM scheme, it provides the overall behavior of the entire body without loosing critical information specific to micro structure. Koynov et al. presented a notable adoptation of this approach in the study of powder compactions for pharmaceutical purposes [35].

1.2.4 Discrete Modeling of Heterogenous Media

Discrete modeling of granular materials is a particle scale research based on detailed micro level information [75]. The state of art paper in this subject was published by Cundall and Strack on method granular dynamics simulation technique soft-sphere [15]. The proposed approach is based on an explicit numerical scheme, through which the particles interactions are calculated over the contact networks and particle motion is determined by the state of force balance equilibrium [15]. The method is applicable for problems on particles of any shape without any limitations over size or distribution. Discrete element method (DEM) is mostly used to simulate dynamic behavior of granular systems such as the trajectories of and transient forces acting on individual particles, and deformations are used to calculate elastic, plastic and frictional forces between particles. Also the integration of discrete element models with computational fluid dynamics models enables the researchers to study the particle-fluid interactions which is important for the geometries where the granular bed is highly interacting with surrounding fluid [75].

The conventional compaction of granular materials mostly accompanied with application of a thermal gradient on the system during consolidation. Thermal contact models are integrated in discrete and continuum modeling of granular media. Vargas et al. provides a detailed background information on the evolution of discrete element methods which integrates thermal contact formulation [68]. Regarding these studies Vargas et al. also investigates the effect of thermal expansion on the stress and heat chain formations within the granular assembly, some of which is revisited in chapter 6 of this study [69, 70].

Feng et al. extended the numerical methodology used in discrete element modeling in order to account for the effective modeling of heat conduction in systems comprising a large number of circular particles in 2D cases [22]. Starting from the well known analytical integral solution for the temperature distribution over a circular body, a linear algebraic system of thermal conductivity equations for each particle is derived in terms of the average temperatures and the resultant fluxes at the contact zones with its neighboring particles [22].

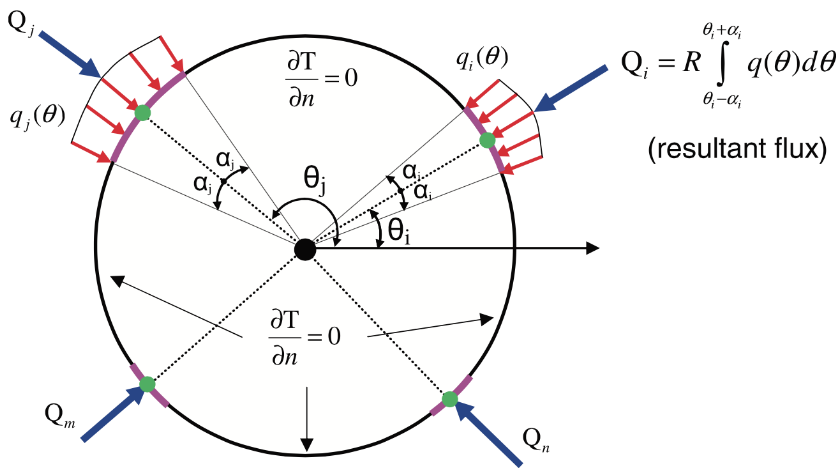

Figure 1.12: Individual particle's contribution to thermal conductivity network, adopted from Feng et al. [2008].

In this method they cast the element thermal conductivity matrix which is dependent on the characteristics of the contact zones, including the contact positions and contact angles. In the illustrative following figure, enhanced discrete thermal element model accuracy in estimating the average temperature variation determined by FEM is compared.

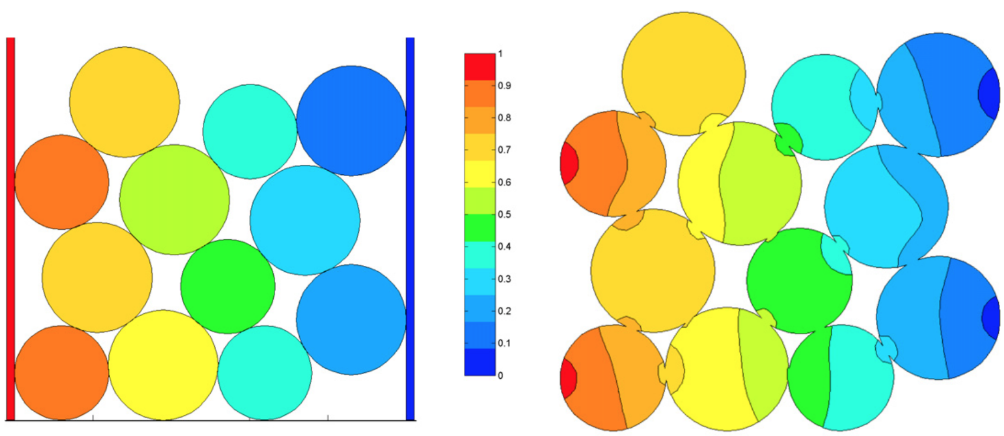

(a) Average particle temperature.

(b) Temperature contour.

Figure 1.13: Comparison of average particle temperature obtained by discrete thermal element method,(a), and temperature variation in each particle obtained by conventional finite element method, (b), adopted from Feng et al. [2008].

Thermal gradient has the effect of increasing the bonding between particles and enhances localization of stress. Kaviany discusses the heat conduction through a granular medium. In his book it is claimed that the allocation of the contacts and contact stress plays an important role in heat conduction [33]. This heterogeneity leads to ‘stress chains’ which is described as forces that follow preferred paths in a granular material [33]. Kaviany illustrates this phenomena using percolation of contacts shown in figure 1.14.

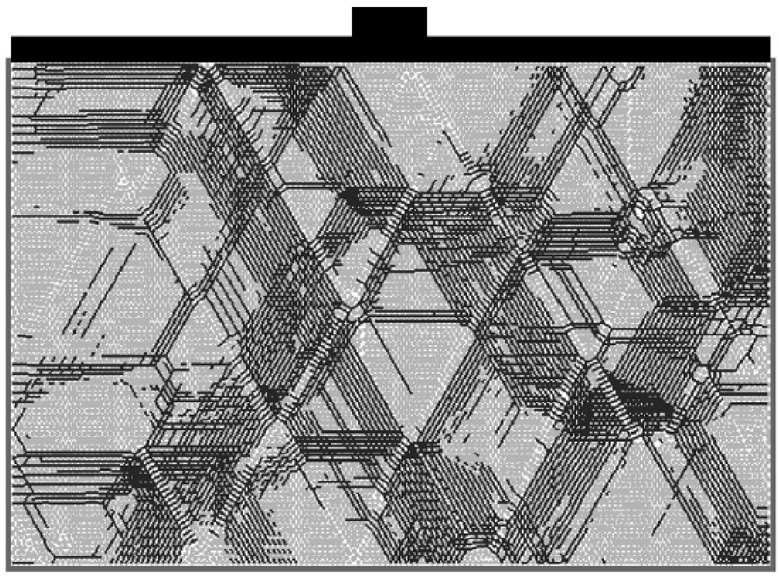

Figure 1.14: Stress chains in heat conduction of compacted granular particles, adopted from Kaviany [1995].

On the other hand Johnson provided a broad overview of the contact mechanics [31], originating from particle interactions and the constitutive relations proposed by various groups (e.g: [27],[15], [48]) and analogous thermal model which is derived in Carslaw and Jaeger [9]. Johnson classified the thermoelastic contact problem into three parts;

- The analysis of heat conduction to determine the temperature distribution in two contacting bodies
- The analysis of thermal expansion of the bodies, to determine the thermal distortion of their surface profiles
- The isothermal contact problem to find the contact stresses resulting from the deformed profiles

Johnson studied the subject with the above three stages, for which he treats the problem as de-coupled [31]. Main assumption is that similar to elastic deformations, whatever the actual profile of the material is, the contact is modeled as an elastic half-space bounded by a plane surface. The temperature gradients that give rise to thermal stress and distortion are large only in the vicinity of the contact region. Also distributed heat flow into a half-space through a restricted area of the surface is solved as point sources in the same way as elastic stress distributions due to surface traction. The linearity of the conduction equations provides the superposition of the solutions. The analogy is constituted between deformation due to uniform pressure applied to a circular area and temperature due to uniform supply of heat to a circular contact area. Therefore the net pressure that obeys the elastic contact mechanics of Hertz Law has two parts, isothermal pressure and thermal pressure that caused the distortion in the contact area.

However the steady state solution of this problem brings discontinuity in temperature profiles of the contacting surfaces as a result of the transition from point contact case to circular contact case. This is contracting with the real physical situations. In an attempt to overcome this problem rough surface models are developed which are also based on statistical averaging techniques [4], [20]. However Barber claimed that the steady state solution of thermo-elastic contact models give negative thermal pressure at certain cases during transition from perfect insulation condition to perfect contact (which is physically impossible) and states that it rises from the thermal boundary conditions which assume perfect contact within the contact area, so the discontinuity in temperature across the interface, and perfect insulation outside the contact area [5]. This difficulty was treated as adding state of imperfect contact which the displacements(elastic and thermal) are such that the surfaces just touch and conduct some heat but the contact pressure is zero. In his one dimensional model, Barber divided the contact zone to three different regimes, perfect contact, imperfect contact and non-contact zone. Perfect contact is the circular contact that is formalized by Hertz theory, the imperfect zone is the annulus where contact pressure drops to zero while passing to non-contact area and also where large thermal resistance is experienced. Barber introduced a pressure dependent thermal contact resistance to overcome the difficulties stemming from the discontinuity of temperature profile. Barber also stated that the nonlinearity of the problem makes the calculations costly for 2D or 3D solutions [5].

1.3 Overview of the Dissertation

The field of granular media keeps attracting researchers in the light of understanding the correlation between material properties of its constituents, geometry of the confinement, loading conditions and anisotropic microstructure formation which determines the macroscopic material behavior of the compacted bed. Specifically experimental results show that thermal gradient applied on the granular assembly has significant effect on the rearrangement of the particles.

Recent studies revived some critical questions which are of great interest to researchers and engineers: what is the role of thermo-mechanical coupling in formation of anisotropic microstructure, and heterogeneously distributed stress, heat chains? how does the cross-property relation between heat and stress chains affect the contact networks, hot zone localization, and how does these microscopic alterations determine the overall performance of the confined granular assembly? Lastly can we engineer/fabricate compacted materials with specific functionalities, by taking advantage of carefully investigating the inverse problem and providing accurate numerical simulations based on inter particle relations.

We propose a mathematical model, namely particle mechanics approach, to investigate the multi-body system behavior of granular materials. We have undertaken in an attempt to understand the thermo-mechanical coupling, taking place during thermally-assisted compaction of packed bed of spherical particles. The set of governing equations, which define prescribed state of the assembly under the thermal and mechanical loading conditions, are expressed in terms of heat and force transfer between the mutual surface of particles that are in contact. For the case the static mechanical equilibrium and steady state heat conduction the system of equations are solved in an explicit numerical scheme.

In this study we are also inspired from the multi scale modeling approach that is introduced by Cuitino et al. [14] and Stainer et al. [64], to model the characteristics of crystalline solids. The main idea of this approach is to determine the controlling unit processes at micro scale, thereby quantifying the energetics and dynamics of these mechanisms, lastly the effect of macroscopic driving force on macroscopic response is understood via microscopic modeling. The bridge between macroscopic driving force to unit-process driving force is constituted in two steps: localization of macroscopic force, and averaging of the unit processes. Similar to this approach, we analyze the driving mechanisms of thermally-assisted compaction of spherical particles and correlate these coupled processes to macroscopic applied boundary conditions. In terms of averaging the effect of thermal expansion at particle level to account for its contribution to the overall stress evolution and heat transfer, we derive an effective thermal expansion formalism.

In chapter 1 we briefly review the theoretical and numerical studies on the deformation mechanism of granular media. Some the groundbreaking studies, which also inspired us along this research, are explained in detailed and compared with similar studies in the literature.

In chapter 2 we explain the particle mechanics approach that we elaborate the exists models to understand the governing mechanisms during thermally-assisted compaction of granular media. We mention the main assumptions used in this model, and provide information about the characteristics of this approach.

Owing to the fact that the nature of the problem leads to highly non-linear coupled equations, regular packings simplifies the problem and makes it mathematically tractable. In chapter 3 we present results regarding one dimensional analysis of this approach in which we focus on the role of thermal expansion, applied mechanical load and thermal gradient on the system.

In chapter 4, we consider the problem from a different perspective. We look for the description of the resembling system in continuum mechanics approach, where we integrate the recent effective medium theories to improve the macroscopic analysis. We recognize that there exists a remarkable discrepancy between conventional continuum solution and discrete particles solution. This stems from the fact that effective thermal expansion of a packed granular bed has not been proposed for the particular problem.

Staring from the pair interactions between particles, we aim to derive an overall thermal expansion expression that can enable the continuum solution to capture the physics of the discrete particle system. In chapter 5 we explain the derivation of the effective thermal expansion coefficient, and state an application of the proposed formula for the particular case. We conclude this chapter by comparing our continuum solution results with conventional continuum solution and discrete solution results.

In chapter 6 another intriguing characteristic of compacted granular systems is investigated. Given the fact that there are major loading paths that cause unevenly distribution of force within the granular material, we present numerical simulations to exploit the generation of heat and force networks, their cross-property relations during coupled phenomena and the dependence of the hot zone formation with regard to the evolution of the prescribed chains.

Chapter 2

Particle Mechanics Approach

2.1 Introduction

Our point of departure for the discrete model is to integrate the well-known theory of Hertzian deformation for quasi-static mechanics and conductive heat transfer for spherical conforming contacts of granular media.

We present a multi-body system model of granular beds starting from the pair interactions of particles defined by thermo-elastic contact models. This concept is similar to recent studies of Vargas and McCarthy ([68], [70]), where they introduce a mathematical model as an extension to the well known discrete element model of granular materials [15]. However, our approach is based on defining particles' final state, such as position and temperature, rather than tracking the particles during the compaction process. Therefore we solve the system of equations for static mechanical equilibrium and steady state heat conduction principles.

The following nomenclature is used in integration of thermal and mechanical deformation models.

Table 2.1: Nomenclature

R^m	Radius of the individual particle m
T^m	Temperature of the particle m
α^m	Thermal expansion coefficient of particle m
E^m	Young Modulus of the particle m
ν^m	Poisson's ratio of the particle m
k^m	Thermal conductivity of the solid particle m
H^{mn}	Thermal contact conductance at that contact of particles m and n
a^{mn}	Radius of contact area at the mutual interface of particles m and n
γ^{mn}	Overlap at the contact of particles m and n
T^{wall}	Temperature of the wall
Tws	Temperature at the wall surface, in contact with the boundary particle
h^w	Convective heat transfer coefficient of the wall

2.2 Mathematical Model

The temperature and position of particles are obtained through the equilibrium for the system particles. The total heat transferred to particle m from neighboring particles n and the total of forces acting on particle m are equated to zero.

$$Q^m = \sum_{n \epsilon \mathcal{N}_m} Q^{mn} = 0 \tag{2.1}$$

$$\mathbf{F}^m = \sum_{n \epsilon \mathcal{N}_m} F^{mn} \mathbf{n}^{mn} = 0 \tag{2.2}$$

where $\mathbf{n}^{mn}$ is the unit normal vector defined from centers of particle n to particle m.

$$\mathbf{n}^{mn} = \frac{\mathbf{x}^m - \mathbf{x}^n}{\|\mathbf{x}^m - \mathbf{x}^n\|} \tag{2.3}$$

Small-strain elasticity of granular media are determined from contact mechanics considerations [31]. These relations define the deformation of locally spherical, elastic particles that are subject to a compression load. Slight deformation of conforming surfaces results in a flat circle of contact area whose dimensions are formulated through Hertz theory [37]. Collinear contact force for elastic contact of two smooth spherical particles m-n is defined through Young's modulus, E^m and E^n; Poisson's ratio, ν^m and ν^n; particle radii, R^m and R^n; and overlap γ^{mn} that occurs along the contact line.

$$F^{mn} = \frac{4}{3} E^{mn} (R^{mn})^{1/2} (\gamma^{mn})^{3/2} \tag{2.4}$$

where

$$R^{mn} = \left[\frac{1}{R^m} + \frac{1}{R^n} \right]^{-1} \tag{2.5}$$

$$E^{mn} = \left[\frac{1 - (\nu^m)^2}{E_m} + \frac{1 - (\nu^n)^2}{E_n} \right]^{-1} \tag{2.6}$$

$$\gamma^{mn} = R^m + R^n - \|\mathbf{x}^m - \mathbf{x}^n\| \tag{2.7}$$

In this study we investigate the effect of thermal expansion on the steady state equilibrium of thermal and mechanical loading conditions. While the temperature and position of each particle is being tracked for any particular loading condition, the particle radius, R^m, is evaluated at the specified temperature T^m, thereby making the active radius R^{mn} temperature dependent.

$$R^m = R^m_{ref}\left[1 + \alpha^m\left(T^m - T^m_{ref}\right)\right] \tag{2.8}$$

where α^m is the thermal expansion coefficient, T_{ref} is the reference temperature and R^m_{ref} is the radius of particle at the reference temperature.

Due to the dependence of contact geometry on thermo-mechanical coupling imposed by the defined problem, it is expected to capture a distribution of contact area formation throughout the compacted medium.

There has been considerable research on thermal-contact models. The major heat transfer mechanisms in compacted particle beds consist of conduction through solid, conduction through the contact area between two touching particles, conduction to/from interstitial fluid, heat transfer via convection, radiation between particle surfaces, radiation between neighboring voids [68]. Under present considerations of thermally-assisted compaction of spherical particles in vacuum, the first two are the driving mechanisms in our work.

Analytical solution of the heat conduction through the solid phase of ordered spherical particles has been proposed by Chan and Tien[10] and Kaganer [32]. The problem of heat transfer regarding the compaction of particles that are in or nearly in contact is deeply investigated by Batchelor and O'Brien.[7]. In an attempt to find the approximate effective thermal conductivity of ordered and randomly packed granular beds, Batchelor and O'Brien states the heat flux across the flat circle of contact between smooth, conforming, and elastic particles. In this study we adopt Batchelor and O'Brien's model for predicting the heat conductance, which is the ability of two touching surfaces to transmit heat through their mutual interface.

$$Q^{mn} = H^{mn}(T^m - T^n) \tag{2.9}$$

$$H^{mn} = 2a^{mn}k^{mn} \tag{2.10}$$

H^{mn} is contact conductance, which defines the ability of two conforming particles to transmit heat across their mutual interface. k^{mn} is the arithmetic mean of the thermal conductivities of two particles in contact, and a^{mn} is the Hertzian contact area.

$$k^{mn} = \frac{1}{2}\left[\frac{1}{k^m}+\frac{1}{k^n}\right]^{-1} \tag{2.11}$$

$$a^{mn} = \sqrt{\gamma^{mn}R^{mn}} \tag{2.12}$$

The total heat flow to an individual particle (eq: 2.1) is calculated by adding the heat flow at each contact of the particle between its neighboring particles (eq: 2.9). Different than the thermal contact models introduced in the literature ([10], [7]), eq. 2.1 requires that at each contact , the temperature is equal to the temperature calculated at the center of the particle. In other words the temperature does not very significantly within the particle, which also imposes that the contact conductance alone the mutual interface of conforming particles is relatively smaller than the heat conductance within the particle.

$$\frac{2k^{mn}a^{mn}}{k^{mn}A/R^m} << 1 \tag{2.13}$$

where A is the cross sectional area, $\pi(R^m)^2$ and eq. 2.13 defines the state of Biot number much less than 1. This assertion is applied by several authors in earlier studies ([68], [60]). The condition of $a^{mn} << R^{mn}$ is also required by the contact mechanics model.

2.3 Wall-Particle Interaction

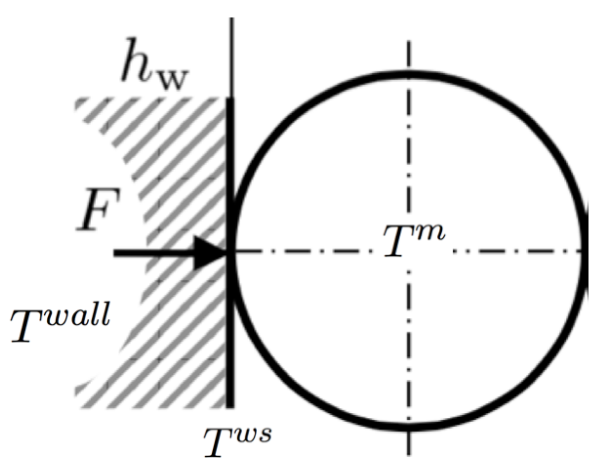

Figure 2.1: Wall-particle interaction.

External loads are exerted on the particles assembly through the circumventing rigid walls at elevated temperatures. Analogous to ghost-cell method, boundary particle-adjacent wall interaction is simulated as the deformed contact between a boundary particle and a ghost particle. Based on the rigid wall assumption, ghost particle is defined to have the same material properties and radius with the boundary particle. The temperature difference between the ghost particle and the wall surface is the same as the temperature difference between the wall surface and the boundary particle. The boundary wall is assumed to be located in the midst of these symmetrically deformed particles. The temperature difference, overlap and contact area are formulated in (2.14), (2.15), (2.16) respectively, where T^{ws} refers to the temperature at the wall surface, and subscript g is used to indicate the ghost particle.

$$\Delta T^{mg} = 2(T^m - T^{ws}) \tag{2.14}$$

$$\gamma^{mg} = 2(R^m - ||\vec{x^m} - \vec{x^{ws}}||) \tag{2.15}$$

$$a^{mg} = (\gamma^{mg}\frac{R^m}{2})^{1/2} \tag{2.16}$$

At the boundary surfaces, heat transfer from granular bed to infinite wall, which is assumed to be kept at constant temperature, can be formulated by two heat transfer mechanisms, (i) heat is conducted over flat circle of contact between the particle and adjacent wall surface; (ii) between wall surface to wall, convective heat transfer, which is dependent on walls' convection coefficient of h_w, is assumed to be the dominant mechanism.

$$\begin{aligned} Q^{m-ws} &= k^m a^{mg} \Delta T^{mg} && (2.17) \\ Q^{ws-wall} &= -h_w \pi (a^{mg})^2 (T^{ws} - T^{wall}) && (2.18) \end{aligned}$$

The final set of equations which define the wall-particle interaction are the following:

$$\begin{aligned} Q &= 4ka^{mg}\big(T^m - \frac{4k^m T^m + h_w \pi a^{mg} T^w}{4k + h_w \pi a^{mg}}\big) && (2.19) \\ F &= \frac{E^m}{3(1-(\nu^m)^2)} R^m \gamma^{mg} && (2.20) \end{aligned}$$

2.4 Assumption of Linear Thermal Expansion

Multi-physics of thermally-assisted compaction problem emphasizes the sensitivity of the thermal-contact solution to the thermal expansion of the particles. Concerning the numerical studies on thermal-contact of granular materials, there exists two approaches of implementing thermal expansion in the coupled solution. Some authors ground their theoretical models by using linear thermal expansion concept, whereas some others implement volumetric thermal expansion concept. We address the question of how these two approaches affect the accuracy of the coupled solution.

Thermal expansion is the tendency of the material to change in volume to a change in temperature. Linear thermal expansion is the expression of the volume change in one major direction, which can be formalized as change in length under the effect of unit increase in temperature.

$$
\begin{aligned}
\frac{\Delta L}{L_i} &= \alpha \Delta T && (2.21)\\
\Delta T &= L_f - L_i && (2.22)\\
L_f &= L_i(1 - \alpha \Delta T) && (2.23)
\end{aligned}
$$

where L_i is the initial length of the material and L_f is the final length. Instantaneous radius of particle m can be calculated as :

$$
\begin{aligned}
R^m &= R^m_{ref}(1 - \alpha \Delta T) && (2.24)\\
\alpha &= \left(\frac{R^m}{R^m_{ref}} - 1 \right) \frac{1}{T^m - T^m_{ref}}
\end{aligned}
$$

In volumetric thermal expansion, we consider a cube with initial volume of $V_i = L_i^3$

$$
\begin{aligned}
V_f &= \big(L(1 + \alpha \Delta T) \big)^3 && (2.25)\\
V_f &= L_i^3 \big(1 + 3\alpha \Delta T + 3(\alpha \Delta T)^2 + (\alpha \Delta T)^3 \big) && (2.26)
\end{aligned}
$$

The last two terms in equation 2.26 are negligible. Mostly volume change is expressed in terms of κ, which is the volumetric thermal expansion coefficient of a bulk material.

$$
\begin{aligned}
V_f &= V_i \big(1 + 3\alpha \Delta T \big) && (2.27)\\
\kappa &= 3\alpha && (2.28)
\end{aligned}
$$

In our numerical simulations we consider spherical particles, such that equation 2.27 can be re-written as:

$$\frac{4}{3}\pi(R^m)^3 = \frac{4}{3}\pi(R^m_{ref})^3\big(1+\kappa\Delta T\big) \tag{2.29}$$

$$R^m = R^m_{ref}\left(1+\kappa\left(T^m - T^m_{ref}\right)\right)^{1/3} \tag{2.30}$$

$$\kappa = \left(\left(\frac{R^m}{R^m_{ref}}\right)^3 - 1\right)\frac{1}{T^m - T^m_{ref}} \tag{2.31}$$

From the numerics point of view, Taylor expansion of volume expansion proves that the radius is indeed a function of linear expansion coefficient, α.

$$R^m = R^m_{ref}\big(1+\kappa(T^m - T^m_{ref})\big)^{1/3} \tag{2.32}$$

$$\simeq R^m_{ref}\left(1+\alpha(1+3\alpha\Delta T)^{-2/3}|_{\Delta T=0}\Delta T + ...\right) \tag{2.33}$$

The dominant terms in equation 2.33 are the first two terms. It is concluded that linear thermal expansion formulation provides significant accuracy when compared with volume thermal expansion formulation. Therefore in our simulations we implemented linear thermal expansion of particles in our coupled system of equations.

$$R^m = R^m_{ref}(1+\alpha\Delta T) \tag{2.34}$$

2.5 Conclusions

We develop a particle mechanics approach that explains the thermo-mechanical coupling observed during compaction processes. The proposed formulation states the governing equations for discrete system of particles, under static equilibrium and steady state heat conduction. The integrated thermal and mechanical model takes into account the thermal expansion during consolidation. The governing field equations are simultaneously solved for the case of static mechanical equilibrium and steady state heat conduction. The wall-particle interaction is formalized in terms of the discussed parameters.

Chapter 3

Chain of Particles' Numerical Experiments

3.1 Introduction

It is the purpose of this chapter to suggest insight into the nature of thermomechanical interaction through numerical experiments. The simulations are evaluated to track the particles' position and determine the temperature under different thermal and mechanical loads. The non-linearity of the stated problem points out alternative aspects of the granular systems.

We focus on a one dimensional model to investigate the effects of thermal expansion, applied mechanical load and thermal gradient on the system of spherical particles. We explain the simulation configuration and the assumptions, which provides the validity of the proposed mathematical model. We mention the numerical methodology that we use to solve the systems of highly non-linear equations. We conclude this chapter with numerical experiments that we concentrate to unveil the characteristics of chain of particles.

3.2 Simulation Configuration

Referring to the previous experimental studies on regular and random packings of granular media, Walton points out that although the regular packing models are based on extreme assumptions, they are capable of capturing vast majority of the characteristics of the real granular beds [72]. We consider a simple cubic packing of identical elastic spheres, where two directions are assumed to be infinity and compression load, temperature gradient are applied along the major direction. Stress and heat flux are defined to solely depend on externally applied thermal and mechanical loads, and weight of the particles are neglected. For such regular packings each layer of arrangement is isothermal normal to the direction of applied load. Also, since these transversely oriented particles are, at most, point contact, for each individual particle there is only one pair of contact area aligned with the direction of applied thermal and mechanical load. Due to the symmetry of the problem, it is sufficient to consider a single column of square cross-section containing the longitudinally compressed spheres together. This concept is similar, in spirit, to the work of Chan and Tien [10] on establishing the effective thermal resistance and to the work of Walton [72] who presents a method to calculate the effective elastic moduli of such packings.

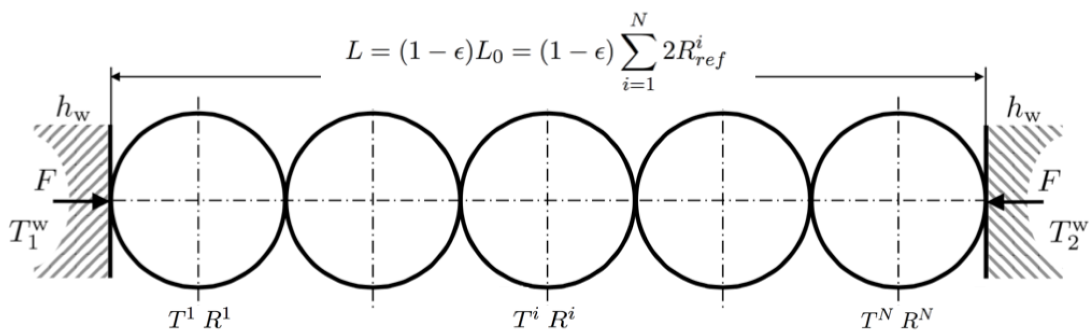

Figure 3.1: Sketch of the initial configuration.

The above description for the specified granular media, which is under thermally-assisted compaction, can be modeled as a chain of elastic particles. The main purpose of this study is to discover the influence of thermal and mechanical coupling at the discrete level and implement the required amendments to continuum level models.

In our numerical experiments, we considered various cases in relation with different materials, such as stainless steel(SS304), aluminum, teflon. The mechanical and thermal properties of these materials are listed in table 6.1.

Table 3.1: Data used in Numerical Analysis

	SS304	Aluminum	Teflon
α	17.3*10^{-6} 1/K	23.6*10^{-6} 1/K	250*10^{-6} 1/K
E	193 GPa	62 GPa	2.25 GPa
k	15 W/mK	243 W/mK	0.5 W/mK
ν	0.29	0.33	0.33
R^m_{ref}	0.003175 m	0.003175 m	0.003175 m
T^m_{ref}	293 K	293 K	293 K

3.3 Methodology

In this section we present the method used for the solution of the non-linear system of equations that we obtain through the thermo-mechanical coupling analysis of a chain of particles. Since we consider the case of static mechanical equilibrium and steady state heat conduction, the sum of forces and heat on each particle can be cast as a system of equations, where we also have the unknowns of each particles' position and temperature. In one dimensional analysis, assuming that we have N number of particles, we have N number of components of force and N heat equations in the system of equations.

$$f(x) = \begin{pmatrix} F^{12} + F^{13} + F^{14} + \cdots + F^{1N} \\ F^{21} + F^{23} + F^{24} + \cdots + F^{2N} \\ \vdots \\ F^{N1} + F^{N2} + F^{N3} + \cdots + F^{N(N-1)} \\ Q^{12} + Q^{13} + Q^{14} + \cdots + Q^{1N} \\ Q^{21} + Q^{23} + Q^{24} + \cdots + Q^{2N} \\ \vdots \\ Q^{N1} + Q^{N2} + Q^{N3} + \cdots + Q^{N(N-1)} \end{pmatrix}$$

The corresponding array of unknowns are listed as:

$$x = \begin{pmatrix} X^1 \\ X^2 \\ \vdots \\ X^N \\ T^1 \\ T^2 \\ \vdots \\ T^N \end{pmatrix}$$

We solve the system of equations by using Newton-Raphson method.

$$f(x) \quad = \quad 0 \tag{3.1}$$

To briefly mention the logic of this method, we can consider the Taylor series expansion of the function $f(x)$ around and initial guess of x_0,

$$f(x) \quad = \quad f(x_0) + f'(x_0)(x - x_0) + \frac{f''(x_0)}{2!}(x - x_0)^2 + ... \tag{3.2}$$

where $f'(x_0)$stands for the derivative of function $f(x)$ with respect to x and evaluated at x_0. By using the first order approximation of this formula, we can find a solution for the first iteration loop,

$$f(x) = 0 \approx f(x_0) + f'(x_0)(x_1 - x_0) \tag{3.3}$$

$$x_1 = x_0 + \frac{f(x_0)}{f'(x_0)} \tag{3.4}$$

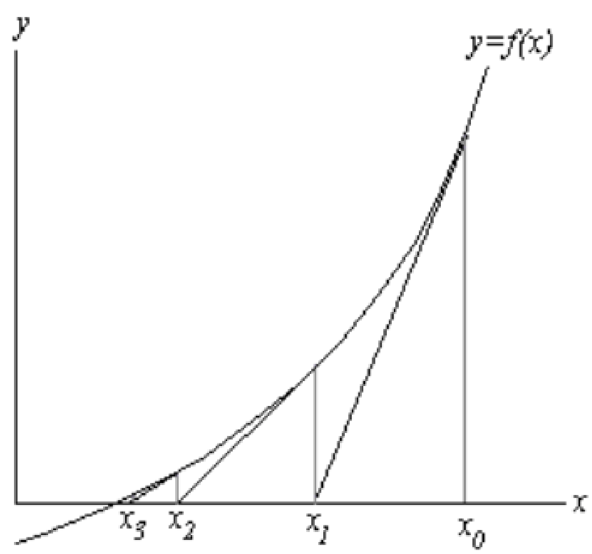

Figure 3.2: Schematic sketch of Newton-Raphson method applied in iterative solution of system of non-linear equations.

The iteration scheme can be generalized by the following equation, where i represents the iteration number;

$$x_{i+1} = x_i + \frac{f(x_i)}{f'(x_i)} \tag{3.5}$$

At the end of each iteration, convergence is checked by comparing the final solution with a prescribed tolerance. In our simulations we compare it with a relative tolerance value, which we set individually for force and heat equations.

3.4 Results

Thermo-mechanical coupling has a significant effect on stress and heat transferred during compaction. According to the Hertz theory [37], collinear force between the elastically compressed particles is nonlinearly proportional to the overlap. This dependency is altered under different thermal loading conditions, as seen in Figure 3.3 and 3.4.

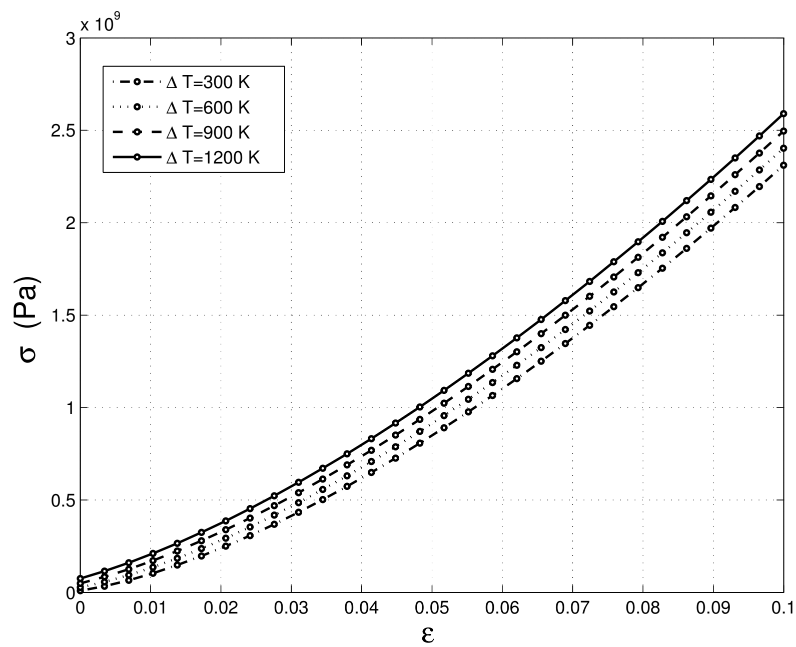

Figure 3.3: Stress vs compaction ratio, ϵ, under different thermal gradient applied at the boundary walls ($\Delta T = T_2^w - T_1^w$).

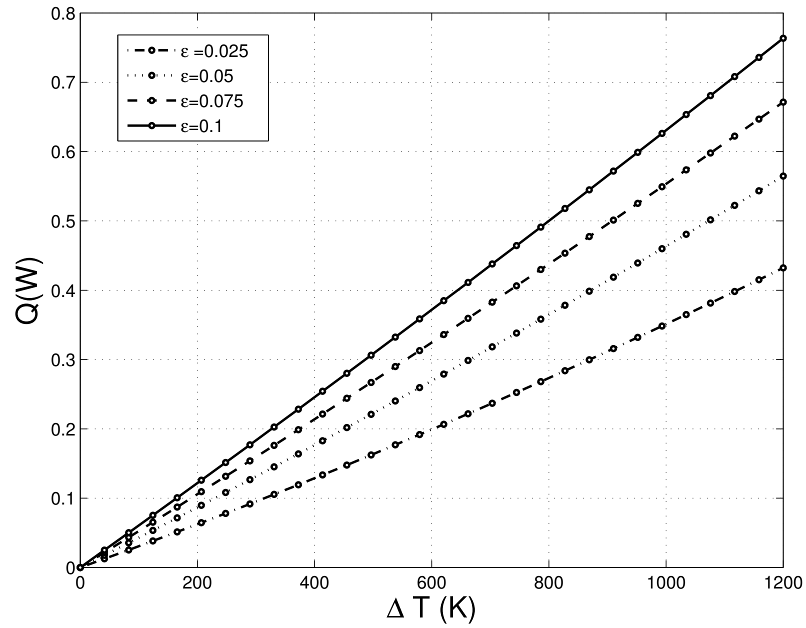

Figure 3.4: Heat vs thermal gradient, ΔT, under various imposed compaction ratios.

The effect of wall-particle interaction is studied through the chain system by applying global thermal gradient of 300 K for three different compaction ratios, % 2.5, %5, %10. For each case, wall heat transfer coefficient (h_w) is ranged from 1 to $10^7 \mathrm{W/m^2K}$. Figure 3.5 indicates the two limiting cases of perfect insulating and perfect conducting walls. The heat transferred increases and reaches a maximum where the walls act as perfect conductors, thereby the particles touching the walls are almost at the prescribed applied temperature.

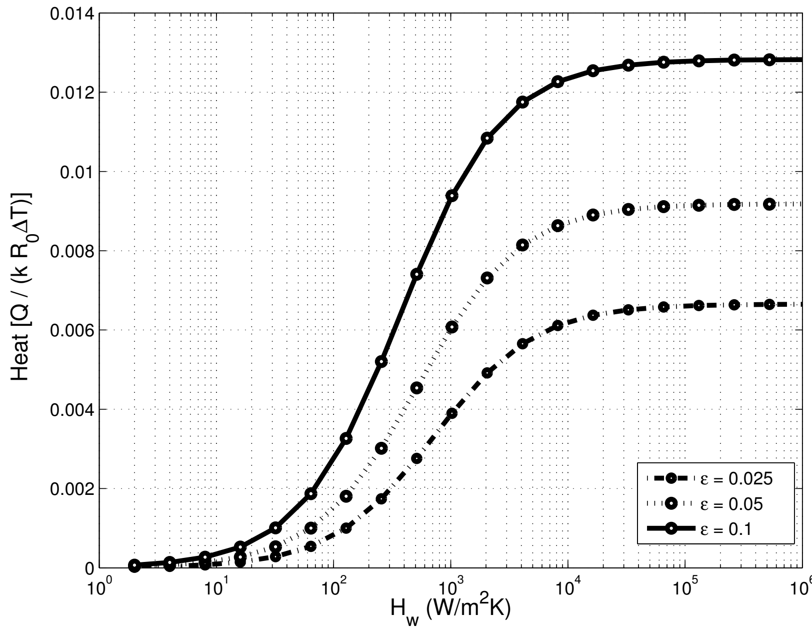

Figure 3.5: Correlation between heat and wall conductance for different compaction strains.

3.4.1 Role of Thermal Expansion

Systems of granular materials with different thermal expansion properties responds in various re-arrangements to a particular thermal and mechanical load. The following experiments compiles the results of three different single particle systems, SS304, Aluminum, and Teflon with different thermal expansion values, $17.3\ 10^{-6}\ 1/K$, $23.6\ 10^{-6}\ 1/K$, $250\ 10^{-6}\ 1/K$, respectively. Alterations due to increase of thermal stress can be traced by plotting the displacement experienced by each particle within the chain system. In Figure 3.6 the relative change in position is divided by the total mechanical deformation, and listed with respect to the non-dimensional position of particle, 0 being the particle at the non-moving boundary and 1 is in contact with the moving boundary. For all these three cases of comparison the chain is system is compacted to the 2.5% of the initial length and a total thermal gradient of 300K is applied. The equilibrium of thermal and mechanical stresses can induce a non-linear distribution of displacements, that can be significant for systems with high thermal expansion property. Moreover as seen in Figure 3.7 steep variation in contact areas appearing at consecutive pairs is another consequence of these systems which also leads to non-uniform thermal contact conductance and non-uniform temperature gradient within the system.

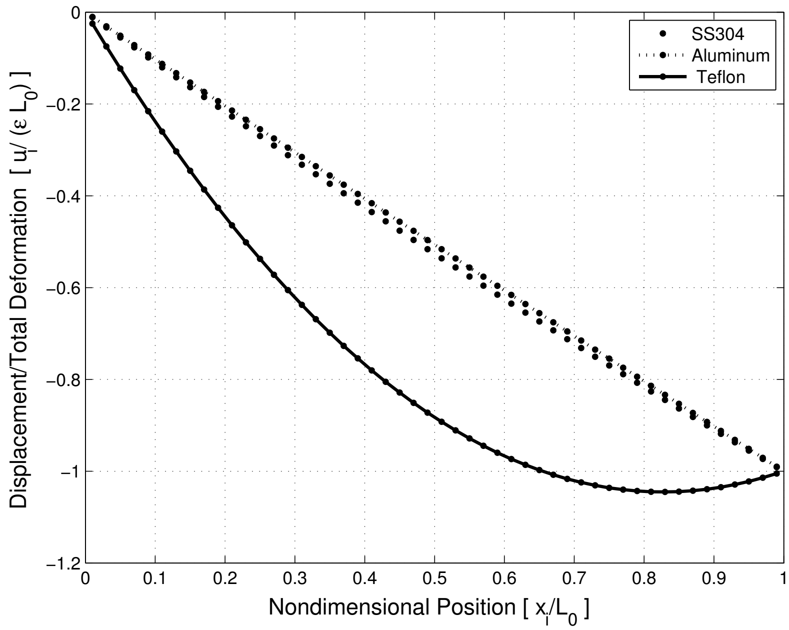

Figure 3.6: Relative displacement of each particle within the chain at $\epsilon = 0.025$ & $\Delta T = 300K$.

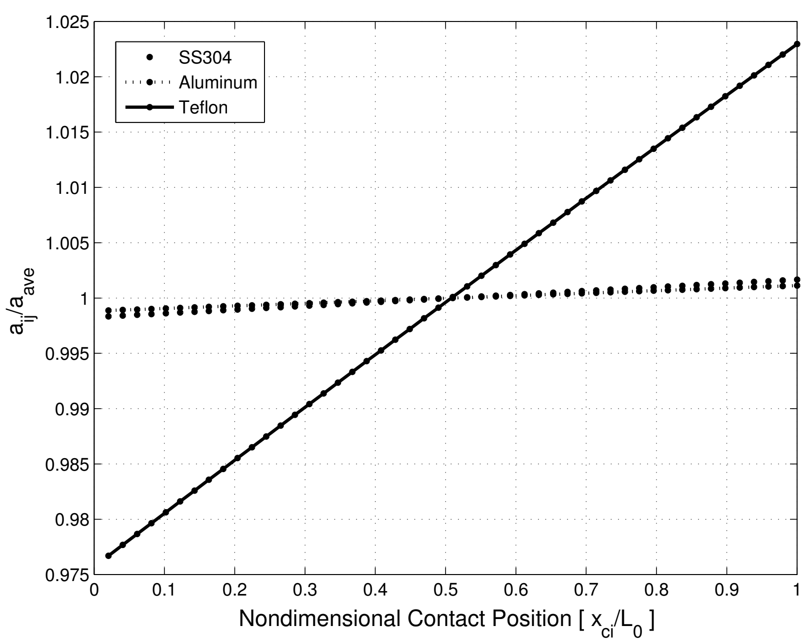

Figure 3.7: Contact radius variation within the chain of particles at $\epsilon = 0.025$ & $\Delta T = 300K$.

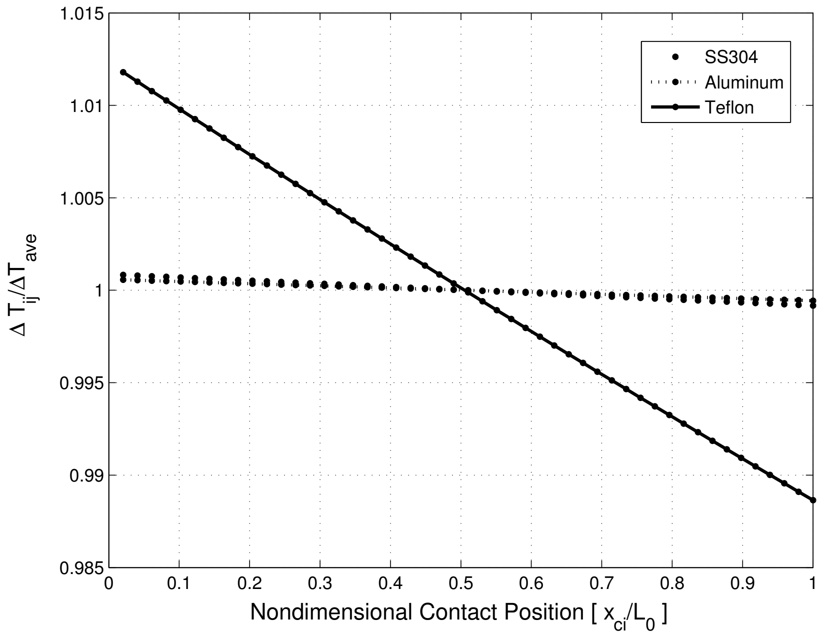

Figure 3.8: Temperature difference at consecutive contacts at $\epsilon = 0.025$ & $\Delta T = 300K$.

Since heat transfer through chain remains the same, the larger contact area the smaller will be temperature difference between the consecutive pairs of particles. Variation from linear distribution of temperature within the chains system is a characteristic of granular systems and enhanced by thermal expansion of individual particles.

3.4.2 Role of Applied Mechanical Load

Under thermal gradient of 300 K, three different mechanical loading conditions are compared in Figure 3.9 when global deformation applied on the system varies from 1%, 2,5% to 10%. In order to compare the coupling effect of thermal gradient and mechanical deformation, 2 extreme cases for wall-particle interactions are considered. In case of perfect insulating walls, h_w is assumed to be $1\mathrm{W/m^2K}$. This particular condition is a simulation of pure mechanical loading where we expect to have linear distribution of non-dimensionalized positions' of particles within the chain system.On the other hand $h_w = 10^7\mathrm{W/m^2K}$ simulates the condition of perfectly conducting walls. As it is seen in Figure 3.9, non-linearity in distribution of displacements is more dominant for low mechanical loading cases such as of 1% compaction ratio.

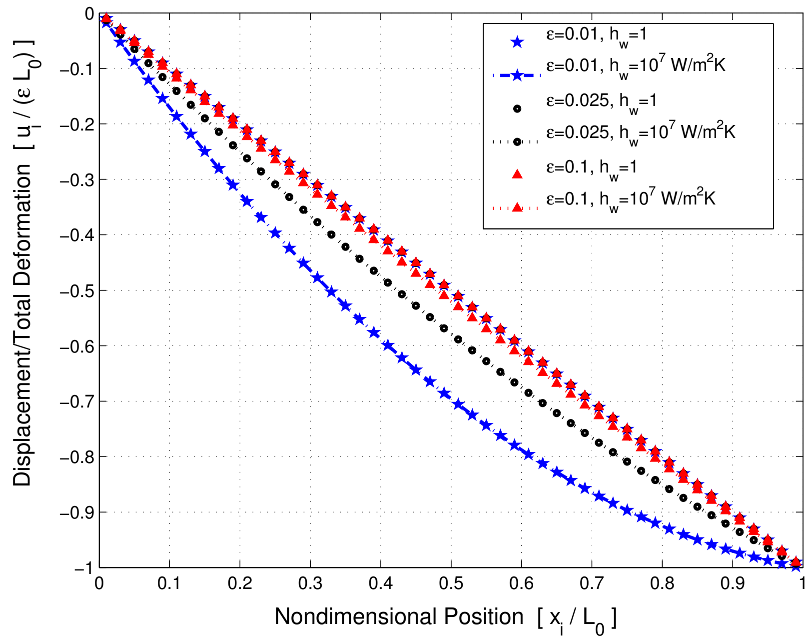

Figure 3.9: Non-dimensional displacement vs initial position of the particles under different mechanical loads, with varying heat convection coefficients of the boundary walls.

3.4.3 Role of Thermal Gradient

Chen et al. [11] proved that temperature changes affect the packing fractions of granular materials in the absence of mechanical compaction in their recent study on grain dynamics induced by thermal cycling. The significant effect of thermal gradient on re-arrangement of particles can be also depicted in one dimensional numerical experiment: A chain of spherical particles is compacted up to 2.5% of their initial length while thermal gradient is varied from 300 K, 600 K and 900 K. Figure 3.10 shows the non-uniform distribution of change in position of particles within the chain. Specifically at high thermal gradient cases this change differs around 30% between the two boundary particles at each end.

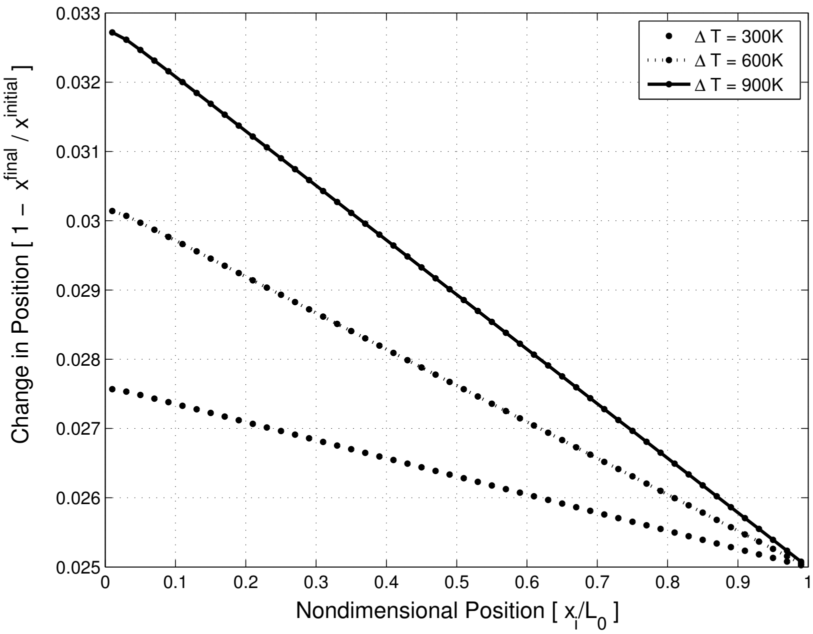

Figure 3.10: Under various imposed thermal gradients between the boundaries, change in particles' position are compared for a fixed compaction ratio of $\epsilon = 0.025$.

3.5 Conclusions

The developed model describes the thermo-mechanical behavior of a confined granular system by adopting a detailed description at the particle level. In order to unveil the physics behind the coupled phenomena, we have restricted attention to one dimensional granular systems.

Thermal contact and Hertzian deformation models are integrated to simulate the temperature and displacement fields of consolidated granular medium. In order to capture the actual physical conditions wall-particle interactions are considered, ranging from perfect insulating to perfect conducting walls. In order to understand the characteristics of thermally-assisted compaction of granular assembly, the effects of thermal expansion, thermal and mechanical loads applied are investigated.

The numerical results shows that integration of thermal deformation with the elastic contact models induces the incongruity seen in mechanical deformation based compaction models. The coupled phenomena introduces highly nonlinear system of equations, and it imposes variation in contact areas and nonlinear temperature distribution within the particulate material. This effect is enhanced for particles with larger thermal expansion coefficient. It appears that the critical regime, where the nonlinearity due to thermo-mechanical coupling becomes more dominant, is low mechanical and high thermal gradient conditions.

Chapter 4

Continuum Mechanics Approach

4.1 Introduction

While the particle mechanics approach elucidates the formation and evolution of microstructure within particle packings, there has been considerable research directed towards describing macroscopic behavior of compacted materials. Some of the early work on theoretical modeling of transport properties are devoted to estimate the thermal, and electrical conductivity, elastic mechanical properties of ordered and disordered arrangements. Starting from the pair interactions between particles, the macroscopic properties are obtained using various homogenization techniques and postulating continuum constitutive laws [34].

In this study we also consider the problem from the point of continuum mechanics approach. For the case of small strain thermoelasticity, governing field equations of motion and energy are the following:

$$\nabla \cdot \boldsymbol{\sigma} = 0 \tag{4.1}$$

$$\nabla \cdot (k \nabla T) = 0 \tag{4.2}$$

where the Cauchy's stress, $\boldsymbol{\sigma}$, is formulated as combination of classical linear elasticity theory and simple linear thermal expansion.

$$\boldsymbol{\sigma} = -\lambda \mathrm{tr}(\boldsymbol{\epsilon})\mathbf{I} - 2\mu\boldsymbol{\epsilon} + (3\lambda + 2\mu)\alpha(T - T_{ref})\mathbf{I} \tag{4.3}$$

where λ and μ are Làme constants.

After a detailed numerical analysis we observe that conventional continuum approach, to which we also integrate the proposed effective mechanical and thermal properties, is insufficient to explain the physics of thermally-assisted compaction. Therefore we focus on derivation of an effective thermal expansion formalism that can account for the thermal expansion at macroscopic level.

4.2 Analytical Solution for 1D Linear Thermoelasticity Continuum Model

We confine our attention to a homogenous and isotropic rod, which is constrained by a pair of vertical walls at points $x = 0$, $x = L_0$. We suppose that the rod is initially stress-free at reference temperature T_{ref}, and upon the applied mechanical load and thermal gradient, the displacement vector measured from the reference state, remains parallel to x-axis. These assumptions ensure the fact in the analysis of an equivalent system similar to discrete solution, we are focused on thermal and mechanical deformations along the primary axis, such that the material is assumed to have $\nu \approx 0$. This concept is similar in spirit to the assumptions considered in William Alan Day's work [16]. One dimensional linear thermoelasticity can be formulated as:

Equation of energy:

$$k\frac{\partial^2 T}{\partial x^2} = c\frac{\partial T}{\partial t} + T_{ref}\alpha(3\lambda + 2\mu)\frac{\partial^2 u}{\partial x \partial t}$$

where T is the absolute temperature, T_{ref} is the reference temperature of the bed, k is the thermal conductivity, c is the specific heat, and α is the thermal expansion coefficient of the rod.

Equation of motion:

$$(\lambda + 2\mu)\frac{\partial^2 u}{\partial x^2} = \alpha(3\lambda + 2\mu)\frac{\partial T}{\partial x} + \rho\frac{\partial^2 u}{\partial t^2}$$

Since we aim to solve for steady state heat conduction, temperature dependent terms are eliminated from the above equations. We consider a simulation where Dirichlet boundary conditions are applied at two boundaries, $T(0) = T_0$ and $T(L_0) = T_N$. The coupled system of equations are solved for the displacement and temperature fields.

$$u(x) = \frac{\alpha}{2}\big(\frac{3\lambda+2\mu}{\lambda+2\mu}\big)\big(\frac{T_N-T_0}{L_0}\big)x^2 - \big[\epsilon + \frac{\alpha}{2}\big(\frac{3\lambda+2\mu}{\lambda+2\mu}\big)(T_N-T_0)\big]x \quad (4.4)$$

$$T(x) = \big(\frac{T_N-T_0}{L_0}\big)x + T_0 \quad (4.5)$$

$$\sigma = -\epsilon(\lambda+2\mu) - \alpha(3\lambda+2\mu)\big(\frac{T_N+T_0}{2} - T_{ref}\big) \quad (4.6)$$

The stress field in thermally assisted compaction of a continuum body is a linear function of elastic moduli and thermal expansion coefficient of the material. It is obvious from equation (4.6) is that the nonlinearity seen in discrete solution can not be expressed through linear thermoelasticity continuum model. As a result, there has been considerable research in the literature that attempt to understand the relationship between the macroscopic physical properties and the physical and geometrical properties of its constituents. Consideration of the thermally-assisted compaction problem requires the definition of effective thermal conductivity, effective elastic moduli, and effective thermal expansion coefficient of the confined body.

4.3 Effective Continuum Approach

Effective mechanical properties of granular beds have been of great interest to large number of researchers and engineers. Some of the groundbreaking studies on determining the elastic moduli of random and ordered packing of spherical particles relies on the early work of Mindlin [47] , Mindlin and Deresiewicz [49], Duffy and Mindlin[19] on describing the particle to particle contact force and work done upon infinitesimal deformation. In this study we are mostly concerned and inspired by the well known studies of Walton (1975, 1987) [72, 73], Norris and Johnson (1997) [51], and Makse et al. (1999, 2001)[44, 45].

Walton proposed the principal elastic modulus, namely the one governing for vertical compression without any lateral extension, for a regular packing model [72]. Regarding on the previous experimental studies, he claimed that although the model is extremely idealized, it is capable of capturing characteristics of granular structure. In this theoretical model he assumes the geometry of interest is infinite in two directions and is compressed along the finite directions under an applied vertical force. The particles are also under the weight of particles that are above them and surrounded by fluid. Neglecting the elastic anisotropic, Walton solved for the equation of equilibrium for a chain of particles, where the appropriate boundary conditions are applied.

In 1987 Walton derived the incremental elastic moduli of a random packing of identical elastic spheres [73]. Randomly distributed spheres are assumed to be subjected to an initially statistically homogenous strain, such that resulted stress is sufficiently small enough to maintain the equations of linear elasticity valid for each sphere. Walton solves the system of equations for a further incremental stress applied on each particle. The effective elastic moduli is determined through the relationship between average incremental stress and average incremental strain. For averaging method, he applied the concept of assuming the packing as statistically isotropic geometrically and the contacts are distributed with uniform distribution over the surface of a spherical particle. This methodology is proposed by Batchelor and O'Brien [7] and applied by many researchers in the field of granular materials.

Norris and Johnson investigated the problem of finite and incremental elasticity of random packing of identical particles using energy methods [51]. They explored the concept of a strain energy function for the granular medium, which is under finite deformation and perform incremental motion. The main principal in effective medium approach is that the global deformation done on the system of particles is equal to the sum of the particle to particle deformation occurring due to infinitesimal work. Starting from single contact models, they extended the derivation to a randomly packed bed of particles, by using ensemble averaging technique. Main assumptions in effective medium theory are:

1) It is based on affine approximation, namely the motion of each grain follows the applied strain.

2) The grains are well-bonded,such that contact number and positioning do not change under the applied load. Norris and Johnson successfully derived the elastic moduli tensor up to second order expansion.

Effective medium theory provides well-rounded derivations in estimating the effective elastic moduli of packed bed of spherical particles to a large extend. Makse et al. searched for the underlying reason of discrepancy observed between the numerical results of effective medium approach and the experimental studies [45]. They point out that this approach is not as successful in estimating shear modulus as in describing bulk modulus [44]. In this regard authors questioned the relevance of force laws defined at single contact level, and the validity of effective medium approach, where they proved that the simplification done in effective medium approach is the misleading element in formulation [44]. Affine motion assumption demolishes the ability of the approach to account for the relaxation and rearrangement of particles that are under shear deformation.

In this study we extend the effective medium approach with the thermal contact model principles by incorporating the particle interactions to account for the local field effects. We reformulated the effective elastic properties and effective thermal conductivity accordingly, and implemented these parameters in continuum mechanics model. We evaluated the effectiveness of continuum model in resembling the system described by the discrete model.

Th effective mechanical properties of granular matter, which is under the effect of a confining stress of σ is listed as

$$C_n = 4\frac{\mu}{1-\nu} = 4\frac{E}{2(1+\nu)}\frac{1}{1-\nu} = \frac{2E}{1-\nu^2} \tag{4.7}$$

$$\tilde{\lambda} + 2\tilde{\mu} = \frac{3}{20\pi} C_n (\phi_s Z)^{2/3} \big(\frac{6\pi\sigma}{C_n}\big)^{1/3} \tag{4.8}$$

$$3\tilde{\lambda} + 2\tilde{\mu} = \frac{1}{4\pi} C_n (\phi_s Z)^{2/3} \big(\frac{6\pi\sigma}{C_n}\big)^{1/3} \tag{4.9}$$

where C_n is actual stiffness that depends on the bulk mechanical properties, ϕ_s is the packing fraction,and Z is the coordination number. Effective mechanical properties and effective thermal conductivity are implemented in continuum mechanics model and listed as continuum solution 1.

4.4 Comparison of Effective Continuum Approach with Particle Mechanics Approach

Taking into account the effective medium approach, we generate the conventional continuum solution, namely conventional continuum solution, and compared these results with a similar discrete solution. Equation (4.6) is now expressed as:

$$\sigma = \phi_s Z C_n \big(\frac{3}{32\pi^2}\big)^{1/2} \big(|-\epsilon\frac{3}{5} - \alpha(\frac{T_N + T_0}{2} - T_{ref})|\big)^{3/2} \tag{4.10}$$

It is worth noting that effective medium approach is describing the elastic moduli of a randomly and/ or ordered system of particles which are deformed in isothermal conditions. Thus the proposed description of elastic moduli are function of bulk material properties and applied mechanical load. Under thermally-assisted compaction conditions we focus on the accuracy of conventional continuum solution in describing the stress evaluation within a chain of particles system.

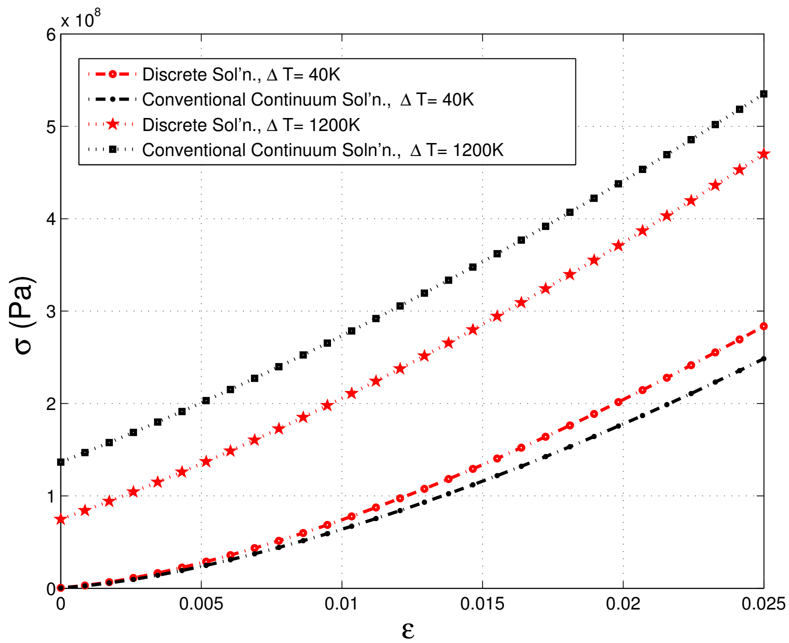

Figure 4.1: Stress vs compaction ratio, ϵ, evaluated for discrete and continuum solutions, at $T_N - T_0 = 40K$ and $T_N - T_0 = 1200K$.

Effective continuum approach renders significant description of granular material regarding the applied stress, however numerical experiments show that the model drastically fails to achieve this for cases of high thermal gradient applied between the two boundary walls (figure 4.1).

4.4.1 Dependence on Definition of Packing Fraction

There exists two definitions that can be used to define the packing fraction of a granular assembly. Among the previous studies it has been a controversial topic whether this has an effect on numerical results of effective medium approach. Thus in this subsection we define the two possible expression of packing fraction and show a numerical example to compare their effect on the final continuum soltuion.

$$
\begin{aligned}
\phi_s^1 &= \frac{n\pi 4/3R_0^3}{V_0} \qquad (4.11)\\
&= \frac{N\pi 4/3R_0^3}{N8R_0^3}\\
&= \frac{\pi}{6}
\end{aligned}
$$

$$
\begin{aligned}
\phi_s^2 &= \frac{\rho_g s}{\rho_t} \qquad (4.12)\\
&= \frac{m_p/v_{gs}}{m_p/V_p} \qquad (4.13)\\
&= \frac{V_p}{V_{gs}}\\
&= \frac{N\pi 4/3R_0^3}{N8R_0^3(1-\epsilon)}\\
&= \frac{\pi}{6(1-\epsilon)}
\end{aligned}
$$

We simulate a case of compaction ratio increasing up to10% under a constant thermal gradient of 600 K. Makse et al. claimed that assuming ϕ_s as a constant for the defined closed packing or modifying it with respect to applied loading has a minor effect in calculation of force in the continuum solution [45]. This is also shown in figure 4.2.

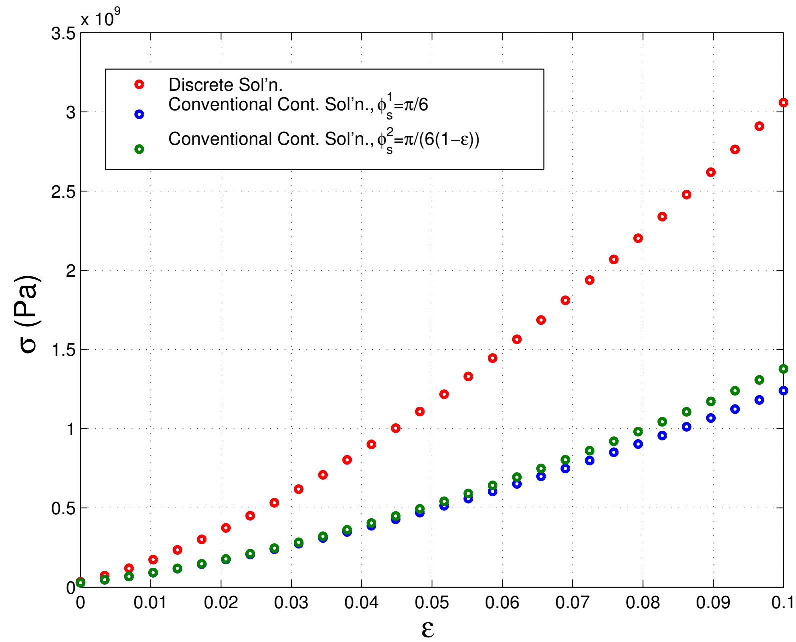

Figure 4.2: Effect of packing fraction definition on stress evaluation is compared for discrete and continuum solution, evaluated at $T_N = 893K$.

4.5 Comparison of Thermal Contact Models

The problem of determining an effective thermal conductivity expression of granular system is mathematically identical with that of finding the effective dielectric constant or the effective magnetic permeability of a disperse system in which the particle have electrical and magnetic properties different from the matrix [7]. The early works in this field roots in Maxwell's expression for the effective conductivity of spherical inclusions [46].

$$\tilde{k} \quad = \quad k_{matrix}\left(1 + \frac{3(k/k_{matrix} - 1)}{k/k_{matrix} + 2}\phi_s\right) \tag{4.14}$$

Jeffrey extended the concept of thermal dipole strength, which is a weighted some of heat fluxes across the areas near contact points [30]. In this study he improved the effective conductivity expression for a dilute dispersion of spherical particles with a correction made on ϕ_s term, changed to ϕ_s^2. However these models lacks accuracy significantly, as the packing fraction is above 0.5. Also for the concerned cases, the particles have much larger conductivity than the surrounding matrix. These two factors urge researches to investigate new approaches for particles systems with high volume fraction and large thermal conductivity.

Thermal contact models aim to propose a description of thermal conductivity through a stationary, ordered and/or random close packing of granular materials. The particles are generally modeled as smooth, perfectly conforming uniform spheres with either point contacts, or small contact spots. Under an externally applied mechanical load and thermal gradient, small contact deformations are calculated as a perturbation from the Hertz theory. Mechanical balance of normal contact reactions on the microscale render the required information of contact network generation within the granular bed. Temperature field within the particle is calculated based on the heat flux through the relevant contact areas. In the case of ordered packings of infinite geometry this calculation is carried out for an limited portion of the granular system such as chain of particles, whereas for random packings different formalisms (i.e: statistical averaging, volume averaging, ensemble averaging) are used to link single contact conductance to the macroscopic heat transport property of the granular bed.

Some of the well known thermal contact models, which have been implemented by recent studies, are proposed by Chan and Tien (1973) [10], Batchelor and O'Brien (1977) [7], Siu and Lee (2000) [59], Kaganer (1966) [32], Zinchenko (1998) [76]. We explain the general methodology used in thermal contact models in section 1.2. In this section we focus on the first three methods, and discuss the effective heat transport formalism proposed in these studies.

Our main objective is to find the effective thermal conductivity coefficient, $\tilde{k}$, that can enhance the continuum solution to achieve the nonlinearity seen in discrete solution. Since the heat flux in continuum solution is a linear function of the thermal conductivity, we look for a formalism that is dependent on the particle size, particle distribution, and boundary conditions of compaction process.

$$q = \tilde{k}\,\frac{\partial T}{\partial x} \tag{4.15}$$

In the following subsections we briefly mention the difference between the three mostly visited thermal contact models in the literature. We re-formulated the effective thermal conductivity formalisms, which are proposed in these studies, in coherence with our continuum solution parameters.

4.5.1 Chan & Tien's Thermal Contact Model

Chan and Tien presents the analytical solution of the steady state heat conduction through a packed bed of solid spheres bounded by two infinite plane surfaces of different temperatures [10]. The overall heat conductance of the ordered system of particles, which is named as regular packing patterns, is predicted in terms of constriction resistance of spheres in contact. Constriction resistance is the resistance to heat flow through a passage, which is a reverse definition of heat conductance concept. In this study they consider thermal contact patterns for different regularly packed spheres, such as simple cubic, body centered cubic and face centered cubic. Moreover they present both exact and approximate solutions for solid, hollow and coated spheres.

Since the packing geometry is finite in only one direction, along which applied mechanical load and thermal gradient are imposed, each layer of arrangement normal to the heat flow has identical point contact and remains isothermal. Thus in calculation of thermal conductance, constriction resistance within each normal direction is neglected, rather the parallel oriented arrangements of spheres are assumed to compose a series of resistance which dominate the overall thermal conductance of the packed spheres.

$$\tilde{k} = \frac{N_a}{N_t}\frac{1}{Res^{mn}} \tag{4.16}$$

where N_t and N_a are the number of particles permit length and unit area, and Res^{mn} is the constriction resistance between particles m and n [10].

Multiple contact areas of a single particle is divided by pair interactions of geometrically opposing contacts with neighboring particles. The overall resistance within a particle is calculated by liner superposition of the resistances due to the contact pairs. And finally the resistance due to each pair is obtained through the solution of steady state heat conduction problem [10]. For simple cubic packing of solid spherical particles the thermal conductivity of the packed bed is calculated as the following:

$$\tilde{k}^{Chan} = S_p k\left(\frac{1-\nu^2}{E}P\right)^{1/3} \tag{4.17}$$

$$P = F\frac{N_a}{S_F} \tag{4.18}$$

$$S_p = \frac{1.56}{S_R S_j}\frac{N_a}{N_t}\left(\frac{3}{4}S_F\frac{R_{ref}}{N_a}\right)^{1/3} \tag{4.19}$$

where for the particular packing pattern, S_R is 0.825, and S_R and S_F are 1. $N_t = 1/(2R_{ref})$, $N_a = 1/(4R_{ref}^2)$. P is the externally applied pressure and F is the contact force alone the normal of contact surface.

$$\tilde{k}^{Chan} = 0.9454k(\frac{3}{4}F\frac{1-\nu^2}{ER_{ref}^2})^{1/3} \tag{4.20}$$

4.5.2 Siu & Lee's Thermal Contact Model

Similar to Chan and Tien's approach, Siu and Lee presents the effective thermal conductivity of ordered packed beds pf spherical particles using constriction resistance and contact angle effects [59]. In this study they claim that the resistance to heat flow has two constituents, (i) bulk resistance that accounts for the distance (i.e.: angle) separating the two areas across the spherical particles, (ii) local resistance that accounts for the presence of constriction at the contact area. The former is dependent on the packing patterns of the spheres, and is specific to simple cubic, body center cubic and face centered cubic. The latter is similar to the contact resistance concept defined in Chan and Tien's model.

Through a series of calculations and proposed correlations Siu and Lee finalize their model by stating that the effective thermal conductivity is a linear function of mean contact radius over particle radius ratio. For simple cubic packing effective thermal conductivity is formulated as:

$$\tilde{k}^{Siu} = 0.8278k\frac{a}{R_{ref}} \tag{4.21}$$

where ratio of contact radius to particle radius can be found through Hertz law of deformation.

$$F^{mn} = \frac{4}{3}E^{mn}(R^{mn})^{1/2}(\gamma^{mn})^{3/2} \tag{4.22}$$

$$a^{mn} = (R^{mn}\gamma^{mn})^{1/2} \tag{4.23}$$

$$F^{mn} = \frac{4}{3}E^{mn}(R^{mn})^{1/2}(\frac{(a^{mn})^2}{R^{mn}})^{3/2} \tag{4.24}$$

For the case of identical spherical particles, which are also initially at same temperature and same size, R_{ref}, the contact radius a can be re-written as:

$$R^{mn} = \frac{R_{ref}}{2} \tag{4.25}$$

$$E^{mn} = \frac{E}{2(1-\nu^2)} \tag{4.26}$$

$$a = \left(\frac{3}{4}F^{mn}\frac{1-\nu^2}{E}R_{ref}\right)^{1/3} \tag{4.27}$$

Since we focus our attention on the compaction of a simple cubic structure that is under a uniaxially applied load of F, and the system is infinite in the other two directions, F^{mn} is equal to F. Equation 4.21 can be expressed in terms of these variables.

$$\tilde{k}^{Siu} = 0.8278k(\frac{3}{4}F\frac{1-\nu^2}{ER_{ref}^2})^{1/3} \tag{4.28}$$

4.5.3 Batchelor & O'Brien's Thermal Contact Model

Batchelor and O'Brien investigates the thermal and electrical conductivity through a granular material embedded in a matrix [7]. Packed bed of particles are either in contact or nearly in contact. A formalism is introduced by Batchelor and O'Brien that connects the overall thermal conductivity of the granular bed to a weighted sum of the thermal fluxes across the surface of contact areas. Starting with evaluation of an integral equation which accounts for the temperature field over the contact, they calculated the average thermal dipole strength of the randomly arrangements packed bed of particles. Assumption of statically isotropic structure cancels the dependence of the thermal conductivity as a second rank tensor, such that it is treated as a unit tensor [6].

Batchelor and O'Brien investigates the problem from a broader perspective. Initially they consider a packed bed of spherical particles embedded in a matrix, which has a comparable thermal conductivity. Later they elaborate their derivation by solving for the asymptotic case of particles having much larger thermal conductivity than the matrix, such that the matrix can be neglected. The particles are initially separated by a small distance h, where this gap is closed upon the application of external load. Lastly the particles are modeled with a flat circle of contact, which is the case of Hertz theory of two touching elastic particles convey a thermal flux along their mutual surface of contact [6].

Although the problem of interest is randomly packed bed of spherical particles, Batchelor and O'Brien provide the solution for ordered systems as well. In general the effective thermal conductivity of a simple cubic arrangement of spherical particles is given as:

$$\tilde{k}^{Batchelor} = k_{matrix}H1.57 \tag{4.29}$$

where the nondimensional total heat flux across a particle surface in the neighborhood of the contact, H, consists of the following terms:

$$H = H_c + \Delta H_m + log_e(\frac{k}{k_{matrix}})^2 + K - 3.9 \tag{4.30}$$

$H_c \Rightarrow$ Nondimensional heat flux at the circle of contact

$\Delta H_m \Rightarrow$ The difference between the flux across the matrix layer and the total flux between the particles in point contact

$log_e(\frac{k_s}{k_{matrix}})^2 + K - 3.9 \Rightarrow$Asymptotic solution for the non-dimensional heat flux between the particles separated by h, where $h \ll R_{ref}$

We focus our attention to the first term in equation 4.30 since we consider the case of particles at vacuum and initially at point contact. Batchelor and O'Brien's solution for the particular case becomes as the following:

$$H_c = \frac{2k(T^m - T^n)a}{\pi k_{matrix}(T^m - T^n)R_{ref}} \tag{4.31}$$

$$\tilde{k}^{Batchelor} = \frac{2k}{\pi}\frac{a}{R_{ref}}1.57 \tag{4.32}$$

$$\tilde{k}^{Batchelor} = \frac{2k}{\pi}(\frac{3}{4}F\frac{1-\nu^2}{ER_{ref}^2})^{1/3}1.57 \tag{4.33}$$

Finally we re-formulate equations 4.20, 4.28, and 4.33 in terms of the parameters that we work with in section 4.3.

$$\tilde{k}^B = k(\frac{6\sigma}{C_n})^{1/3} \tag{4.34}$$

$$\tilde{k}^C = 0.9454k(\frac{6\sigma}{C_n})^{1/3} \tag{4.35}$$

$$\tilde{k}^L = 0.8278k(\frac{6\sigma}{C_n})^{1/3} \tag{4.36}$$

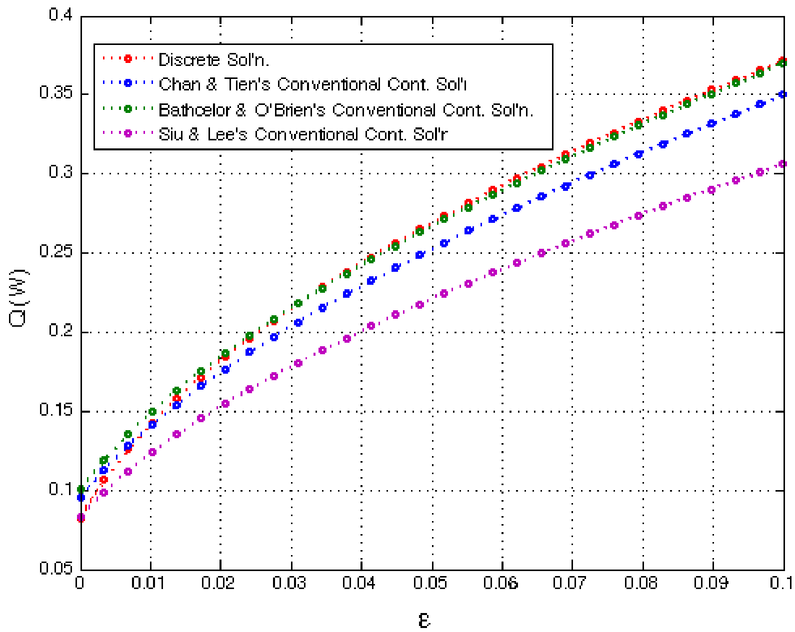

Figure 4.3: Comparison of continuum solutions adopting three different thermal contact models with discrete solution. Heat vs compaction ratio, ϵ, is evaluated at $\Delta T = 600K$.

It is known that for ordered granular packings thermal contact models provide accurate results in estimating steady and average temperature profiles [36]. Since, among the discussed thermal contact models, Batchelor and O'Brien's solution stays in remarkable agreement with the discrete case in terms of heat transferred through the chain (as seen in Figure 4.3), this solution is adopted for calculation of effective thermal conductivity in this study.

As a multi-physics problem, thermally-assisted compaction shows a significant dependence on the thermal expansion of the particles. Discrete solution based on the particle mechanics approach that also adopts the thermal contact model, carries out this dependence and the nonlinearity enhanced by thermal strains, successively. Despite the fact that effective medium approach improves the continuum solution to a large extend, it fails to capture the characteristics of the coupled physical phenomena unless the integration of thermal expansion is resolved. For this purpose we aimed to present an effective thermal expansion coefficient that depends on the applied loading conditions and particles' material properties (both thermal and mechanical).

4.6 Optimum Thermal Expansion Coefficient

Discrepancy between discrete solution and continuum solution indicates that the thermal expansion of a confined granular bed is different than the bulk thermal expansion property of its constituents. We focus our attention to the characteristics of this difference. We address the question whether there exists a certain pattern that continuum solution deviate from discrete solution, if so which material properties are dominant, and to which extend the particle size and applied mechanical load, thermal gradient play a role in the final solution.

The treatment of this problem is based on numerical simulation of two similar cases generated for discrete and continuum solution. Under particular mechanical compression load and thermal gradient, we estimate the displacement of each node in continuum analysis that corresponds to a particle center in discrete analysis. Displacement of each node under the particular thermal and mechanical loading is given by the following equation:

$$u(x) \;=\; \frac{\alpha}{2}\Big(\frac{3\tilde{\lambda}+2\tilde{\mu}}{\tilde{\lambda}+2\tilde{\mu}}\Big)\Big(\frac{T_N-T_0}{L_0}\Big)x^2-\big[\epsilon+\frac{\alpha}{2}\Big(\frac{3\tilde{\lambda}+2\tilde{\mu}}{\tilde{\lambda}+2\tilde{\mu}}\Big)(T_N-T_0)\big]x \qquad (4.37)$$

We look for the optimum thermal expansion coefficient, α_{opt}, that diminishes the residual between discrete and continuum solutions.

$$Res \;=\; u_{disc}-u_{cont} \qquad (4.38)$$

$$F \;=\; \sum_{i=1}^{N} Res^2 \qquad (4.39)$$

In these analysis we use MATLAB curve fitting toolbox to find the optimum thermal expansion coefficient for different loading conditions, particle sizes, and materials.

Case 1: We simulate a case where thermal gradient applied on the system and mechanical load is increased incrementally. Wall 1 is kept at reference temperature $T_{ref} = 293$K, and wall 2 is heated to a higher temperature incrementally, $T_N^{max} = 1493K$. Also the maximum compaction ratio is 6%, $\epsilon^{max} = 0.06$. For the discrete analysis we consider stainless steel particles which have thermal expansion coefficient of $17.3 * 10^{-6}\ 1/K$. ($R_{ref} = 0.003175$ m). Below is shown the deformation steps, on the left, and the results of the optimum thermal expansion coefficient calculated,on the right, respectively.

Deformation: $T_N - T_0$ & ϵ $\qquad\qquad$ $\alpha_{opt} * 10^{-6}$

$$\begin{pmatrix} 400\&\ 0.02 & 400\&0.04 & 400\&0.06 \\ 800\&0.02 & 800\&0.04 & 800\&0.06 \\ 1200\&0.02 & 1200\&0.04 & 1200\&0.06 \end{pmatrix} \qquad \begin{pmatrix} 11.2489 & 11.3102 & 11.3668 \\ 10.5720 & 10.6396 & 10.7115 \\ 10.5059 & 10.5724 & 10.6466 \end{pmatrix}$$

Case 2: In order to understand the effect of particle size, we compare there different cases under the same applied mechanical load and thermal gradient. Below the deformation steps applied in numerical analysis are listed, which are followed by the ratio of optimum thermal expansion coefficient to bulk thermal expansion coefficient.

Deformation: $T_N - T_0$ & ϵ

$$\begin{pmatrix} 240\&0.02 & 240\&0.04 & 240\&0.06 & 240\&0.08 & 240\&0.1 \\ 480\&0.02 & 480\&0.04 & 480\&0.06 & 480\&0.08 & 480\&0.1 \\ 720\&0.02 & 720\&0.04 & 720\&0.06 & 720\&0.08 & 720\&0.1 \\ 960\&0.02 & 960\&0.04 & 960\&0.06 & 960\&0.08 & 960\&0.1 \\ 1200\&0.02 & 1200\&0.04 & 1200\&0.06 & 1200\&0.08 & 1200\&0.1 \end{pmatrix}$$

Simualtion 1: $R_{ref} = 0.003175$ m. $T_N^{max} = 1493$ K. $\epsilon^{max} = 0.1$.

α_{opt}/α:

$$\begin{pmatrix} 0.7472 & 0.7514 & 0.7579 & 0.7635 & 0.7580 \\ 0.6340 & 0.6370 & 0.6414 & 0.6449 & 0.6477 \\ 0.6135 & 0.6173 & 0.6213 & 0.6251 & 0.6294 \\ 0.6086 & 0.6125 & 0.6164 & 0.6206 & 0.6242 \\ 0.6072 & 0.6113 & 0.6150 & 0.6190 & 0.6229 \end{pmatrix}$$

Simulation 2: $R_{ref} = 0.0015875$ m. $T_N^{max} = 1493$ K. $\epsilon^{max} = 0.1$.

α_{opt}/α:

$$\begin{pmatrix} 0.6764 & 0.6764 & 0.6801 & 0.6839 & 0.6864 \\ 0.6150 & 0.6188 & 0.6231 & 0.6269 & 0.6305 \\ 0.6078 & 0.6118 & 0.6157 & 0.6196 & 0.6237 \\ 0.6067 & 0.6105 & 0.6144 & 0.6183 & 0.6224 \\ 0.6063 & 0.6103 & 0.6143 & 0.6183 & 0.6223 \end{pmatrix}$$

Simulation 3: $R_{ref} = 0.00635$ m. $T_N^{max} = 1493$ K. $\epsilon^{max} = 0.1$.

α_{opt}/α:

$$\begin{pmatrix} 0.8741 & 0.8719 & 0.8755 & 0.8767 & 0.8800 \\ 0.6739 & 0.6785 & 0.6789 & 0.6828 & 0.6862 \\ 0.6289 & 0.6323 & 0.6361 & 0.6393 & 0.6443 \\ 0.6147 & 0.6188 & 0.6225 & 0.6262 & 0.6304 \\ 0.6098 & 0.6136 & 0.6176 & 0.6214 & 0.6253 \end{pmatrix}$$

Case 3: We investigate the effect of thermal expansion coefficient of the bulk material in determining the overall thermal expansion property of the granular system of particles. We consider simulations with two different materials of same initial radius, $R_{ref} = 0.003175$ m: (i) stainless steel particles (SS304) of $\alpha = 17.3 * 10^{-6}$ $1/K$; (ii) teflon particles of $\alpha = 250 * 10^{-6}$ $1/K$. The analysis are held for gradually increasing mechanical load and thermal gradient, $\epsilon^{max} = 0.1$ and $T_N^{max} = 1493K$, respectively.

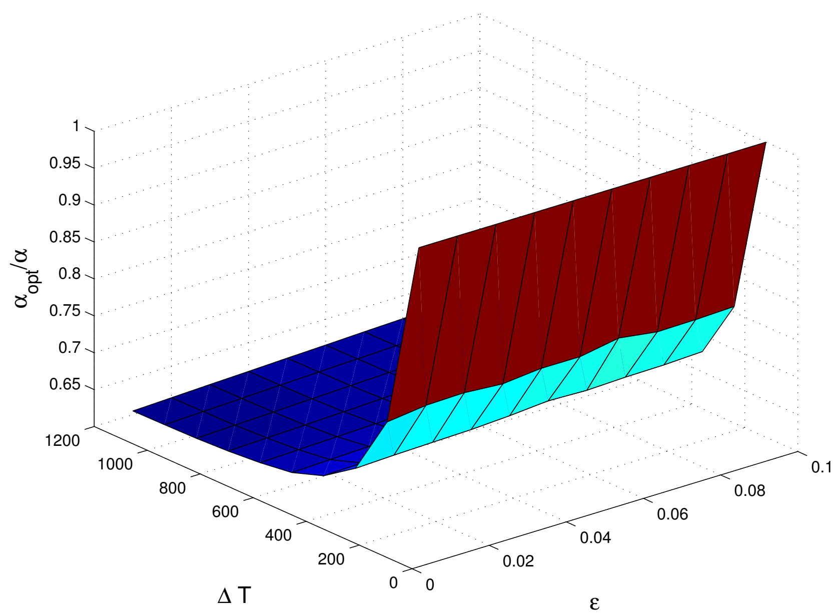

Figure 4.4: Change in optimum thermal expansion coefficient for a system of steel, SS304, particles, under various loading conditions.

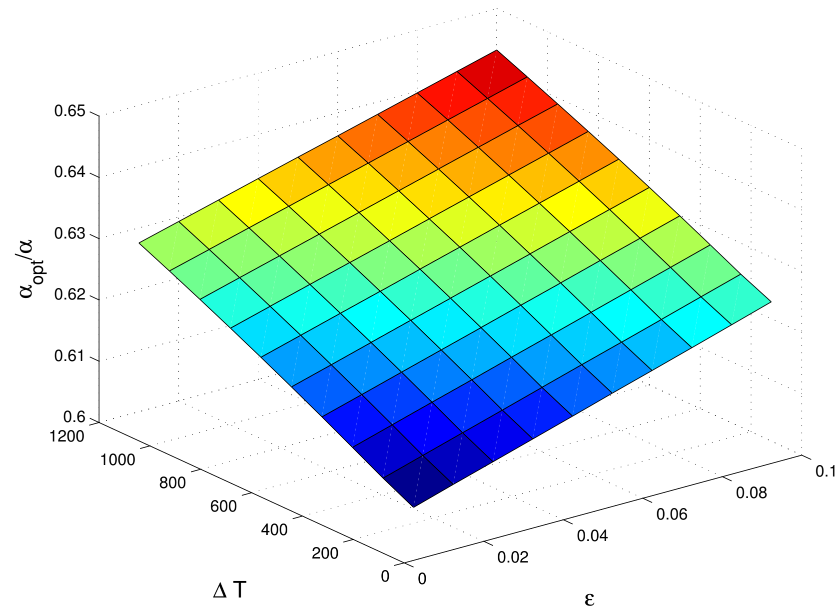

Figure 4.5: Change in optimum thermal expansion coefficient for a system of teflon particles, under various loading condition.

Simulation results show that the optimum thermal expansion coefficient of a granular system varies between 0.60 to 0.85 of the thermal expansion coefficient of the bulk material. Moreover the optimum thermal expansion expression is a function of the particle size and the applied boundary conditions. Thus as stated in effective mechanical properties, the effective thermal expansion can be expressed in terms of R_{ref}, σ, T_N.

4.7 Conculision

In chapter 4 we focus on the basic problem of one dimensional steady state thermoelasticity of continuum media, where the body forces are neglected. The solution depends linearly on elastic constants (λ, μ), thermal expansion, α, and conduction coefficient,k, compaction ratio and thermal gradient. Effective elastic moduli and thermal conductivity that are proposed in earlier studies are adopted in the continuum solution. However it is observed that the continuum solution deviates from the discrete solution particularly for cases of low mechanical load and high thermal gradient.

Taking advantage of the optimization techniques we look for the optimum value of thermal expansion that minimizes the difference between the discrete solution. For a range of deformation conditions, it is concluded that effective thermal expansion of a granular assembly varies between 0.60-0.80 of the bulk material property. Moreover it is shown that effective thermal expansion formalism is a function of applied boundary conditions, similar to effective elastic moduli.

Chapter 5

Derivation of Effective Thermal Expansion Coefficient

5.1 Introduction

Regarding the subject of one dimensional thermoelasticity of continuum media, we formulate the Cauchy's stress as combination of classical linear elasticity theory and simple linear thermal expansion. In chapter 4 we improved the continuum solution by incorporating the effective medium theory, which aims to express the elastic contacts, λ, μ , and thermal conductivity, k, in terms of bulk properties of the individual particles and loading conditions. Although the improved continuum solution achieves to explains the non-linearity seen in discrete solution, we notice that the lack of effective thermal expansion plays a significant role in the diverging result.

The treatment of this problem is based upon derivation of an effective thermal expansion formalism that can account for the physics of particle rearrangement and temperature variation within the granular assembly.

$$\sigma \quad = \quad -(\tilde{\lambda} + \tilde{\mu})\epsilon + \tilde{\alpha}(3\tilde{\lambda} + 2\tilde{\mu})(T - T_{ref}) \qquad (5.1)$$

We define the contact force that is needed to compress two identical and elastic particles undergoes thermal expansion due to temperature increase. Starting from single contact level analysis, we derive an overall thermal expansion formalism that can replace $\tilde{\alpha}$ in equation 5.1, thereby providing a continuum solution that can explain discrete particles system under thermally-assisted compaction.

5.2 Formulation

In this section we use upper letters of mn to refer for the particle interactions at the contact of individual particles m and n, as previously used in chapters 2 and 3. Similarly superscript notation of m/n stands for the nodal interactions between the center of particle m, X^m and the center of particle n, X^n.

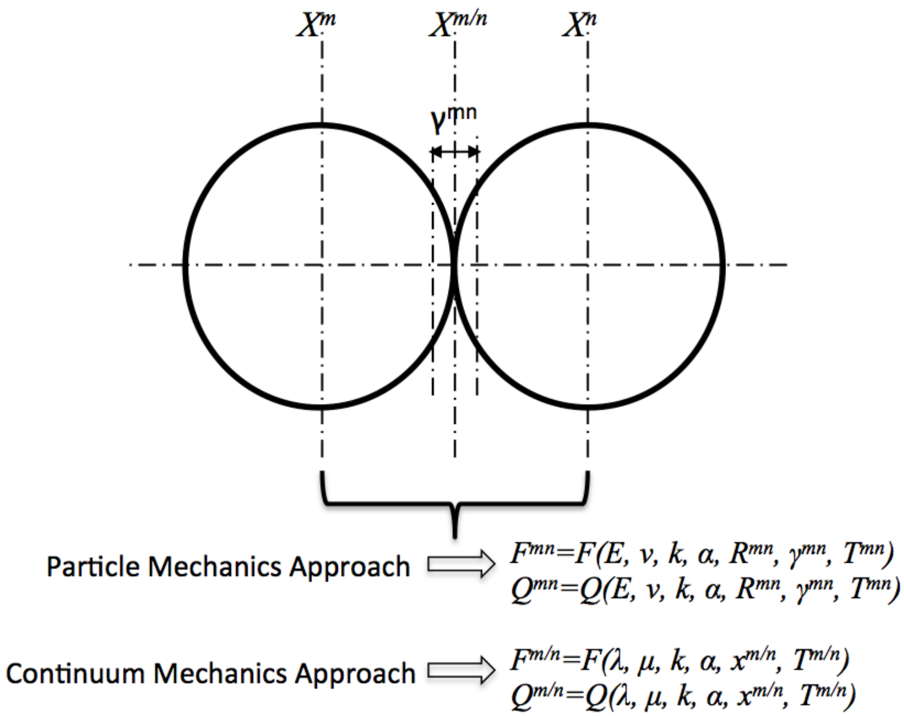

Figure 5.1: Effective thermal expansion derivation sketch.

We consider two identical spheres each of radius R_{ref} and at temperature of T_{ref} initially. Upon the applied thermal gradient, the particles experiences thermal expansion, which increases the stress at the contact. Temperature variation between the two particles is assumed to smooth such that we assume equilibrium is maintained at an average temperature which we can evaluate as:

$$T^{mn} = \frac{T^m + T^n}{2} \tag{5.2}$$

Since the particles are assumed to be identical and the difference between T^m and T^n is negligible, the contact is positioned at the middle of the contact line of these particles.

$$x^{mn} = \frac{x^m + x^n}{2} \tag{5.3}$$

Radii of particles and contact can be formulated in terms of the average temperature.

$$R^m = R^n = R_{ref}(1 + \alpha(T^{mn} - T_{ref})) \tag{5.4}$$

$$R^{mn} = \frac{R_{ref}(1 + \alpha(T^{mn} - T_{ref}))}{2} \tag{5.5}$$

The overlap between two adjacent particles positioned in a chain of particles can be expressed as the following equations.

$$\gamma^{mn} = R^m + R^n - \sqrt{(x^m - x^n)^2} \tag{5.6}$$

$$x^m = (2m - 1)R_{ref}(1 + \epsilon^{mn}) \tag{5.7}$$

$$x^n = (2(m + 1) - 1)R_{ref}(1 + \epsilon^{mn}) \tag{5.8}$$

$$|x^m - x^n| = 2R_{ref}(1 + \epsilon^{mn}) \tag{5.9}$$

Equation 5.6 becomes:

$$\gamma^{mn} = 2R_{ref}(\alpha(T^{mn} - T_{ref}) - \epsilon^{mn}) \tag{5.10}$$

where a convergent solution can be reached under the following valid constraint:

$$\alpha(T^{mn} - T_{ref}) > \epsilon^{mn} \tag{5.11}$$

As a results the contact for between identical particles of same elastic constants, E and ν can be expressed as the parameters that we also use in effective medium approach.

$$F^{mn} = \frac{4}{3}E^{mn}(R^{mn})^{1/2}(\gamma^{mn})^{3/2} \tag{5.12}$$

$$E^{mn} = \left(\frac{1 - (\nu^m)^2}{E^m} + \frac{1 - (\nu^n)^2}{E^n}\right)^{-1} \tag{5.13}$$

$$E^{mn} = \frac{E}{2(1 - \nu^2)} \tag{5.14}$$

$$C_n = 4\frac{\mu}{1 - \nu} \tag{5.15}$$

$$\mu = \frac{E}{2(1 - \nu)} \tag{5.16}$$

$$E^{mn} = \frac{C_n}{4} \tag{5.17}$$

The local force at the contact of particles m and n and the average stress are formulated as:

$$F^{mn} = \frac{4}{3}\frac{C_n}{4}\left(\frac{R_{ref}(1 + \alpha(T^{mn} - T_{ref}))}{2}\right)^{1/2}\left(2R_{ref}(-\epsilon^{mn} + \alpha(T^{mn} - T_{ref}))\right)^{3/2} \tag{5.18}$$

$$\sigma^{mn} = \frac{C_n}{6}(1 + \alpha(T^{mn} - T_{ref}))^{1/2}(-\epsilon^{mn} + \alpha(T^{mn} - T_{ref}))^{3/2} \tag{5.19}$$

In equation 5.19, ϵ^{mn} and T^{mn} is dependent on position of the contact, x^{mn}.

Similar methodology can be traced to obtain a consistent solution from the perspective of continuum mechanics approach. The stress at a nodal point which stays in the mid-way of x^m and x^n, is a function of the effective properties and compaction ratio at $x^{m/n}$ and temperature increase, $T^{m/n}$.

$$\sigma^{m/n} = \sigma^{m/n}(\epsilon^{m/n}, T^{m/n}, \tilde{\lambda}, \tilde{\mu}, \tilde{\alpha}) \tag{5.20}$$

where

$$T^{m/n} = \frac{T^m + T^n}{2} \tag{5.21}$$

$$x^{m/n} = \frac{x^m + x^n}{2} \tag{5.22}$$

As also shown in chapter 4, the stress at continuum solution can be expressed as:

$$\sigma^{m/n} = -(\tilde{\lambda} + \tilde{\mu})\epsilon^{m/n} + \tilde{\alpha}(3\tilde{\lambda} + 2\tilde{\mu})(T^{m/n} - T_{ref}) \tag{5.23}$$

$$\sigma^{m/n} = \phi_s Z C_n \Big(\frac{3}{32\pi^2}\Big)^{1/2} \Big(|-\epsilon^{m/n}\frac{3}{5} - \tilde{\alpha}(\frac{T^{m/n} + T_{ref}}{2} - T_{ref})|\Big)^{3/2} \tag{5.24}$$

We are looking for a definition for stress in continuum solution which is equal to the expression derived in discrete solution. Therefore equations 5.19 and 5.24 are equal where x^{mn}, ϵ^{mn} and T^{mn} corresponds to $x^{m/n}$, $\epsilon^{m/n}$ and $T^{m/n}$, respectively. By using this equality we can express $\tilde{\alpha}$ in terms of stress σ^{mn}, T^{mn}, bulk properties of the particles, and packing fraction.

$$\tilde{\alpha} = \alpha\frac{3}{5} + \frac{4\pi}{T^{m/n} - T_{ref}}\Big(\frac{\sigma}{C_n}\Big)^{2/3}\Big[\Big(\frac{1}{\phi_s Z(6\pi)^{1/2}}\Big)^{2/3} - \frac{3}{20\pi}\Big(\frac{6}{(1 + \alpha(T^{m/n} - T_{ref}))^{1/2}}\Big)^{2/3}\Big] \tag{5.25}$$

Numerical analysis on investigation of the asymptotic limits of this formalism, provides an accurate approximation, which is dependent on the applied load σ and temperature T.

$$\tilde{\alpha} = \frac{3}{5}\alpha + \frac{4\pi}{T - T_{ref}}\Big(\frac{\sigma}{C_n \phi_s Z(6\pi)^{1/2}}\Big)^{2/3}\Big[1 - \Big(\frac{1}{1 - \alpha(T - Tref)}\Big)^{1/3}\Big] \tag{5.26}$$

The overall effect of the two terms contributing eq. 5.26 is summarized in figure 5.2. Continuum solution is generated for the following two cases: (i) with the first order approximation of eq. 5.26, (ii) the full proposed formula. It is concluded that the first order approximation is significantly dominant in the continuum solution.

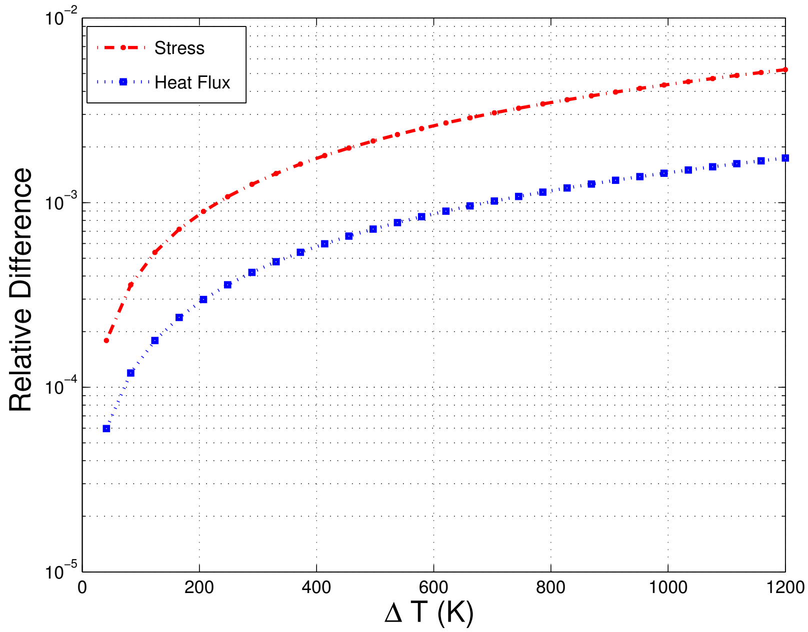

Figure 5.2: Two cases of continuum solution are simulated with: (i) first order approximation, and (ii) full version of the proposed thermal expansion coefficient. Relative difference between these two solutions are shown in terms of stress and heat (results are evaluated at low compaction ratio, $\epsilon = 0.005$).

5.3 An Application Of The Proposed Effective Thermal Expansion Formula

Similar to the system discussed in discrete analysis, a one dimensional continuum system is modeled which is under uniaxial compressive stress of σ and thermal gradient of $T_N - T_0$. In addition to the effective material properties developed in effective medium approach, the proposed effective thermal expansion formalism is implemented in solution of the coupled system of equations.

The effective properties are listed as :

$$\tilde{\lambda} + 2\tilde{\mu} = \frac{3}{20\pi} C_n (\phi_s Z)^{2/3} \left(\frac{6\pi\sigma}{C_n}\right)^{1/3} \tag{5.27}$$

$$3\tilde{\lambda} + 2\tilde{\mu} = \frac{1}{4\pi} C_n (\phi_s Z)^{2/3} \left(\frac{6\pi\sigma}{C_n}\right)^{1/3} \tag{5.28}$$

$$\tilde{k} = \frac{2k}{\pi} \left(\frac{6\sigma}{C_n}\right)^{1/3} 1.57 \tag{5.29}$$

$$\tilde{\alpha} = \frac{3}{5}\alpha + \frac{4\pi}{T - T_{ref}} \left(\frac{\sigma}{C_n \phi_s Z (6\pi)^{1/2}}\right)^{2/3} \left[1 - \left(\frac{1}{1 - \alpha(T - Tref)}\right)^{1/3}\right] \tag{5.30}$$

$$\begin{aligned}
\frac{\partial u}{\partial x} &= \tilde{\alpha}(\frac{3\tilde{\lambda}+2\tilde{\mu}}{\tilde{\lambda}+2\tilde{\mu}})(T-T_{ref}) - \frac{\sigma}{\tilde{\lambda}+2\tilde{\mu}} && (5.31)\\
\frac{\partial u}{\partial x} &= \alpha(T-T_{ref}) + \frac{20\pi}{3}(\frac{\sigma}{C_n\phi_s Z(6\pi)^{1/2}})^{2/3}(\frac{1}{1-\alpha(T-Tref)})^{1/3} && (5.32)\\
u(x) &= \int \frac{\partial u}{\partial x} + C_1\\
C_1 &= -[\int \frac{\partial u}{\partial x}]_{x=0}\\
\epsilon L_0 &= [\int \frac{\partial u}{\partial x}]_{x=L_0} + C_1
\end{aligned}$$

In this regard analytical solution for the system of equations given in 4.1, and 4.2 are the following :

$$\begin{aligned}
T(x) &= \frac{(T_N-T_0)\,x}{L_0} + (T_0 - T_{ref}) && (5.33)\\
u(x) &= \alpha x\left(\frac{(T_N-T_0)\,x}{2L_0} + (T_0-T_{ref})\right) - \frac{10\pi L_0}{(T_N-T_0)}\left(\frac{\sigma}{C_n\phi_s Z(6\pi)^{1/2}}\right)^{2/3}\ldots\\
&\left[-(1-\alpha\,(T_0-T_{ref}))^{2/3} + \left(1-\alpha(\frac{(T_N-T_0)\,x}{L_0} + (T_0-T_{ref})\right)^{2/3}\right]
\end{aligned}$$

$$\sigma = C_n\phi_s Z(6\pi)^{1/2}\left(\frac{\alpha(\alpha\,(T_N-T_0)^2 - 2\epsilon\,(T_N-T_0) + 2\alpha\,(T_N-T_0)\,(T_0-T_{ref}))}{20\pi\,(1-\alpha(T_N-T_{ref}))^{2/3} - 20\pi(1-\alpha\,(T_0-T_{ref}))^{2/3}}\right)^{3/2} \quad (5.34)$$

As expected in the limit of zero thermal gradient, the derived solution for stress, eq. 5.34, approaches to the solution offered by conventional continuum mechanics where also no thermal gradient is considered.

$$\begin{aligned}
\lim_{\alpha\to 0}\sigma &= \sigma_{EMT}\\
\lim_{T_N-T_0\to 0}\sigma &= \sigma_{EMT}
\end{aligned}$$

5.4 Comparison of Improved Continuum Solution with Discrete Solution

Based upon the highlighted characteristics of discrete particulate system analysis, our aim is to compare the accuracy of continuum scale models from the point of convergency to the discrete solution. In this regard the required stress to compact the linear system of particles and heat to be transferred through the chain are evaluated for various compaction ratios and thermal loading conditions. Conventional continuum solution refers to the traditional thermo-mechanical model which integrates effective mechanical properties obtained from Effective Medium Approach and effective thermal conductivity as derived in Batchelor and O'Brien's study [7] ($\tilde{\mu}$, $\tilde{\nu}$, $\tilde{k}$). Improved continuum solution is the proposed solution in this paper through sections 5.2, and 5.3 ($\tilde{\mu}$, $\tilde{\nu}$, $\tilde{k}$, $\tilde{\alpha}$).

At constant thermal loads Hertzian stress is plotted with respect to the compaction ratio in figures 5.3 and 5.4. As it is seen even for small thermal loads, continuum models lacks predicting the required values for stress. Furthermore as applied thermal gradient is increased, this discrepancy between discrete and continuum models ascends. However integration of effective thermal expansion coefficient clearly improves the continuum system analysis.

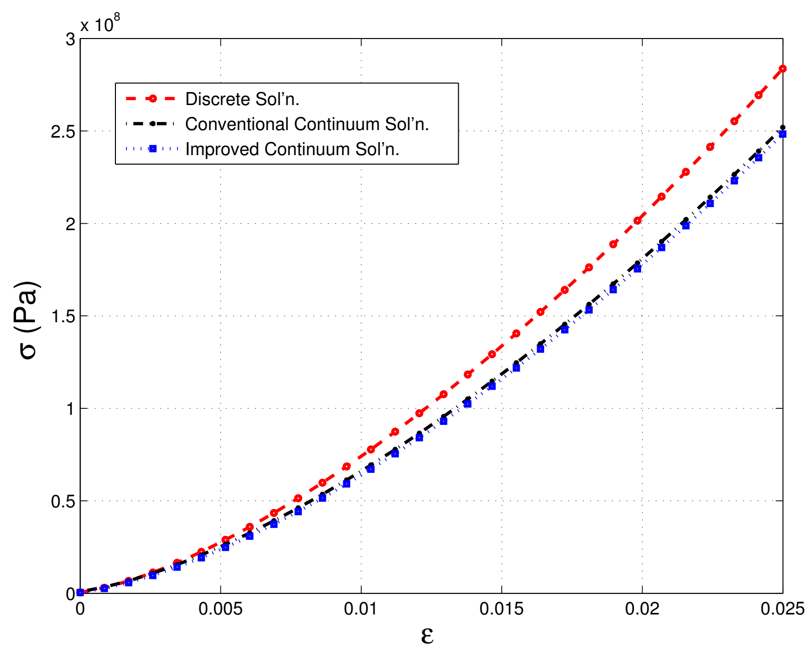

Figure 5.3: Comparison of continuum and particle mechanics models in terms of stress vs compaction ratio, ϵ, under the particular thermal gradient imposed between the boundary walls, $\Delta T = 40K$.

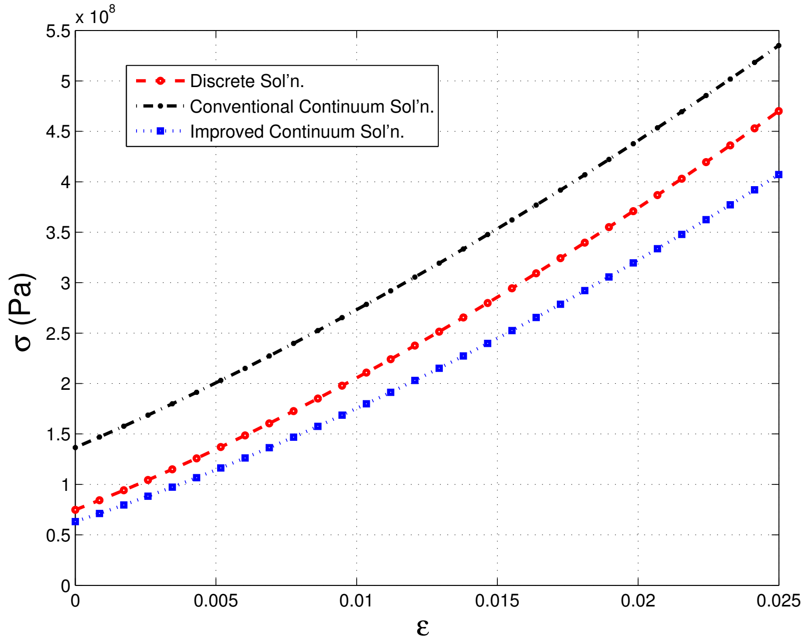

Figure 5.4: Comparison of continuum and particle mechanics models in terms of stress vs compaction ratio, ϵ, under the particular thermal gradient imposed between the boundary walls, $\Delta T = 1200K$.

Previously shown in discrete system analysis that nonlinearity plays a significant role, specifically in low mechanical and high thermal load condition. In the case of compacting the system of particles by 0.5% of the total length, conventional continuum solution overestimates the required stress to 1.5 times larger than the discrete solution (figure 5.5) . This difference is significantly decreased by improved continuum solution. On the other hand under larger compressive load both continuum solutions shows 10% deviation from the discrete model when there is no thermal gradient applied on the system. This is due to the fact that the present effective mechanical properties and thermal conductivity brings particular limitation to the problem.

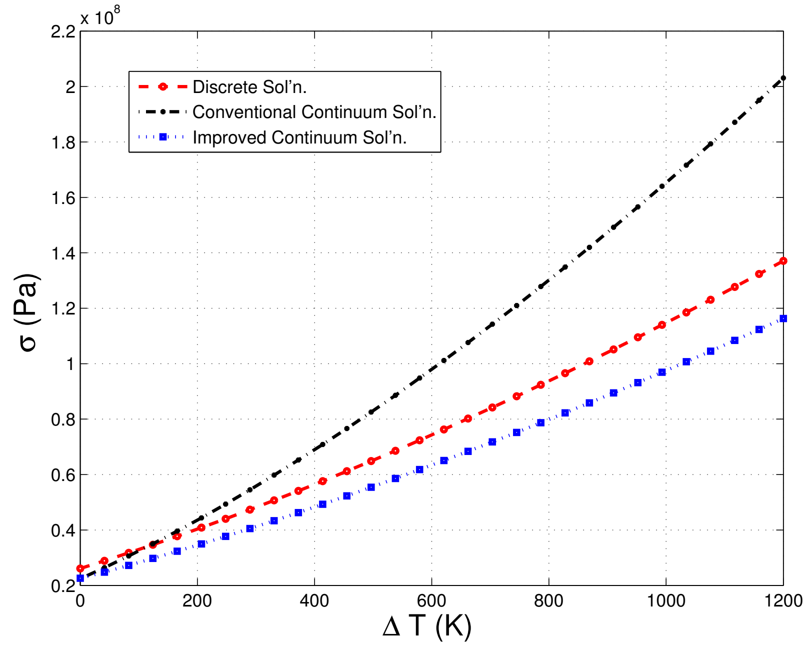

Figure 5.5: Comparison of continuum and particle mechanics models in terms of stress vs thermal gradient, ΔT, for the compaction ratio of $\epsilon = 0.005$.

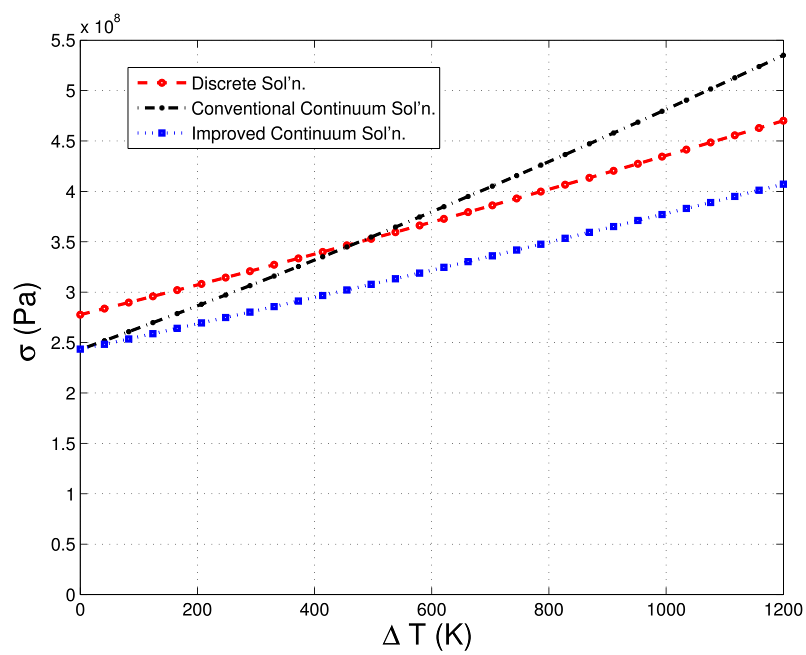

Figure 5.6: Comparison of continuum and particle mechanics models in terms of stress vs thermal gradient, ΔT, for the compaction ratio of $\epsilon = 0.025$.

Heat transferred within the particle chain is dependent on the current radius and the temperature of particles that are coming into contact. In general the continuum solutions that are addressed in this study provide decent accuracy with the discrete system analysis under constant compaction ratios (figs. 5.8).

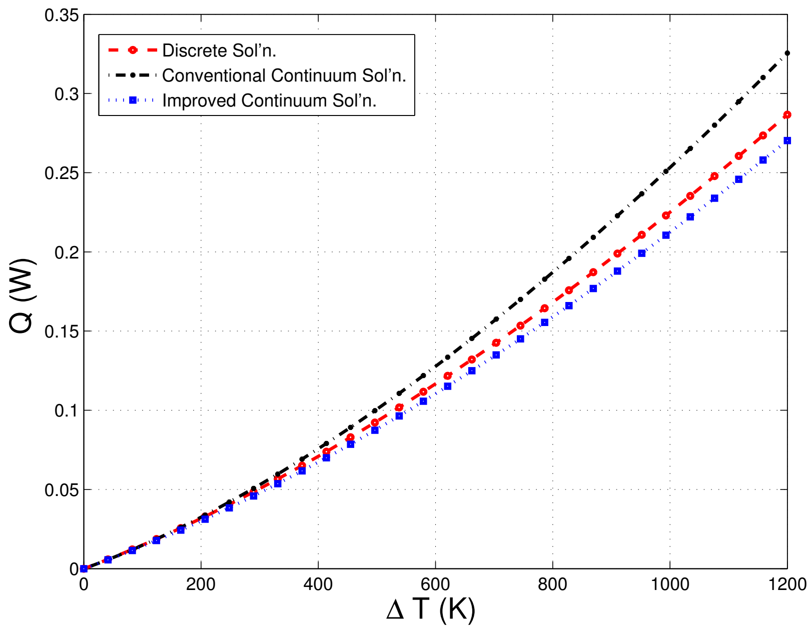

Figure 5.7: Comparison of continuum and particle mechanics models in terms of heat vs thermal gradient, ΔT, evaluated at the compaction ratios of $\epsilon = 0.005$.

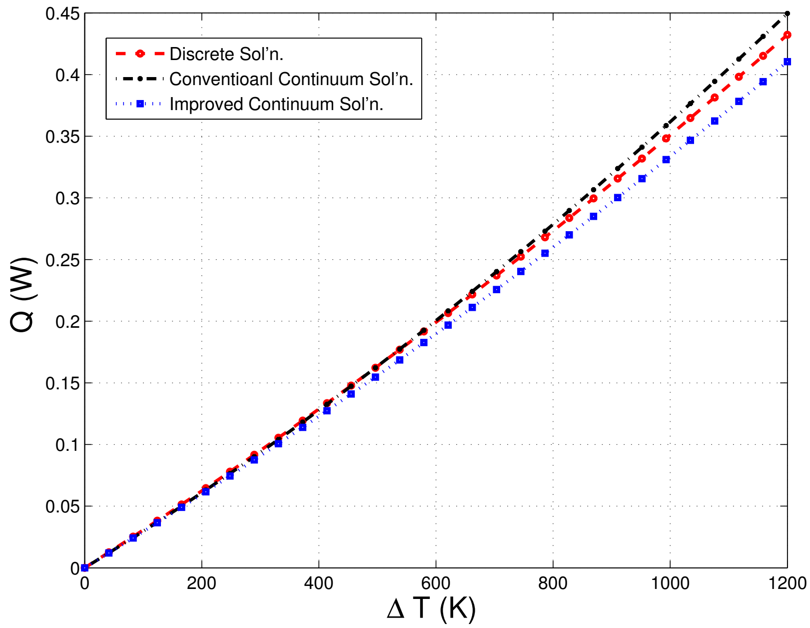

Figure 5.8: Comparison of continuum and particle mechanics models in terms of heat vs thermal gradient, ΔT, evaluated at the compaction ratios of $\epsilon = 0.025$.

However, once heat transferred with respect to compaction ratio at constant thermal loads is traced, the deviation from the discrete solution is noticed. The thermo-mechancially coupled system imposes a dependency such that the overestimation and/or underestimation of stress results in diversification in calculated temperature profiles and contact radii. Figures 5.9 and 5.10 reflect this correlation for two limiting cases.

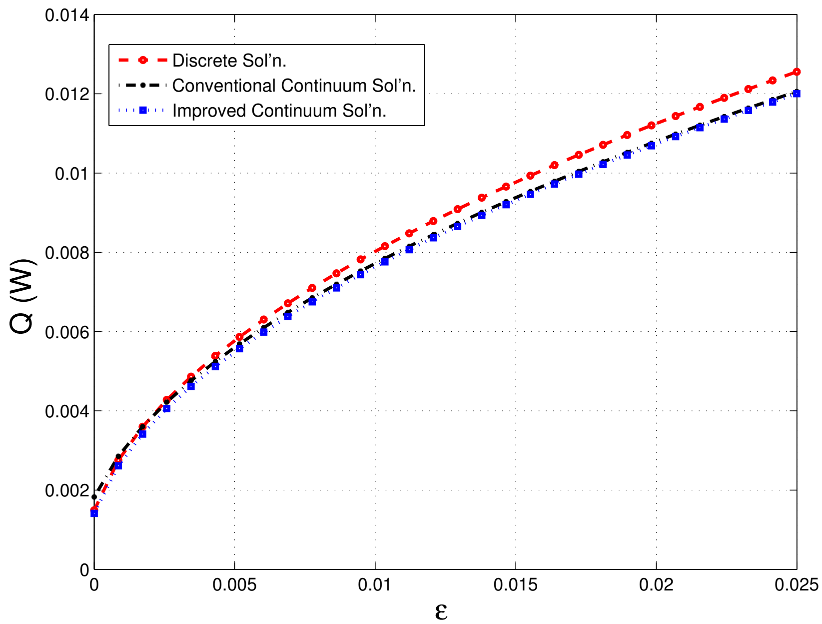

Figure 5.9: Comparison of continuum and particle mechanics models in terms of heat vs compaction ratio, ϵ, evaluated for the thermal gradient imposed at the boundary walls, $\Delta T = 40K$.

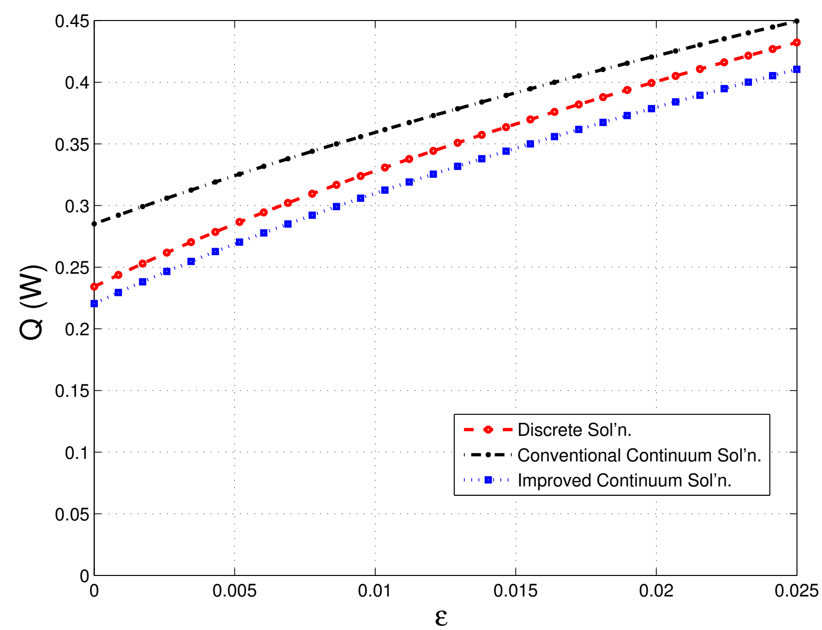

Figure 5.10: Comparison of continuum and particle mechanics models in terms of heat vs compaction ratio, ϵ, evaluated for the thermal gradient imposed at the boundary walls, $\Delta T = 1200K$.

In order to test the overall performance of the continuum solutions, we plotted the displacement of particular points with respect to their initial position. In the following figures 5.11 and 5.12, the node in contact with the non-moving boundary is positioned at $x = 0$. It is worth stating that the equilibrium of thermal expansion due to thermal gradient applied on the system and the change in position due to compaction results in nonlinear distribution of displacements at each individual node. In addition to effective medium approach, taking into consideration the effective thermal expansion of particulate bed introduces a significant improvement in continuum analysis in terms of accuracy.

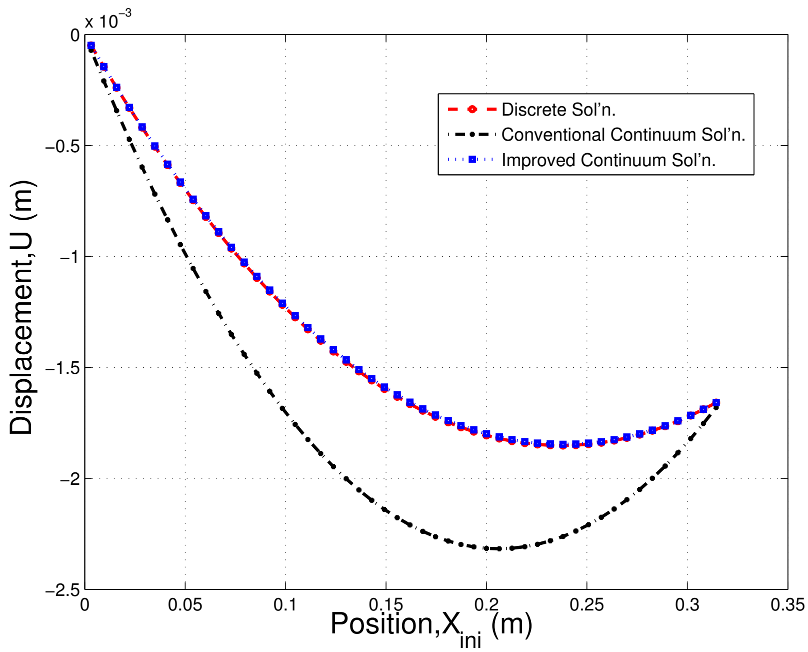

Figure 5.11: Tracking each particles displacement under the boundary conditions of $T_N - T_0 = 1200K$ and $\epsilon = 0.005$.

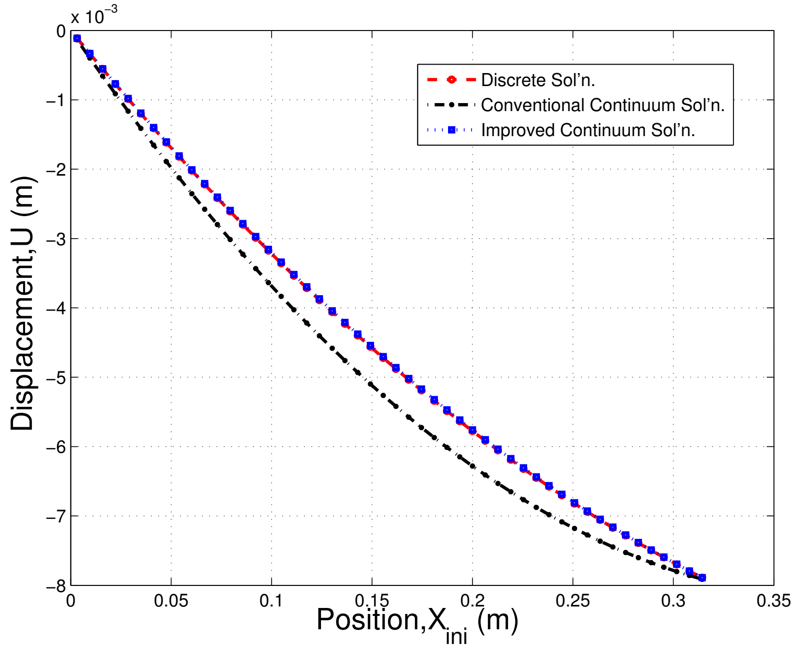

Figure 5.12: Tracking each particles displacement under the boundary conditions of $T_N - T_0 = 1200K$ and $\epsilon = 0.025$.

The discrepancy between the continuum and the discrete system analysis also points out the importance of the effective thermal expansion coefficient in the thermo-mechanically coupled systems. In this regard relative difference between the above mentioned solutions for a range of loading conditions are evaluated. Relative difference is basically the ratio of average difference between discrete and continuum solutions over discrete solution.

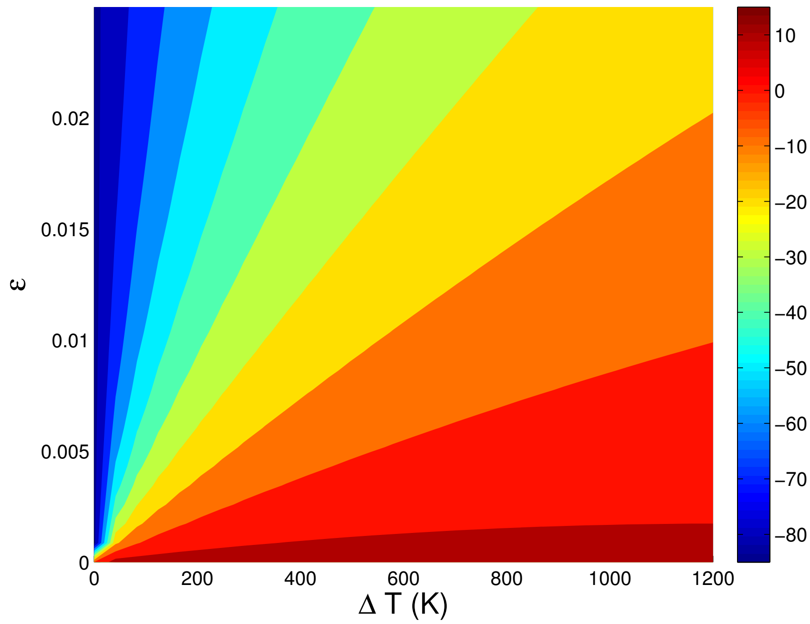

Figure 5.13: Relative difference between discrete solution and conventional continuum solution in terms of stress evaluation under various loading conditions.

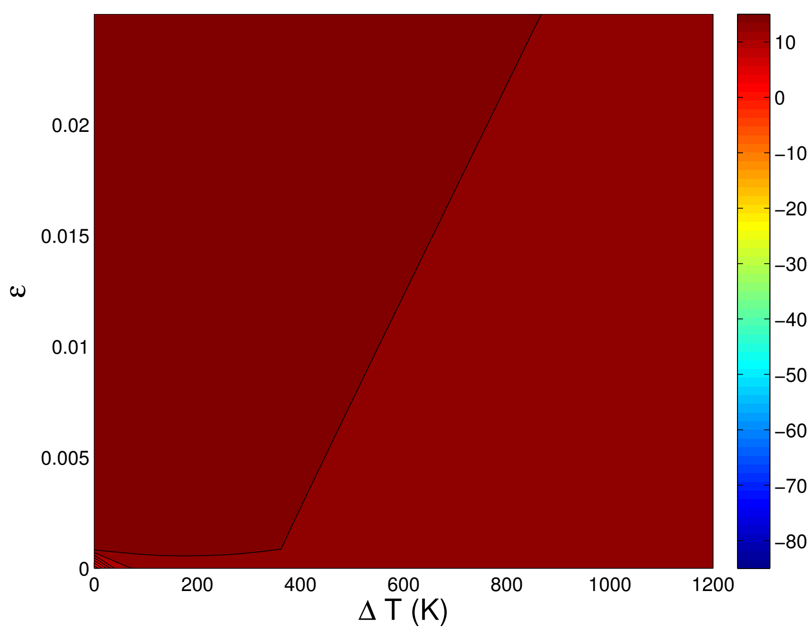

Figure 5.14: Relative difference between discrete solution and improved continuum solution in terms of stress evaluation under various loading conditions.

Figure 5.13 shows that conventional continuum solution differs up to 80% with respect to discrete solution in terms of stress, whereas this is only up to 15% for the improved continuum solution in this study as seen the figure 5.14 .

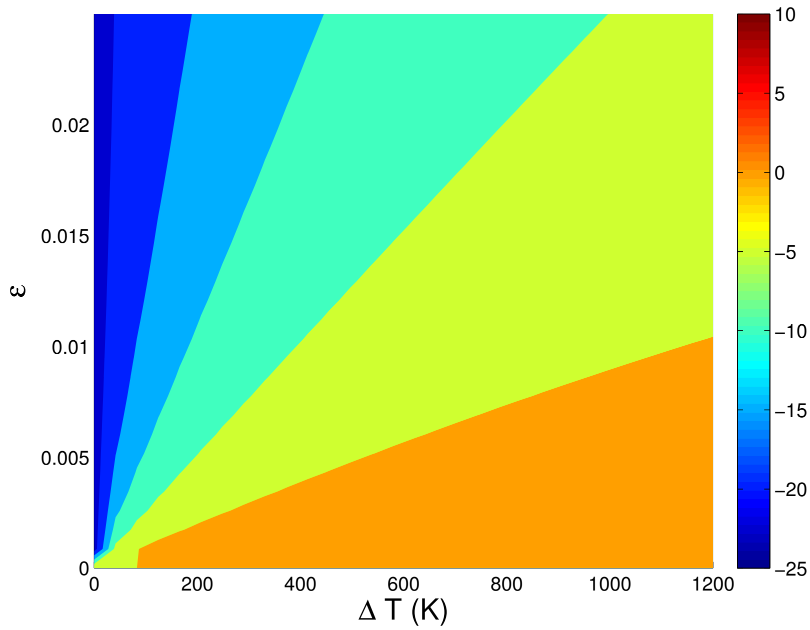

Figure 5.15: Relative difference between discrete solution and conventional continuum solution in terms of heat flux evaluation under various loading conditions.

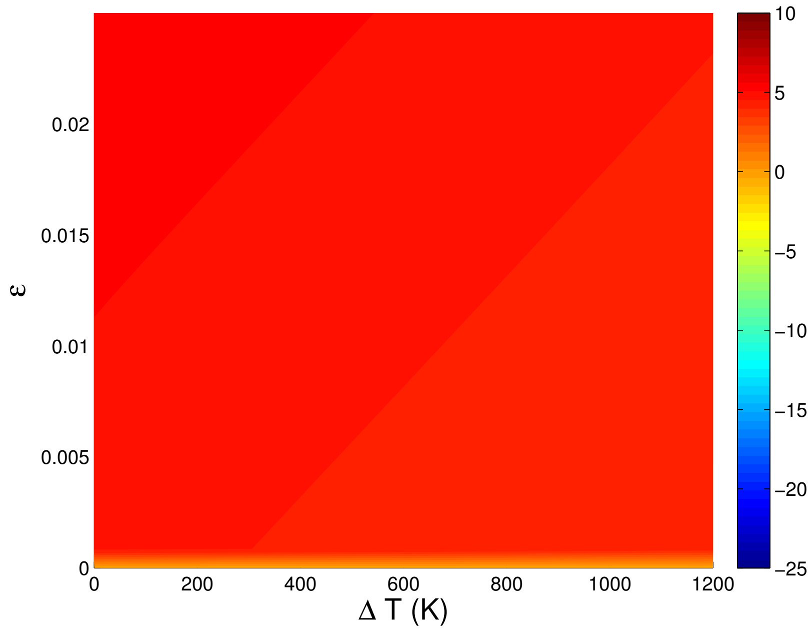

Figure 5.16: Relative difference between discrete solution and improved continuum solution in terms of heat flux evaluation under various loading conditions.

Similarly there is remarkable accuracy achieved in improved continuum solution in terms of heat transferred. As shown in figures 5.15 and 5.16 the maximum deviation from the discrete solution is minimized four times less in improved continuum solution.

To sum up, it is proved that the proposed continuum model predicts the required stress and heat transferred within 10% and 5% accuracy, respectively. This derivation enhances the conventional use of continuum-scale analysis to simulate the discrete particulate systems that are under thermally-assisted compaction. The implementation of the newly proposed formula for determining the effective thermal expansion of granular beds is crucial in acquiring more realistic results.

5.5 Conclusions

In this section we consider a simple thermally-assisted compaction setup, where the system is under the effect of uniaxial stress of σ, and a thermal load of $T_N - T_0$. We investigate the prescribed coupled system in terms of particle mechanics approach that we elucidate in chapter 2, and conventional continuum mechanics approach for a incremental temperature increase at the neighborhood of two adjacent particles.

From theoretical point of view, we claim that the stress evaluation obtained in both solutions remain equal. This allows us to express the effective thermal expansion formalism in terms of bulk properties of the particles, and loading conditions.

We implement the proposed formalism to account for the thermal expansion effect on the overall solution of stress and heat flux generated in continuum solution. The results show that significant improved is achieved in expressing the discrete system characteristics in continuum approach by our proposed expression.

It is also clear that the dominant term in effective thermal expansion expression, $(3\alpha)/5$, provides a good approximation that can be easily implemented in numerical analysis based on conventional continuum approach.

Similar to the well-established paradigm of micromechanical modeling, meticulous implementation of the proposed effective thermal expansion formalism renders truly predictive models of the mechanical and thermal behavior of the granular assembly.

Chapter 6

2D Numerical Experiments

6.1 Introduction

Understanding the fundamental multi-physics behind the thermo-mechanically coupled deformation of granular systems and its projections in macroscopic scale, provide the essentials to fabricate particulate assemblies with specific functionalities. The long-standing problem of remarkable reduction in raw material resources and the increasing costs empower the prevalence of particulate materials in vast array of industrial applications. As a consequence the course of manufacturing changed from materials for design to design for materials.

It is worth noting that the rapid progress being made in atomic force microscopy and particle characterization techniques provides the opportunity of monitoring inter-particle connections experimentally. Recent improvements in additive manufacturing enhanced the wide range of particulate materials applications. It is no longer a dream to seek for science integrated technology applications where particle interactions are engineered to fabricate consolidated assemblies with desired macroscopic mechanical, thermal, and electrical properties. Concerning a vast majority of materials and manufacturing techniques, however it remains inefficient and impractical to test experimentally for individual design, with the aim of describing the bulk characteristics of the the compacted product.

A proper estimate of the mechanical strength, thermal and electrical conductivity of a compacted solid is contingent upon the knowledge of the amount of inter-particle contact area created during the deformation stage of the compression. In this regard discrete thermal element methods has been used by different groups to understand the influence of thermo-mechanical coupling. Majority of the papers, estimating the overall characteristics of there confined granular beds, relies on statistical mechanics approaches where mainly mean field theory and ensemble averaging techniques are widely used.

It is the purpose of this chapter to suggest that insight into the nature of thermo-mechanical interaction which determines the microstructure of the confined granular materials. Particle mechanics approach, which is introduced in Chapter 2, is extended to investigate the two dimensional particle arrangement of packed beds compressed by heated boundary walls. We trace the evaluation of contact networks at each quasi-static equilibrium state and address the intriguing question of how the force chains are related to heat chains. We also consider the effect of loading conditions, and the role of particle size and distributions on the final microstructure.

6.2 A Survey of Related Literature

Recent experimental studies elucidate the long-standing problems in collective behavior of granular assemblies and become an inspiration to the areas of theoretical physics, applied mathematics, and engineering fields. One of these ground breaking studies is conducted by Chen and his co-workers on packing particulate assemblies by thermal cycling that unwinds the nature of grain packing under the sole effect of thermal loading without any mechanical energy input [11]. They investigated the influence of thermal cycling on packing fraction. As a results they managed to explain a well known phenomena of packing re-arrangement due to temperature changes and the changes in stress state of a granular pile through a serious of temperature increase and decrease applied on a pile of glass beads in a plastic container.

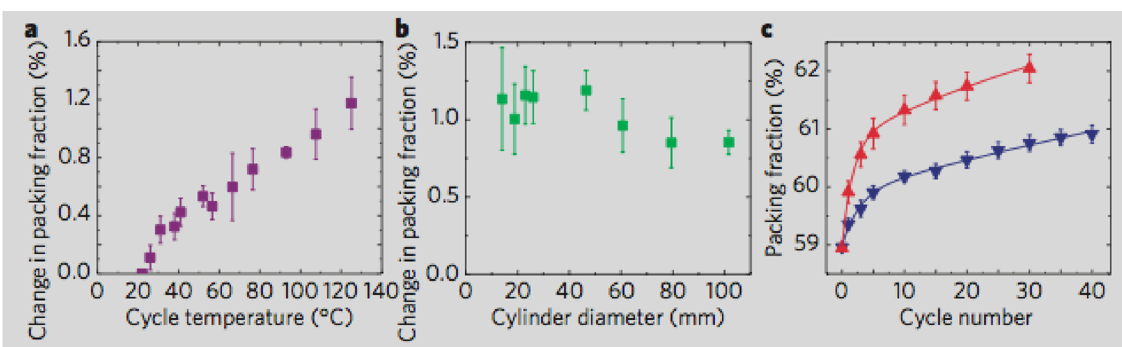

Figure 6.1: Change in packing fraction with thermal cycling for glass spheres in a plastic cylinder, adopted from Chen et al. [2006]. Change in packing fraction as, **(a)** a function of cycle temperature from room temperature for a single cycle, **(b)** a function of cylinder diameter for a single cycle . **(c)** Change in packing fraction after multiple thermal cycles.

Chen et al. showed that the difference between the thermal expansion of the glass beads and of the container, induces thermal stress, which can be characterized as an alternative to mechanical agitation for altering grain packing [11].

Moreover regarding the study of static granular systems, a very common geometry, namely silo, is an unique example where small thermal perturbations can lead to giant stress fluctuations. Experiments on the weight carrying elements in a system of large number of loosely packed particles contained in a box, shows that the apparent weight on the bottom and side walls can change drastically under a variation of temperature of a few degrees [39]. These giant stress fluctuations is associated with the extreme sensitivity of stress paths to small perturbations, and recalled as the result of arch formations in silos [12].

One of the fascinating properties of granular materials is the organization of contact networks, thereby formation of highly heterogeneous distribution of force network that determine the macroscopic strength characteristics [43, 61]. Upon the application of compaction forces, special structural arrangements arose to serve the purpose of supporting most of the external load, leaving the other particles unloaded or less loaded. These force chains can be treated as the load bridges, which usually stand several times larger forces than the rest of the system. Surprisingly these structural elements constitute only a limited portion of all contacts [1]. Antony names these chains as ‘granular brains’, and memory networks, which are influenced by the loading conditions and the initial packing arrangement of the structure [1].

In various studies it has been postulated that stress chains are responsible for localized fracture and hot spot formations, which causes unexpected failure of the confined material [23]. For the cases of compaction where the process may trigger chemical wave front propagation or phase transition due to the instant change of temperature or surplus pressure, it is important to control the process to prevent the undesired formations. Widely used traditional material examination methods, such as destructive testing and post process characterization, provide very poor or inaccurate information in the prospect of revealing the mechanisms of failure. For instance, stress bridges occurred at the early stage of loading event increase the stress concentrations leading to crystal fracture, whereas a later formation of stress chains can only be responsible for viscoelastic shear deformation [23].

After clarifying the critical issues of experimentation, it is useful to mention some of the mostly used techniques that are widely accepted in the study of force measurements in granular systems. One of the mostly used technique is stress-induced birefringence experiments that takes advantage of the photo elasticity property of some materials. A plane stress is induced to deform a set of thin discs of particles, where some of them cause light to propagate through them at different speeds along two perpendicular axes. Using different polarization techniques and comparing the birefringence patterns, statistical information on particle's characterization and measurements on contact forces are obtained.

Majmudar and Behringer conducted a high-impact study on contact force measurements, in which they pointed out the stress-induced anisotropy in granular materials [43]. Their uniaxial and biaxial compaction experiments reveals that sheared systems have long-range correlations in the direction of force chains, whereas isotropically compressed systems have short-range correlations. Uniaxialy compressed systems, which are highly under the effect of sheared forces, show two distinct aspects of anisotropy: (i) solely a geometric effect, that is the loading conditions induce anisotropy in the contact network, (ii) mechanical effect, that is they develop uneven distribution of force chain networks and alter stress distribution in the system [43]. Figure 6.2 briefly describes their experiment set-up and results of the experiment [43].

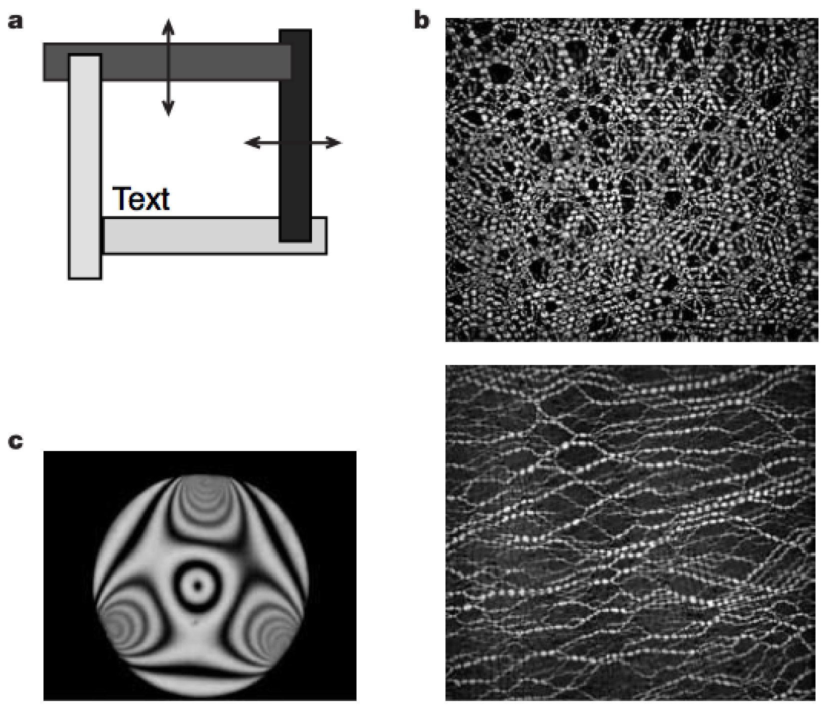

Figure 6.2: Contact force measurements using photoelastic techniques, adopted from Majmudar and Behringer [2005]. **(a)** Schematic diagram of the biaxial test cell, **(b)** Typical system size images for an isotropically compressed state (top) and a sheared state (bottom), **(c)** Observed stress pattern for a single disk.

The second mostly used experimentation technique is carbon paper method, which is based on the direct measurement of the contact area traces left on special paper placed at the bottom of a uniaxialy compacted particles' assembly. By using this method, Mueth et al. proposes an empirical functional form that estimates the probability of force distributions at bottom, top and side walls [50]. Lovoll et al. extended this method to discover the relationship between particle bed height and weight distribution [42]. They placed a probe in the assembly to detect the effect of perturbation on distribution of forces. Tsoungui et al. uses a similar method to determine the interparticle contact forces [67]. In this study they analyze the two dimensional compacted bed with a limited number of particles. The basic idea in this study is that they color the compacted thin disks by red crushed chalk, and when the particles are separated smoothly, the white areas designates the contact areas. By using calibration tests, they provide an estimate of the contact force, thereby contact force distribution.

There exists significant number of studies that aims to understand the force distributions, and probability of arch formations, based on the tools provided by statistical mechanics. The well-known paper in this approach is by Liu et al. who propose a model to explain the force fluctuations in bead packs, and name it as 'q-model' [38]. In this model, they assume that the dominant physical mechanism that leads to inhomogeous force chains is the unequal distribution of weights on the beads supporting a given grain. They generate a stochastic equation to estimate the force carried by each bead which is at a particular depth and in contact with neighboring beads. The key concept in their model is the 'q' fraction, which is a random variable and accounts for the generic randomness of the disordered granular system. Liu et al. verifies the accuracy of their model by comparing experimental observations and numerical results [38]. Coppersmith and her colleagues explain the methodology used developing q-model in details [13]. They solve the system of equations for a countable infinitely number set of q distributions and present mean field results compares their q-model estimation for force distribution with molecular dynamics simulations generated for a set of 1024 particles, where they observe quite good agreement [13]. Both studies agrees on the fact that very strong contact forces within a granular assembly are exponentially rare.

For the purpose of defining the global description of a granular system, Radjai and Roux focus on the frictional motion of a linear array of parallel identical cylinders on a plane where all interparticle and particle-plane contacts are described by a Coulomb friction law [55]. Based on this model Radjai et al. develop contact dynamics simulations to study the statistical distribution of contact forces inside a confined packing of circular rigid disks with solid friction [54]. In this study they compared the effect of different particle size beds with varying number of particles. The normal force distributions at the particle contacts agrees well with the q-model results. Concerning the statistical homogeneity of the sample bed, they conclude that despite local force fluctuations, the linear scale of homogeneity is reached when conduction computational studies at a sample size of a few tens of particle diameters [54]. This hypothesis is also proved in earlier studies which take account for the effect of spatial patterns of motion during compaction of spherical particles [56, 21].

Beside these mathematical models which relies on fundamentals of statistical mechanics, there is a well-known methodology to estimate the macroscopic characteristics of compacted granular materials by the knowledge obtained through understanding the particle interactions. Starting from the early work of Cundall and Strack [15], significant number of studies are intended to provide a discrete thermal element formulation of the coupled problem. Vargas and McCarthy approached this problem to solve for the heat conduction through the confined granular system [68]. By their thermal particle dynamics model, they are capable of tracking the formation of stress and heat front during thermally-assisted compaction of binary size particles. They showed that similar to stress chains, theres exists preferable paths to conduct heat within the granular bed, which are recalled as heat chains. Surprisingly stress chains and heat chains are not identical, however they share the same characteristic of being unevenly distributed and being dependent on the loading conditions [68]. Vargas and McCarthy compared the solution with the improved continuum solution in which effective medium approach is integrated, and physical experiments [36]. In this study they show that stress chains serve to augment the heat flow along their axis and they effectively hamper the perpendicular heat flow, thereby inducing hot spots and well-bonded areas within the particulate bed. In a more recent study Vargas and McCarthy considered the effects of thermal expansion on heat condition in granular materials [70]. The striking conclusion in this research states that thermal expansion not only enhances the compaction, but also reforms the stress and heat chains. The nonlinearity induced by thermal expansion is mostly important for ‘unconsolidated or mildly consolidated’ packings. They mapped the stress field for a particle bed under external loading. In figure 6.3 the lines joining the centers of particles in contact represent the force network and have thickness proportional to the contact force [70].

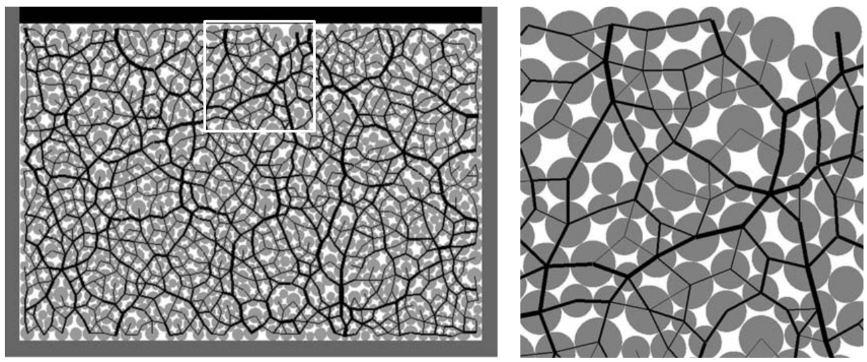

(a) (b)

Figure 6.3: Stress chains in an athermal particle bed under external loading, adopted from Vargas and McCarthy [2007]. **(a)** Experimental set-up with moving top wall, **(b)** Rescaled region close to top wall.

Figure 6.4 is the evaluation of temperature and stress field at steady state solution [70]. The black lines represent particle contacts, which experience forces above the average with thickness proportional to the contact force, while colors represent dimensionless temperatures (red corresponds to hot).

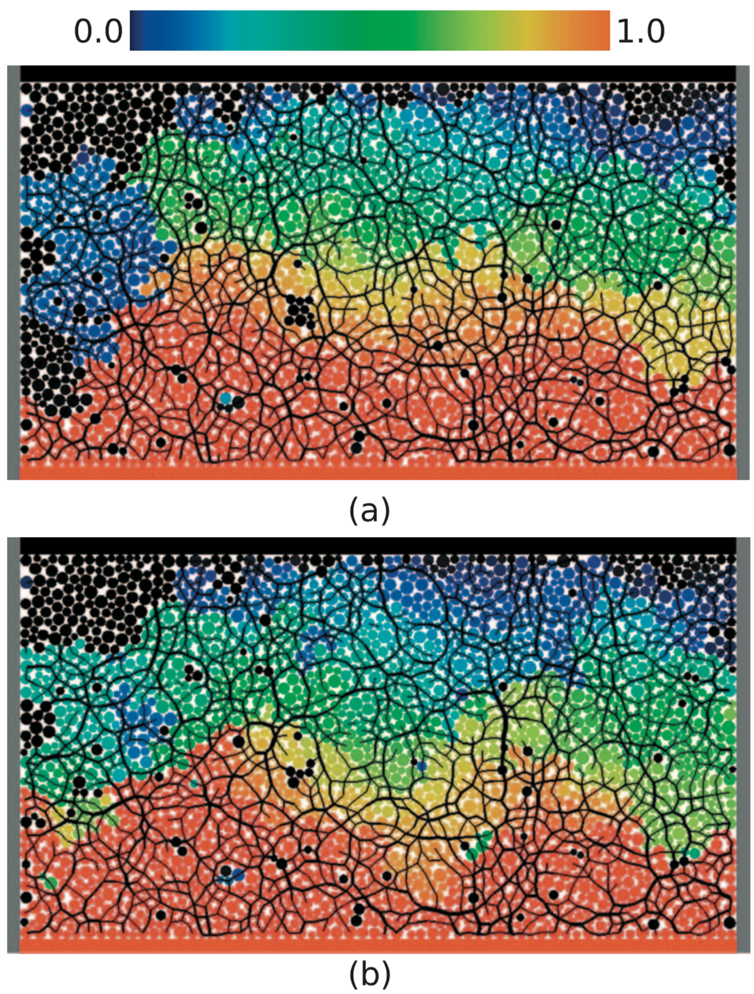

Figure 6.4: Thermal particle dynamics model estimating temperature and stress fields at steady state solution for thermally-assisted compaction of particle bed, adopted from Vargas and McCarthy [2007]. **(a)** Particle bed with a fixed top wall, **(b)** Particle bed with a top freely moving wall.

6.3 Simulation Configuration

We extend our mathematical model that is based on particle mechanics approach to study the two dimensional system of particles. The spherical particles are shown as circles, and the boundary walls are presented with solid lines. Initially the particles are assumed to be at point contact, upon the application of thermal and mechanical loads the particles change place and settle down while reaching a steady state temperature to adjust with the overall temperature gradient of the system. Initial configuration of two-dimensinal granular is assembly is obtained through the numerical simulations developed by Gioia et al. [24] by using ballistic deposition technique.

We investigate different configurations under different boundary conditions. In order to avoid the dominant influence of boundaries and minimize the local fluctuations of spatially dependent properties, we study two dimensional assemblies of sample size which is a few tens of particles diameters. This approach is similar in spirit to the statistical mechanics perspective improved on the subject of granular media. Radjai et al. explains the validity of this approach in search of statistical homogeneity and verifies his solution with experimental studies [54].

Initial sample configuration that we focus is a randomly arranged bed of 2077 stainless steel particles, as shown in figure 6.5. The particles are 4mm in radius and contained in a bed of 0.4m in height and width. The packing density of the undeformed system of particles is 0.72.

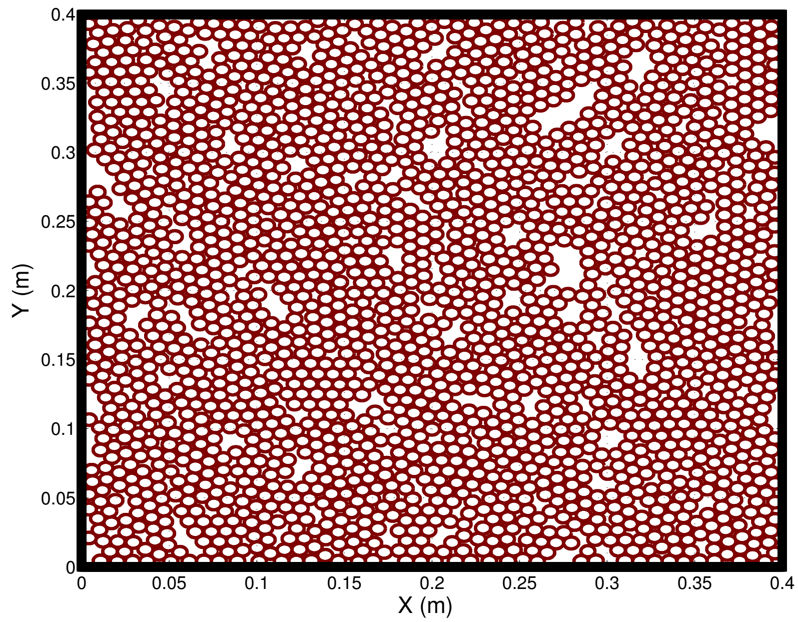

Figure 6.5: Initial configuration used in two dimensional analysis.

6.4 Methodology

Initial random distribution of particles within the compacted sample is generated by using ballistic deposition technique. The boundary conditions are imposed on the system of equations that defines the sum of the forces and heat transferred to each particle to be zero. The particle-particle and wall-particles interactions are classified according to the instantaneous position of the particles. Similar to chain of particles numerical experiments, rigid wall assumptions are used in two dimensional analysis. Newton-Raphson method is implemented as a direct iterative method to solve nonlinear system of coupled equations. Although the interdependence of mechanical and thermal properties introduces highly intricate system of equations while calculating the jacobian of the system of equations, the computational challenge is carried out carefully. Convergent solutions are achieved at a relative tolerance check of 10^{-2}, which basically continues the iteration till the next solution differs less than 1 percent of the solution in the previous iteration step. Finally in the post processing part, we study the generation of contact networks, the interrelation between force chains and heat chains within the confined assembly, the indicators of hot zone localizations and arching, the force and heat distributions in the overall solution.

The following flowchart explains the main steps completed in numerical experiments.

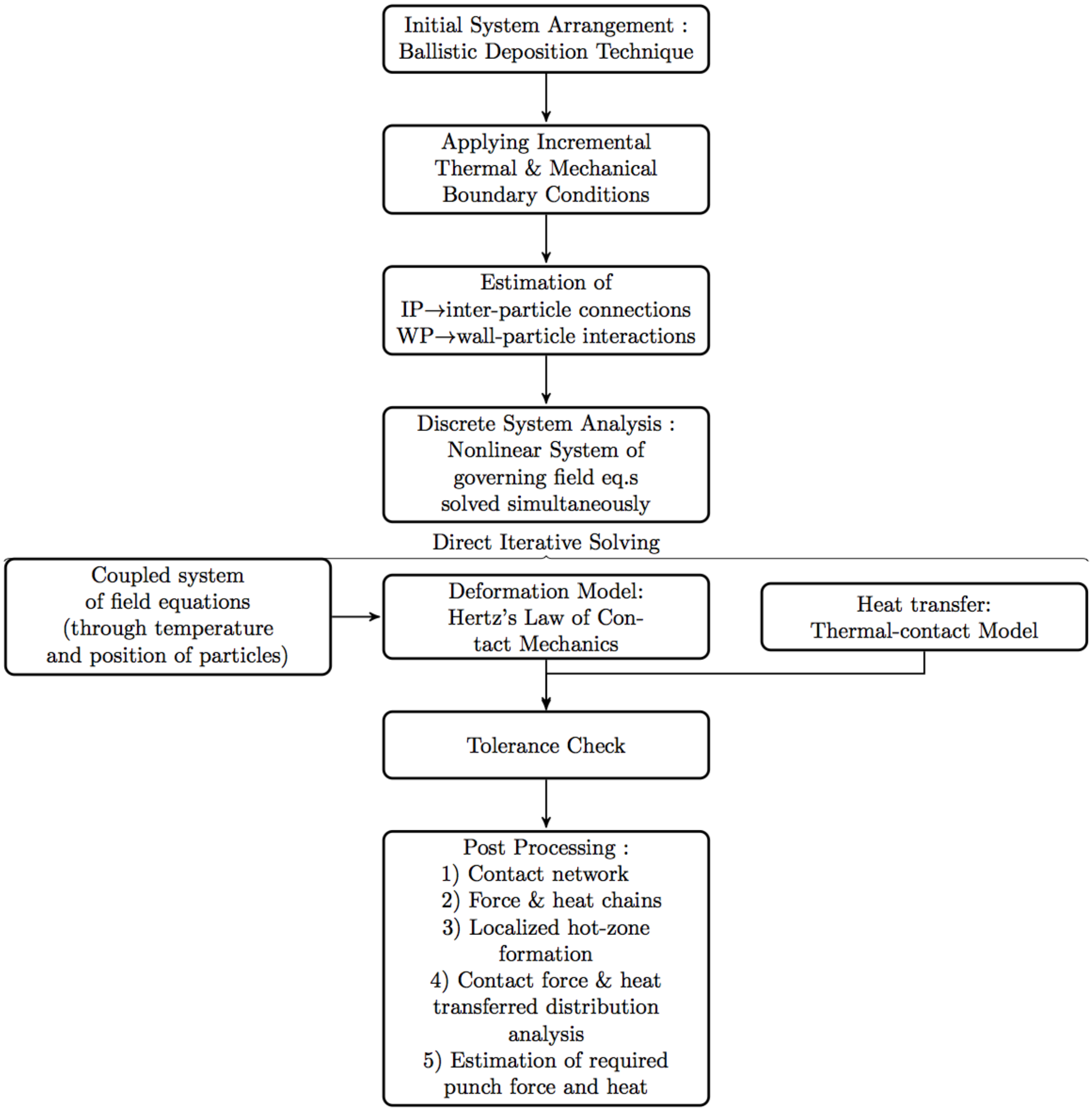

Figure 6.6: Flow chart of two dimensional numerical experiments.

6.5 Fundamental Concepts in 2D Discrete Modeling of Granular Materials

In this section we present the fundamental concepts that are introduced by previous experimental and numerical studies in the literature. Based on the proposed particle mechanics approach in this study, we conduct numerical analysis to exploit the dependence of the contact network with regard to the formation of force and heat chains within the confined granular bed. We simulate the force and heat distributions along the normal of the particle-particle contacts and wall-particle interactions. Lastly we investigate the cross-property relation between force and heat distributions.

The primary compaction configuration is the case where the initial system of 2077 particles are compressed by the top horizontal boundary. This top wall is heated, thereby thermal gradient is imposed on the system of particles. As expected the thermal force contribute to the rearrangement of the particle bed. It is worth noting here that similar to chain of particles' experiments, the weight of there particles are neglected in two dimensional analysis.

6.5.1 Contact Network

During the process of consolidation, particles come into contact in newly arranged configurations under compressive loading. Contact network generation is highly dependent on the initial positioning of the particulate matter within the confinement, applied boundary conditions and the material properties of the individual particles that support the external load. Since the contact network determines the preferred paths of force transfer within the compacted granular media, it indicates the unevenly distributed force distributions. These are the highways, that contribute to the percolation of the system concerning not only force transfer, but also heat and electrical conductivity. Moreover they serve as significant tools that indicate hot zones localizations, and propagation of chemical wave fronts during the compaction process.

In figure 6.7 we trace the contact network generation of our 2077 particles system that is compacted by a ratio of, ϵ, 8%.

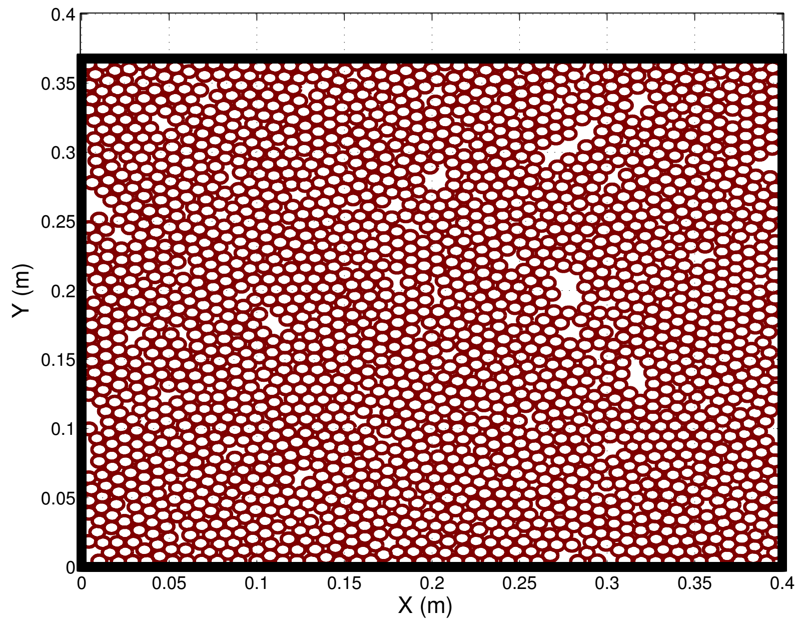

Figure 6.7: Contact network generation.

6.5.2 Force Chains

Force chains form the skeleton of compacted granular materials [53]. Visualization of force chains can be achieved by representation of forces at contacts as bonds between the conforming particles. The thickness of line connecting the particles is proportional to the magnitude of the contact force. In force and heat chain representations, we plot the particles as circles filled with black color, and surrounded by a red line. The force chains are shown as blue lines. For the case of pure mechanical compaction, the force chain formation of the particular configuration is seen in figure 6.8

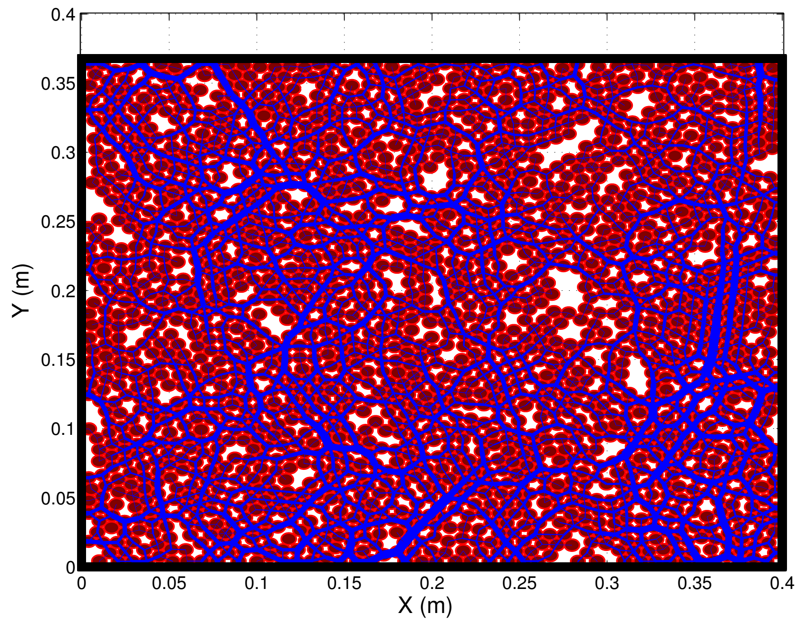

Figure 6.8: Force chains developed in athermally compaction of 2077 stainless steel particles' system. The total granular assembly is compacted by 8% in height, and constrained by the side vertical walls.

6.5.3 Heat Chains

Concerning the process of thermally-assisted compaction, the confined granular bed is imposed to a thermal gradient, which triggers the formation of preferred paths of heat transport within the assembly. In order to visualize the heat transport chains, we use a similar algorithm that we study in force chains. The heat transferred at each contact is mapped into the contact network, shown in lines whose thickness is proportional to the heat flux. In figure 6.9, we represent the heat chains developed in a system of 2077 randomly packed particles that are compacted by a ratio of 8% and heated through the top horizontal wall, which is kept at 493 K.

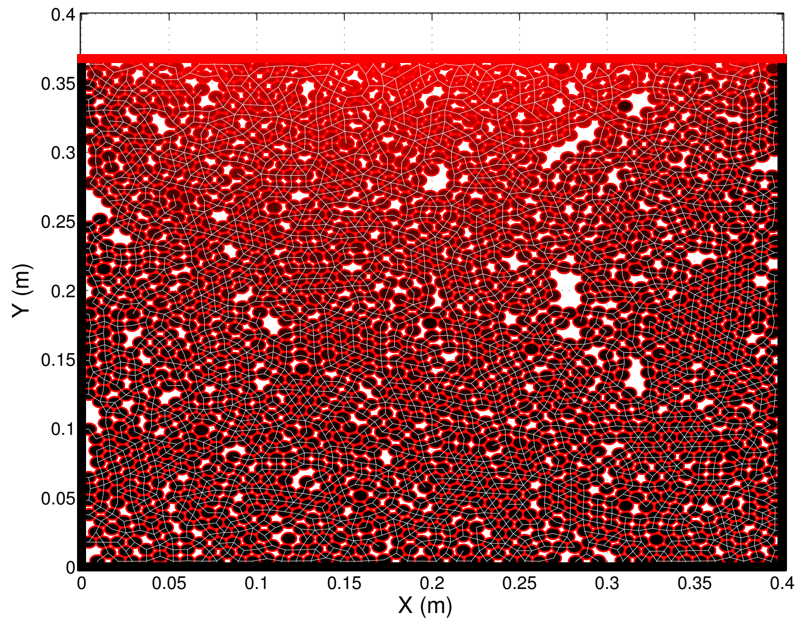

Figure 6.9: Heat chains developed in thermally-assisted compaction of 2077 stainless steel particles system. The granular assembly is heated through the top horizontal wall which is kept at 493 K, and moved down by % 8 of the initial height of the system.

Despite the unevenly distributed force chains, the map of heat chains displays that the heat distribution within the particulate bed is more uniform. It is worth noting that the heat flux illustration as solid lines at the particle contacts is more convenient for small systems with relatively less particles. To provide o more trackable visualization we prefer to show the heat gradient within the particulate bed, by altering the color filling of each particle. In the following figures the filling color of circles is changed to brighter red, as the temperature of particles increases.

6.5.4 Contact Force Distribution

The simplest characterization of force chains is probability distribution of individual contact forces. There exists a broad spectrum of statistical mechanics approaches developed to estimate the probability of very large and very small force loads within the particle-particle contacts. As mentioned in section 6.2 there also exists significant experimental studies that validate these mathematical models, specifically for the case of thermal compaction of spherical particles. The force distributions are expressed in terms of a non-dimensional variable, f, that defines the normal force at the contact divided by the average of these contact forces. In typical granular packings, the probability distribution, $P(f)$, has an exponential tail at large f, and a plateau at small f.

In our numerical analysis, we are capable of tracing normal contact forces at each contact. In figure 6.10 we plot distribution of non-dimensionalized contact forces f for the system of 2077 particles, which are compacted by 8% in one direction in the absence of any thermal load. We estimate the normalized force distribution, which are above the average force, by a power law decay. As seen in the semilogaritmic plot of the normalized distributions, $D(f)$ decays by $exp(-1.3413f)$. For the case of pure mechanical compaction, our simulations agree quite well with both the experimental [67] and the numerical studies [38, 54], in which this power law is given as $D(f) \approx exp((-1.4 \pm 0.1)f)$.

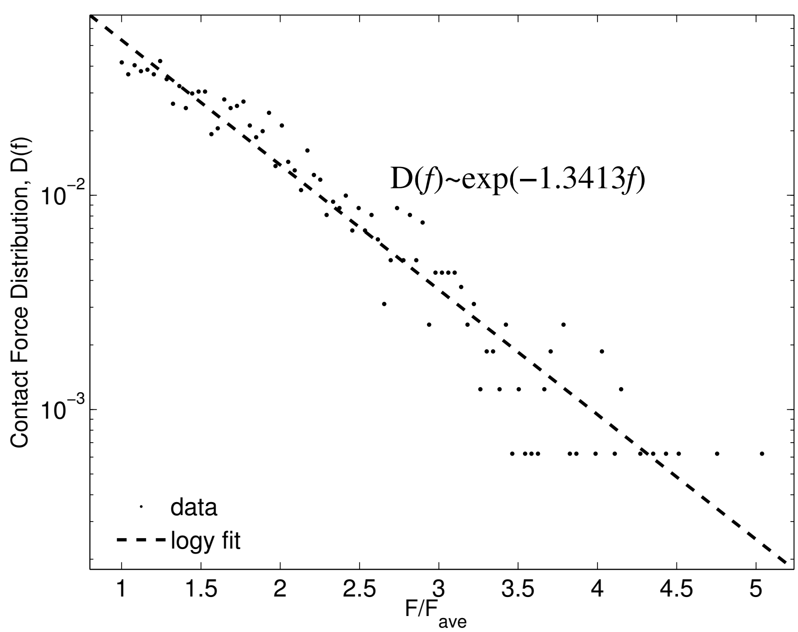

Figure 6.10: Normalized contact force distribution of athermally compacted 2077 stainless steel, SS304, particles system.

We investigate the dependence of packing fraction on the contact force distribution. The system of 2077 particles is gradually compressed by lowering the top wall, which is kept at 493 K. The normalized force distributions at the contacts are evaluated at compaction rates, 2%, 4%, 6% and 8%.

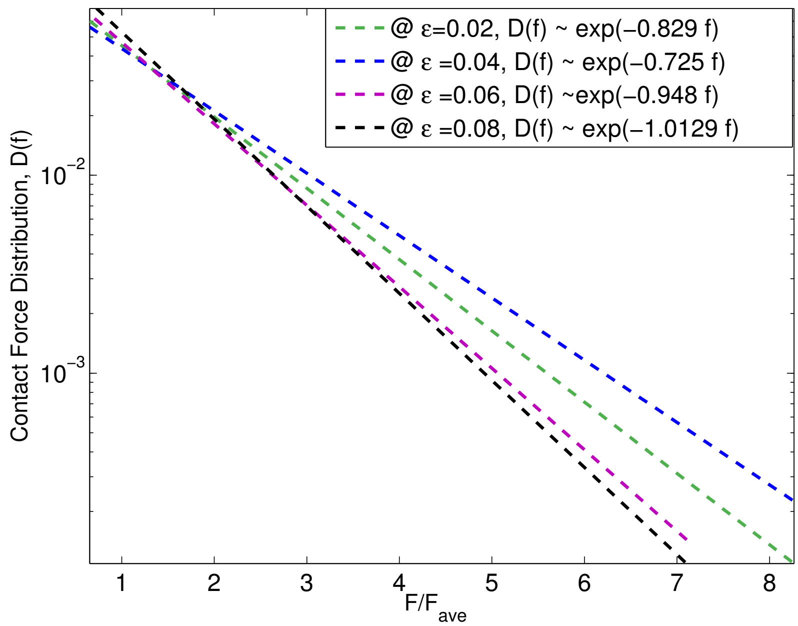

Figure 6.11: Comparison of force distributions for a gradually compacted SS304 particles' system which is under the particular thermal gradient, 200 K, imposed between the top and bottom boundary walls.

Figure 6.11 indicates that force distribution in a thermally-assisted compaction is correlated with the packing fraction and re-arrangement of particles determined by the coupled thermal and mechanical stresses.

6.5.5 Heat Distribution

Similar to force distribution analysis, we investigate the heat distribution within the contact network. The numerical simulations point out that the normalized heat distribution can be distinctly expressed in log-log plots. In figure 6.12 the heat distribution of 2077 particles system is shown for the particular loading of compaction ratio, ϵ, 8% and the top wall kept at 493 K.

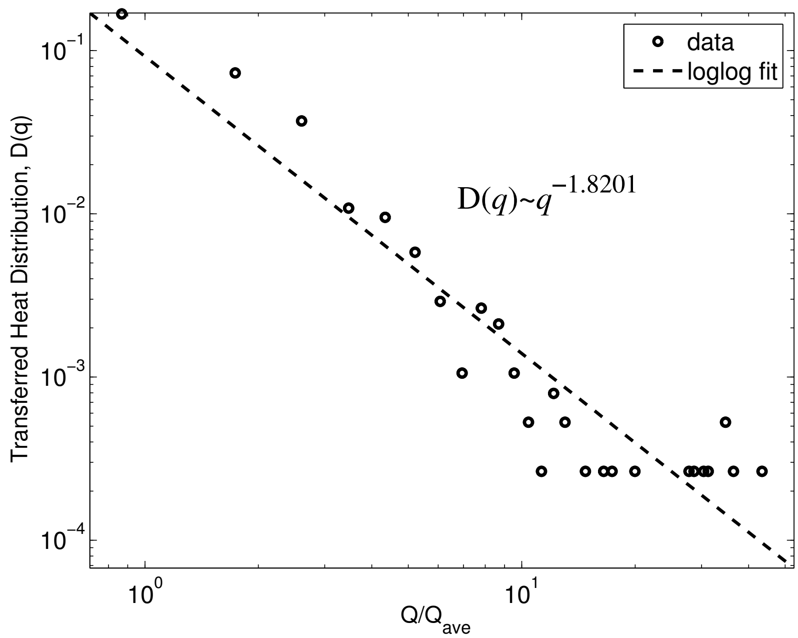

Figure 6.12: Normalized heat distribution of 2077 stainless steel particles' system which is under the imposed thermal gradient of 200 K. The total granular assembly is compacted by 8% in height.

In order to understand the effect of boundary wall temperature, the same system is investigated in a gradually heated numerical experiment. The particle assembly is compacted by a ratio of 8%, and the temperature of the top horizontal wall is increased from 293 K to 493 K, by increments of 40 K.

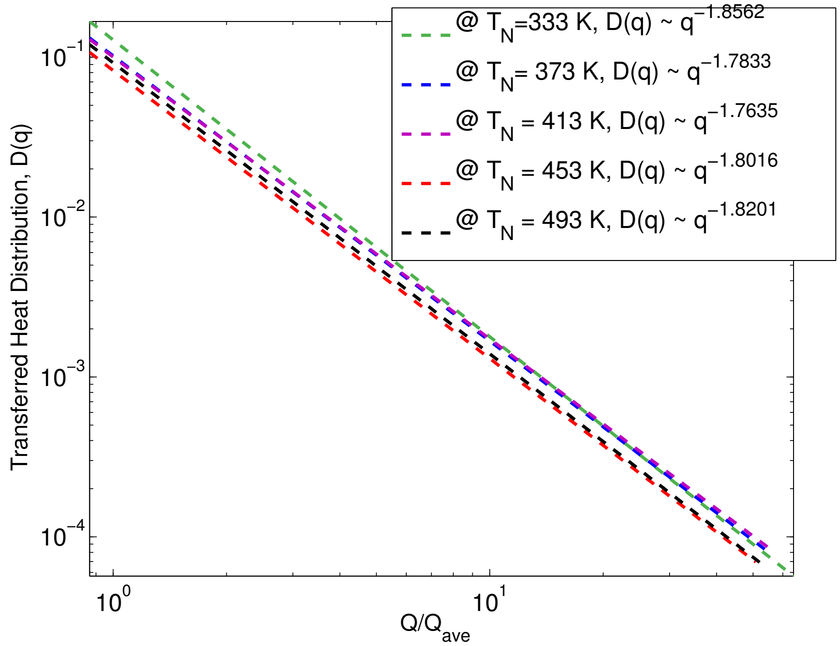

Figure 6.13: Comparison of heat distributions for a gradually heated system of 2077 particles, under effect of the thermal gradient of 200K and compacted by % 8 in height.

6.5.6 Cross-Property Relation Between Force and Heat Distributions

In their recent study Vargas et al. argued that force chains serve to augment the heat flow along their axis and they effectively hamper the perpendicular heat flow [70]. They traced the evolution of force chains and propagation of temperature gradient for a two dimensional system of particles. In this study we aim to explain quantitatively the influence of heat transfer to contact force distribution and the compaction ratio to heat transfer distribution within the particulate bed.

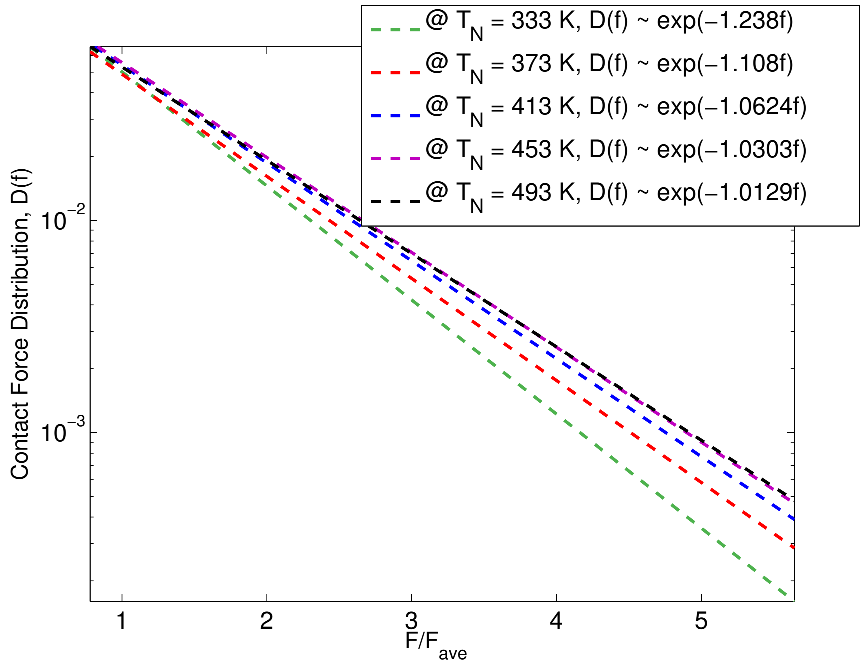

Figure 6.14: Evolution of force distribution under different thermal boundary conditions. System of 2077 stainless steel particles is compacted by a ratio of % 8, while the thermal gradient imposed between the top and bottom boundary walls is increased from 40 K to 200 K, gradually.

Figure 6.14 points out one of the unique characteristic of thermally-assisted compaction. The exponential power decreases for the cases of higher thermal load on the system.

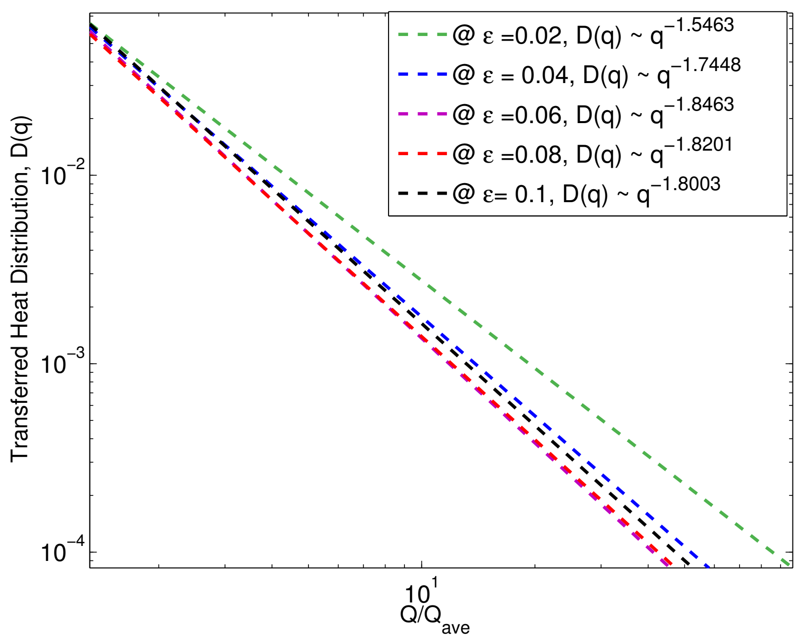

Figure 6.15: Evolution of heat distribution under different mechanical loading conditions. System of 2077 stainless steel particles is under the effect of a thermal gradient, 200 K, imposed between the top and bottom boundary walls, while it is compacted up to % 10, gradually.

The correlation between heat distribution and compaction ratio reveals that throughout the process of compaction when the densely packed bed of particles reaches a certain limit, the heat distribution mechanism is dominantly controlled by contact network evolution.

6.6 Simulation Results

6.6.1 Role of Particle Size

In an attempt to understand the effect of particle size on the microstructure of the compacted granular matter, two different cases are compared. Under the same thermal and mechanical loading conditions, a square container of 0.4m edge is compacting a bed of spherical particles by the downward movement of the top horizontal boundary wall. Case 1 is a system of 1486 particles, 1195 of them has a radius of 4mm and the rest of 8mm. The total area of the small particles are equal to the total area of the large particles. With the same concern we also generate, case 2, a system of 1760 particles, where 1225 of them are 4mm in radius and rest is 6mm.

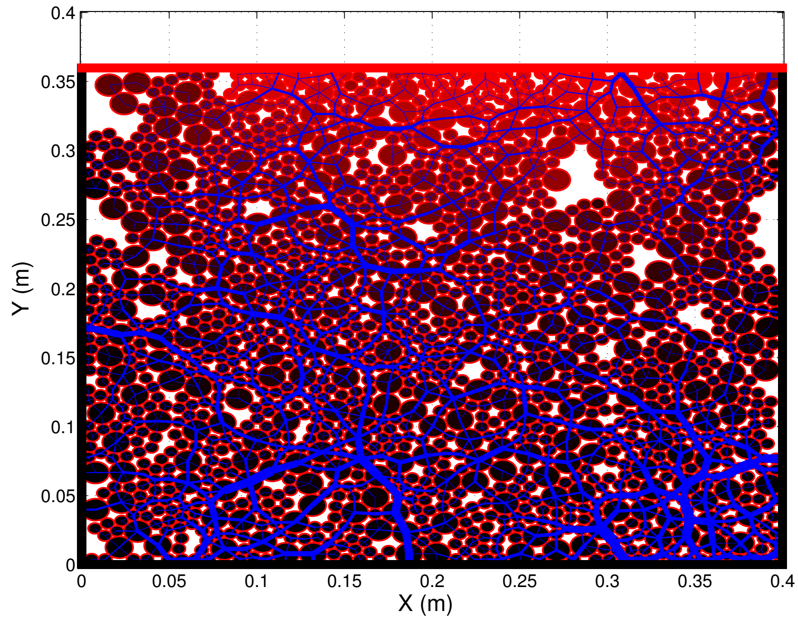

Figure 6.16: Force chains in a system of 1486 particles, under $\epsilon = 0.10$ and $T_N = 493K$. 1195 of the total number of particles are 4mm in radius, rest is 8mm in radius.

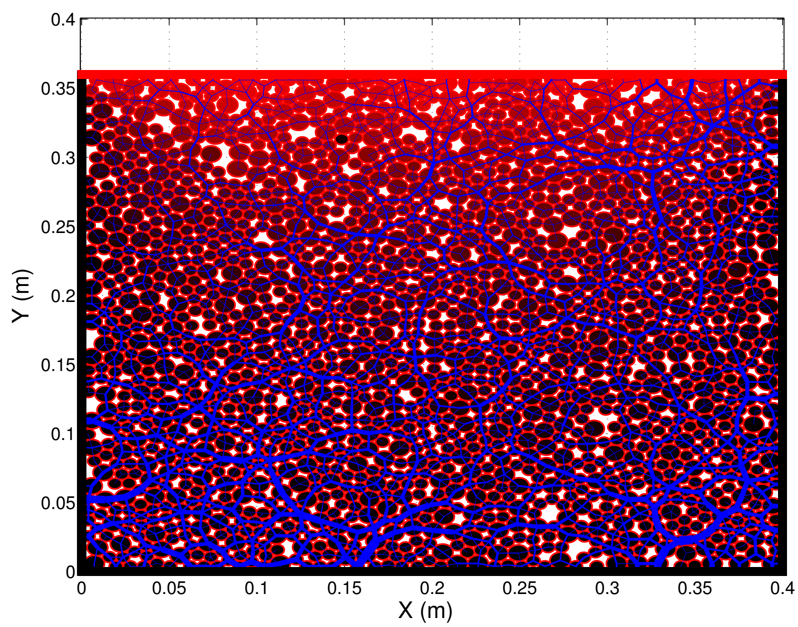

Figure 6.17: Force chains in a system of 1760 particles, under $\epsilon = 0.10$ and $T_N = 493K$. 1225 of the toal number of particles are 4mm in radius and rest is 6mm in radius.

Force chain maps given in figures 6.16 and 6.17 shows that systems which have particles that are similar in size, have more uniform distribution of contact forces. Under modest thermal gradients applied on the system, this statement remains valid. In figure 6.18 normalized force distributions of the considered cases are compared for three different compaction ratios.

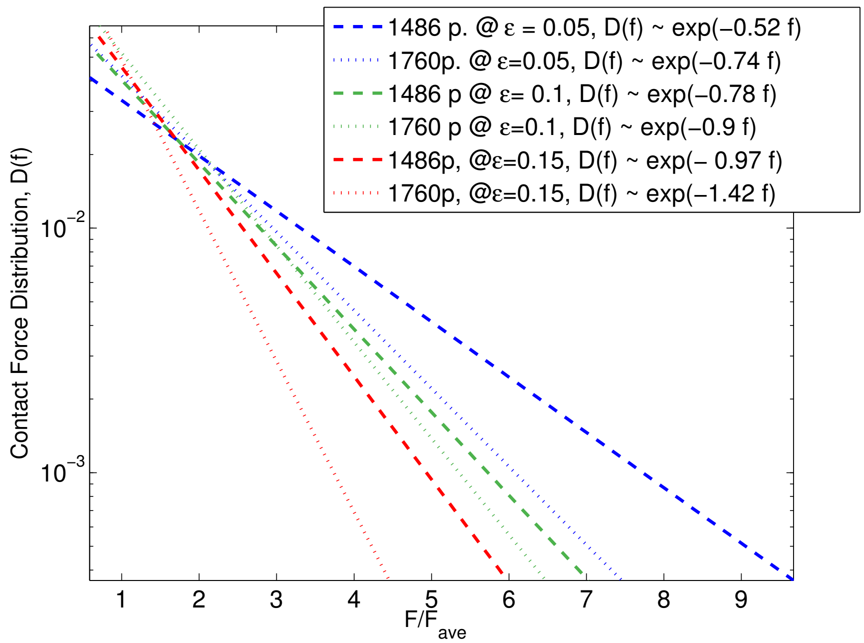

Figure 6.18: Comparison of normalized contact force distribution is evaluated for two binary size systems. As the packing density of granular assembly increases, the characteristic exponential tail of force distribution decays faster. Moreover the system with particles similar in size, develop more uniform distribution of contact forces.

6.6.2 Role of Thermal and Mechanical Material Properties

In most of the engineering practices, different material powders are consolidated through thermally-assisted compaction. Particularly for the cases where the thermal and mechanical properties of the binary particles system vary significantly, the estimation of microstructure characteristics become more robust.

In this study we consider a binary assembly that consists of teflon and stainless steel (SS304) particles. The system is compacted by a ratio of 8% and the top horizontal wall is kept at 393 K. We compare the force chains developed in the binary system with the ones developed in primary system of 2077 single type particles of SS304 compacted under the same loading conditions.

Table 6.1: Thermal and mechanical properties of teflon and stainless steel

	SS304	Teflon
α	17.3*10^{-6} 1/K	250*10^{-6} 1/K
E	193 GPa	2.25 GPa
k	15 W/mK	0.5 W/mK
ν	0.29	0.33
R^m_{ref}	0.004m	0.004 m
T^m_{ref}	293 K	293 K

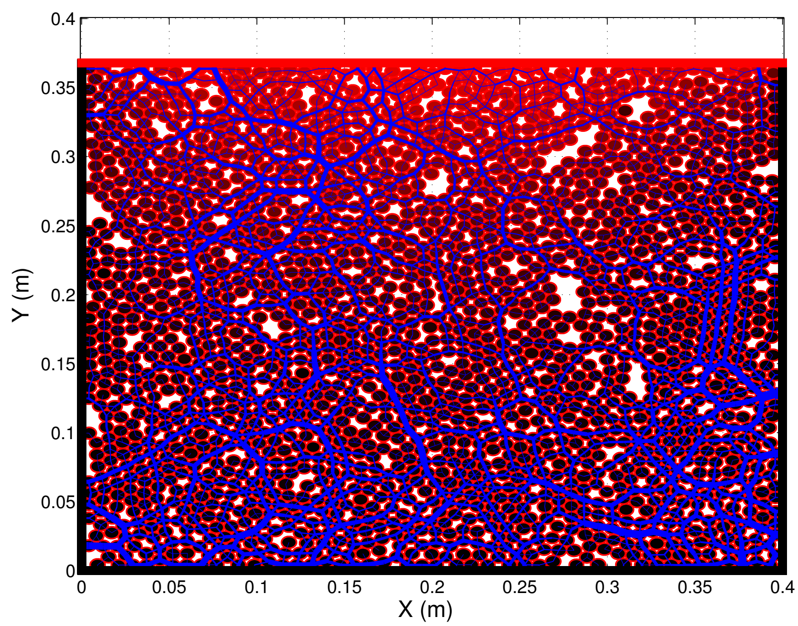

Figure 6.19: Force chains for a system SS304 particles, developed under $\epsilon = 0.08$ and $T_N = 393K$.

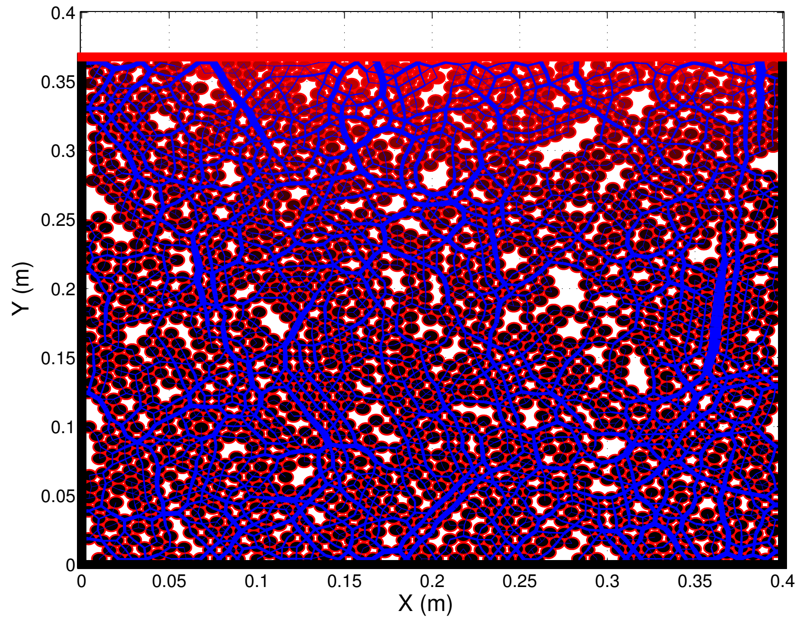

Figure 6.20: Force chains for a binary system of Teflon and SS304 particles, developed under $\epsilon = 0.08$ and $T_N = 393K$.

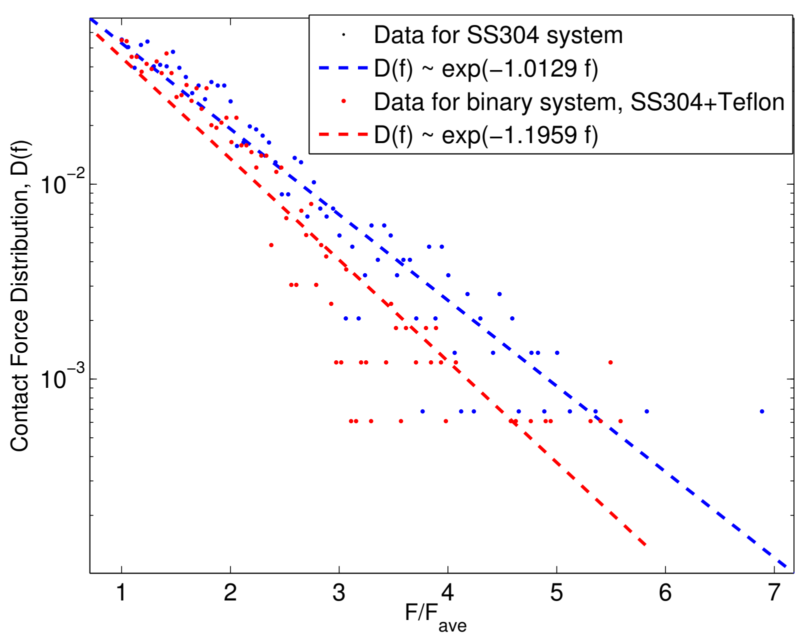

Figure 6.21: Comparison of normalized contact force distributions for binary, %50 Teflon and %50 SS304, and single, SS304, particle systems, developed under $\epsilon = 0.08$, and $T_N = 493K$.

Compared to the single particle system, binary system has a more evenly distributed contact force distribution. This is quantitatively shown in figure 6.21.

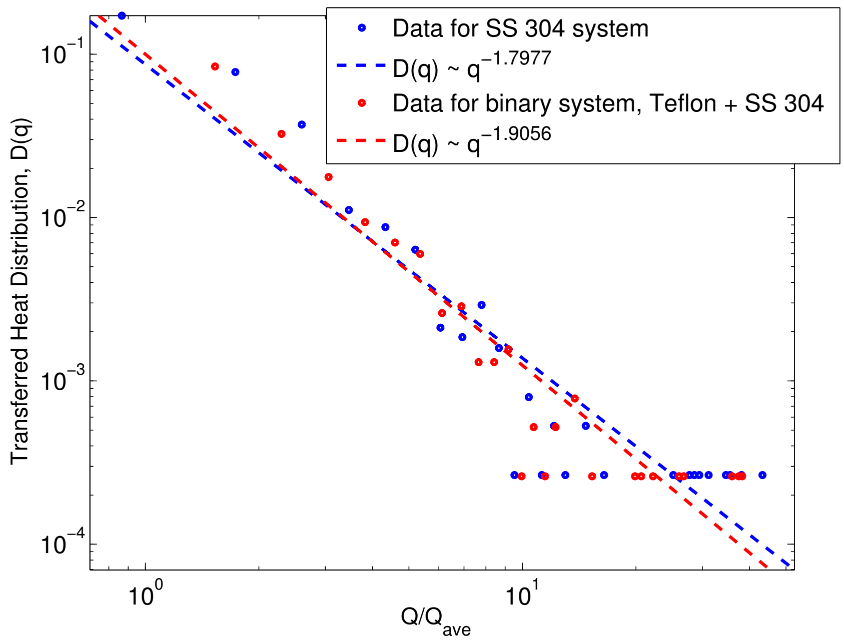

Figure 6.22: Comparison of heat distributions for binary, %50 Teflon and %50 SS304, and single, SS304, particle systems, developed under $\epsilon = 0.08$, and $T_N = 493K$.

Although thermal properties of the binary system particles vary significantly, comparison of the heat distribution in these two systems do not reflect a characteristic variation in terms of heat transfer.

6.6.3 Role of External Applied Thermal and Mechanical Boundary Conditions

Another controversial topic in thermally- assisted compaction is the effect of consolidation conditions on the microstructure. We consider four different boundary conditions (BC): (i) BC. 1: the system is compacted by the downward movement of the top horizontal wall which is kept at an elevated temperature, (ii) BC. 2: the system is compressed by the top horizontal wall, and heated from the side walls, (iii) BC. 3: the system is compressed by the top wall and the top and bottom horizontal walls are heated, (iv) BC. 4 the system is compacted by the top horizontal and right vertical walls, which are also heated. A schematic sketch of the described boundary conditions is illustrated for a small size system in figure 6.23.

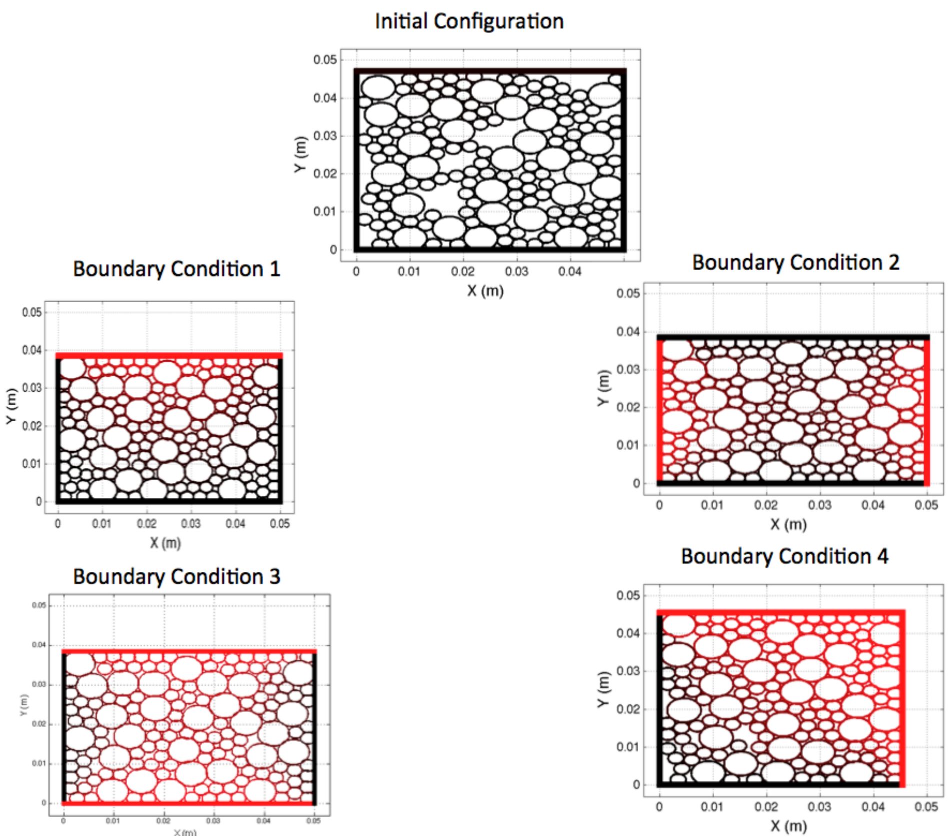

Figure 6.23: Schematic sketch of different boundary conditions.

Boundary conditions 1,2, and 3 are similar to uniaxial compaction and boundary condition 4 is names as isotropic compaction in the literature. We consider the case when the heated wall temperature is set to be 393 K, and compaction ratio is 8%. For the case of isotropic compression $\epsilon_x = \epsilon_y = 0.04$.

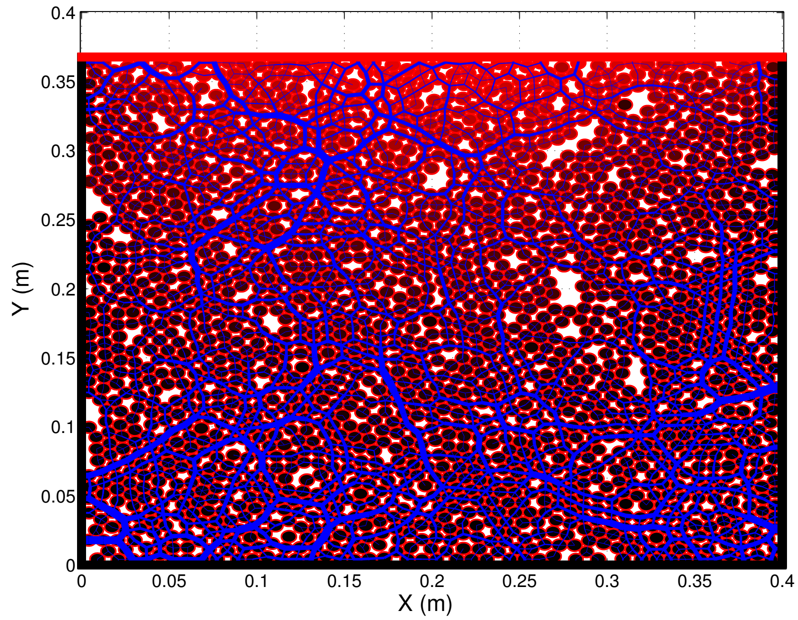

Figure 6.24: Force chains developed under boundary condition 1.

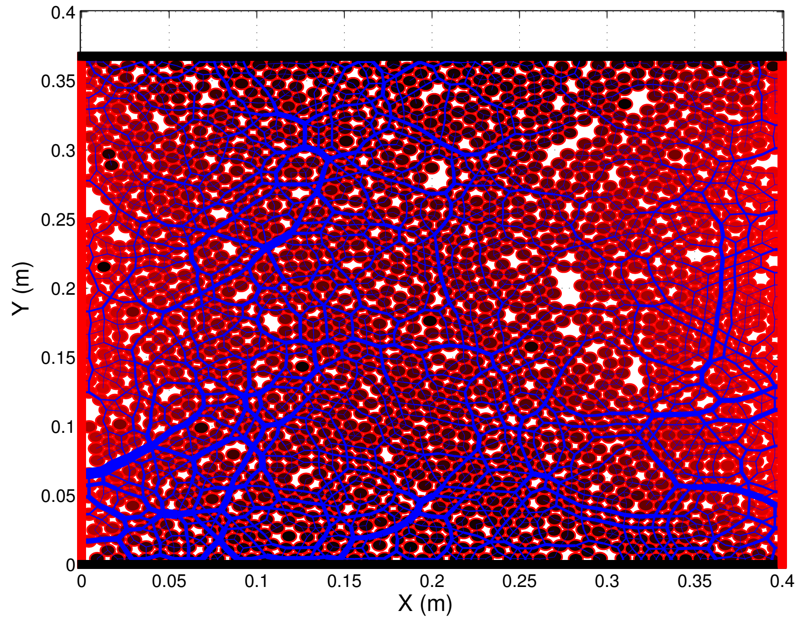

Figure 6.25: Force chains developed under boundary condition 2.

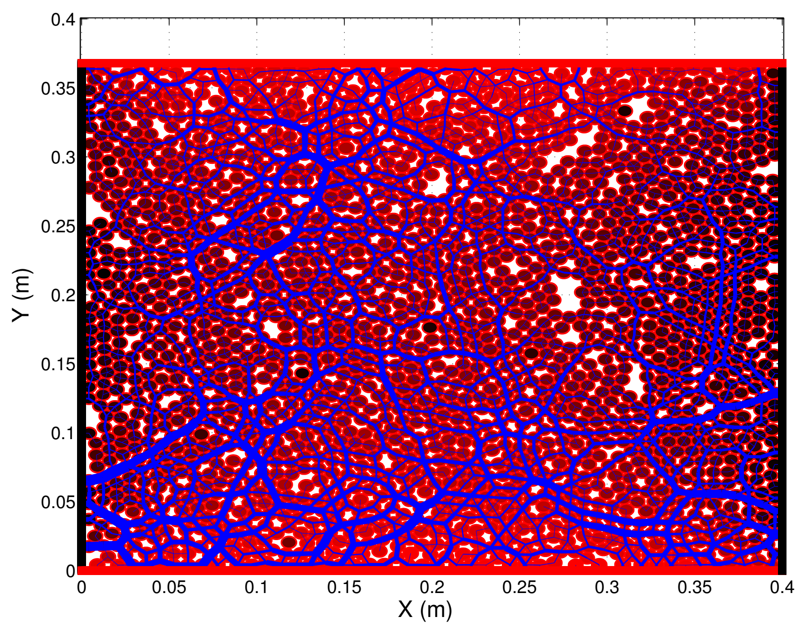

Figure 6.26: Force chains developed under boundary condition 3.

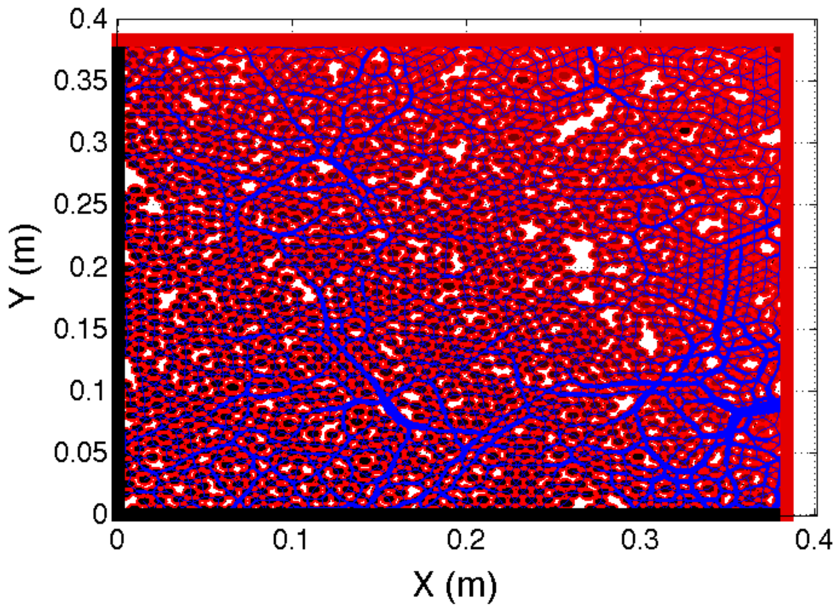

Figure 6.27: Force chains developed under boundary condition 4.

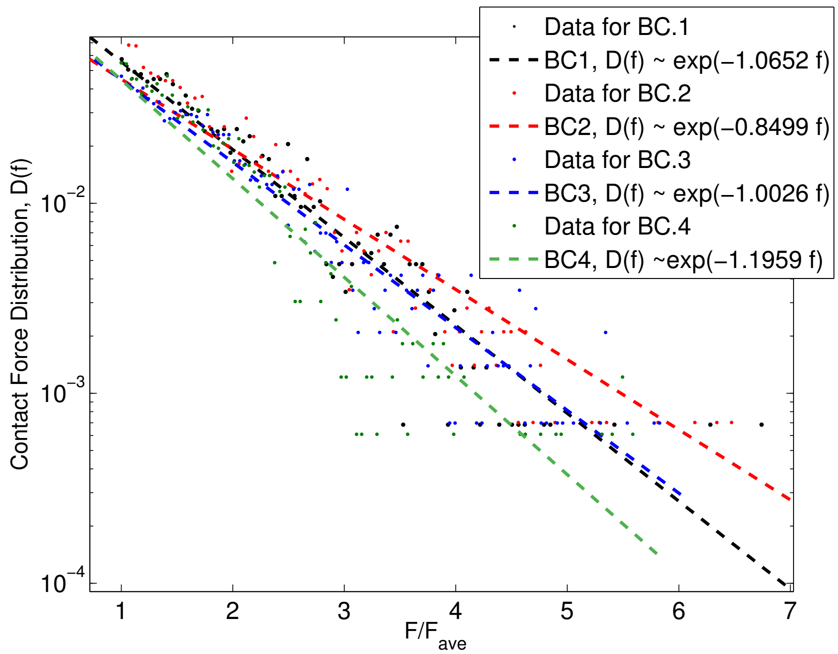

Figure 6.28: Comparison of normalized contact force distributions for different boundary conditions.

In figure 6.28 we compare the force distributions for these four boundary conditions. It is concluded that boundary condition 4 provides the most uniform distribution of contact forces. The difference between the force distributions of boundary condition 1 and 3 are relatively small, which demonstrates that the direction of applied heat transfer and external force plays an important role in microstructural rearrangement of particles.

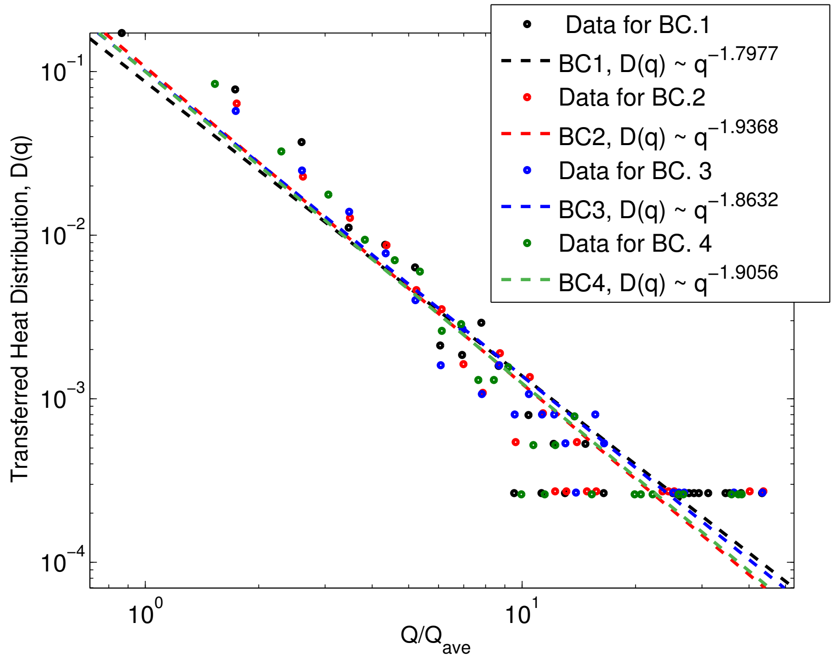

Figure 6.29: Comparison of heat distributions for different boundary conditions.

Figure 6.29 compares the heat distributions of the particulate assemblies under the four different boundary conditions. Under the thermal and mechanical boundary conditions, the distribution of heat at the contacts do not vary significantly for the current system of particles.

6.7 Conclusions

Particle mechanics approach is implemented to unveil the key characteristics of the thermally-assisted compaction in two dimensional numerical experiments. Our methodology is capable of capturing the contact networks, force and heat chains within the granular bed. Despite the fact that these chains visually reveal the hot zone localizations and the potential arching spots, it is not feasible to trace the evolutions of them on microstructural scale, particularly for the case of large system. However the force and heat distributions provide significant insight about understanding the mechanisms which determine the microstructure of compacted granular beds quantitatively.

Our numerical simulations show that force distribution of a densely packed spherical particles system is cumulated around an average normal contact force value, which is determined by the loading conditions, and material properties of the compacted sample. This distribution tends to decay out obeying an exponential power law. The extremely large values of normal contact force can be used in estimation of potential of micro-crack in further analysis. We show this distribution in terms of a normalized contact force in semilogaritmic plots.

Similar to contact force distribution analysis, we investigate the heat distributions and their correlation with the heat chains formations. We trace the normalized heat transferred at each contact. The distribution of them obeys a general power law, therefore the log-log plot is chosen for illustration purposes. As expected the normalized heat distribution is independent of the thermal gradient applied on the system.

In recognition of the ubiquity of thermally-assisted compaction problem, there is an inevitable need for granular material simulations to search for the cross property relation of the force and heat chain formation with respect to thermal gradient imposed on the system and compaction ratio. Our numerical results show that the thermo-mechanical coupling enhances the uneven distributions of force chains. The exponential decay seen in force distribution analysis is extended, revealing the fact that thermally-assisted compaction not only induces larger contact forces, but also the frequency to experience forces larger than average is increased. The correlation between heat distribution and compaction ratio reveals that the contact network formation becomes dominant in determining the heat distribution after a certain compaction is reached.

We focus our attention to consider the effects of particle size, material properties and boundary conditions on the microstructural arrangement of the particulate system. Concerning compacted granular assemblies of varying particle size, it is concluded that system which have particles similar in size, experience more uniform heat and force distributions. In order to understand the effect of thermal expansion particularly for the cases of binary particles systems, we consider a packed of particles which constitutes 60% teflon particles and 40% stainless steel particles, approximately. Under the same thermal and mechanical loading conditions force distribution of the binary system shows more uniformity. This indicates that thermal loading enhances the particles rearrangement such that the system has a tendency to develop a more evenly distributed contact network relatively. Regarding the effect of loading conditions in determining the microstructural evolution of force and heat chains, we compare four boundary conditions which are in practice similar to the conventional compaction methods. The three uniaxial compaction case which alter by the application of thermal load reveals that the coincided loading of thermal and mechanical deformation provides to most uniform distribution of contact forces. Whereas the transversely applied thermal load enhances larger heat flux and normal force at the contacts.

Chapter 7

Concluding Remarks

7.1 Overview

In this study we developed a model to describe the thermo-mechanical behavior of confined granular systems. Thermal contact and Hertzian deformation models are integrated to simulate the temperature and displacement fields of consolidated granular medium. We name this method as particle mechanics approach, since it adopts a detailed description at that particle level.

We focused on one dimensional numerical experiments to understand the effects of thermal expansion, thermal and mechanical loading conditions. The coupled phenomena introduces highly nonlinear system of equations, and it imposes variation in contact areas and nonlinear temperature distribution within the particulate material. This effect is enhanced for particles with larger thermal expansion coefficient. It appears that the critical regime, where the nonlinearity due to thermo-mechanical coupling becomes more dominant, is low mechanical and high thermal gradient conditions.

We studied the conventional continuum mechanics approach to understand the problem, and we integrated the effective medium theories to account for the overall properties of the compacted granular assembly. We adopted the effective elastic moduli and thermal conductivity that are proposed in earlier studies. The continuum solution deviates from the discrete solution particularly for cases of low mechanical load and high thermal gradient. Taking advantage of the optimization techniques we looked for the optimum value of thermal expansion that minimizes the difference between the discrete solution. For a range of deformation conditions, it is concluded that effective thermal expansion of a granular assembly varies between 0.60-0.80 of the bulk material property.

Starting from the particle-particle interactions, we proposed an effective thermal expansion coefficient for the particular case of thermally-assisted compaction. It is shown that meticulous implementation of the effective thermal expansion formalism renders truly predictive models of the mechanical and thermal behavior of the granular assembly.

We extended the numerical simulations to account for the two dimensional analysis of thermally-assisted compaction of densely packed granular beds. We implemented the proposed particle mechanics approach in this study to unveil the key characteristics of the thermally-assisted compaction in two dimensional numerical experiments. Our methodology is capable of capturing the contact networks, force and heat chains within the granular bed. Understanding such chains, and their correlation, we represent the key characteristics of granular media by using contact force and heat distribution. We quantitatively prove that contact force distribution within the densely packed particle bed becomes more uniform as the system is heated. Referring also the related literature we conclude that applied thermal gradient is effective on particle rearrangement, thereby formation of force chains. In loosely packed particle systems, heat distributions are mainly controlled by the thermal load and orientation of boundary conditions, however in densely packed systems contact networks plays a dominant role in heat distribution within the particulate bed.

Two dimensional numerical experiments show that particulate systems, which are of similar size particles, experience a more evenly distributed system of contact forces. Binary systems that constitute of particles with higher thermal expansion coefficient perform more uniform force and heat distributions. Concerning different boundary conditions, imposed thermal gradient aligned with the externally applied force induces a more uniform distribution of contact forces. Isotropic compaction provides the most uniformly distributed contact forces and heat transport within the granular system.

7.2 Future Work

In recognition of the ubiquity of thermally-assisted compaction of granular materials and the importance to a wide variety of technological processes, we focus our interest on how the forces supporting the microstructure is distributed, and how the preferred paths of heat transfer is oriented. Visualizations of two-dimensional granular systems demonstrate the influence of thermo-mechanical coupling. Heat and force distribution plots indicate this alterations quantitatively. It is natural to expect that similar concentrations of forces and heat will occur in three dimensions. The distinctive contact network formations in particulate systems give rise to distinctive macroscopic material properties in the confined bed. Extension of this model to three dimensions will serve as an optimum platform to analyze cases where the third dimensionality of the consolidated sample is comparable with the first two considered.

The basic idea to explain the giant stress fluctuations induced by temperature changes is that the network of stress paths is extremely sensitive to small perturbations. In this study the potential of extreme normal forces at contacts are correlated to imposed temperature gradient on the system. It is also known that a proper estimate of the mechanical strength of a compacted solid is contingent upon the knowledge of the amount of inter-particle contact area created during the plastic deformation stage of the compression. In this sense a further study, which also considers the plastic deformation of particles upon the coupled loading conditions, can be rewarding.

In order to study system with significantly larger number of particles, an adaptive meshing method can be developed to an integrated multi-scale model. In this study it is observed that not all particles undergo a rapid change at each deformation step. Depending on the boundary condition a portion of the particles, which are close to the moving boundary or heated boundary, experience larger changes in terms of position an temperature. For larger systems it can be critical to increase the computational efficiency by location these active zones, and analyzing with micro-scale models such particle mechanics approach introduced in this study, while analyzing the rest in a macro-scale model such as an finite element modeling tool. Similar concepts has recently acquired attention, particularly by the implementation of adaptive meshing in the subject of granular matter.

Current thermal contact models assume that neighboring particles of a particle sees the same temperature for the particle, such that multiple contacts on a single particle are at the same temperature. A model similar in spirit to the mathematical formulation developed by Gonzalez and Cuitino on nonlocal contact formulation for confined granular systems, can be developed to release the restriction of independents contacts [25]. Regarding the case of multiple contacts, the contribution of thermal load from different contacts of a single body will have an additional nonlocal effect beside the current thermal models for contacting bodies.

References

[1] SJ Antony. Link between single-particle properties and macroscopic properties in particulate assemblies: role of structures within structures. *Philosophical Transactions of the Royal Society A: Mathematical, Physical and Engineering Sciences*, 365(1861):2879–2891, 2007.

[2] M Bahrami, JR Culham, and MM Yovanovich. A scale analysis approach to thermal contact resistance. In *ASME International Mechanical Engineering Congress, Nov*, pages 15–21, 2003.

[3] Majid Bahrami. *Modeling of Thermal joint resistance for sphere-flat contacts in a vacuum*. PhD thesis, Citeseer, 2004.

[4] Majid Bahrami, M Michael Yovanovich, and J Richard Culham. Effective thermal conductivity of rough spherical packed beds. *International journal of heat and mass transfer*, 49(19):3691–3701, 2006.

[5] JR Barber. Contact problems involving a cooled punch. *Journal of Elasticity*, 8(4):409–423, 1978.

[6] GK Batchelor. Transport properties of two-phase materials with random structure. *Annual Review of Fluid Mechanics*, 6(1):227–255, 1974.

[7] GK Batchelor and RW O'Brien. Thermal or electrical conduction through a granular material. *Proceedings of the Royal Society of London. A. Mathematical and Physical Sciences*, 355(1682):313–333, 1977.

[8] Daniel L Blair, Nathan W Mueggenburg, Adam H Marshall, Heinrich M Jaeger, and Sidney R Nagel. Force distributions in three-dimensional granular assemblies: Effects of packing order and interparticle friction. *Physical Review E*, 63(4):041304, 2001.

[9] HS Carslaw. Jc jaeger conduction of heat in solids. *Clarendon, Oxford*, 1959.

[10] CK Chan and CL Tien. Conductance of packed spheres in vacuum. *J. Heat Transfer;(United States)*, 95(3), 1973.

[11] K Chen, J Cole, C Conger, J Draskovic, M Lohr, K Klein, T Scheidemantel, and P Schiffer. Granular materials: Packing grains by thermal cycling. *Nature*, 442(7100):257–257, 2006.

[12] Philippe Claudin and Jean-Philippe Bouchaud. Static avalanches and giant stress fluctuations in silos. *Physical review letters*, 78(2):231, 1997.

[13] SN Coppersmith, C-h Liu, Satya Majumdar, Onuttom Narayan, and TA Witten. Model for force fluctuations in bead packs. *Physical Review E*, 53(5):4673, 1996.

[14] Alberto M Cuitiño, Laurent Stainier, Guofeng Wang, Alejandro Strachan, Tahir Çağin, William A Goddard Iii, and Michael Ortiz. A multiscale approach for modeling crystalline solids. *Journal of computer-aided materials design*, 8(2-3):127–149, 2001.

[15] Peter A Cundall and Otto DL Strack. A discrete numerical model for granular assemblies. *Geotechnique*, 29(1):47–65, 1979.

[16] William Alan day. *Heat Conduction Within Linear Thermoelasticity*. Springer Tracts in Natural Philosophy, 1985.

[17] Frank L Dimaggio and Ivan S Sandler. Material model for granular soils. *Journal of the Engineering mechanics Division*, 97(3):935–950, 1971.

[18] Daniel Charles Drucker and William Prager. Soil mechanics and plastic analysis or limit design. *Quarterly of applied mathematics*, 10, 2013.

[19] Jacques Duffy and R Do Mindlin. Stress-strain relations and vibrations of a granular medium. Technical report, DTIC Document, 1956.

[20] AB Duncan, GP Peterson, and LS Fletcher. Effective thermal conductivity within packed beds of spherical particles. *Journal of heat transfer*, 111(4):830–836, 1989.

[21] F Emeriault and B Cambou. Micromechanical modelling of anisotropic non-linear elasticity of granular medium. *International Journal of Solids and Structures*, 33(18):2591–2607, 1996.

[22] YT Feng, K Han, CF Li, and DRJ Owen. Discrete thermal element modelling of heat conduction in particle systems: Basic formulations. *Journal of Computational Physics*, 227(10):5072–5089, 2008.

[23] Joseph C Foster Jr et al. Dynamic stress chain formation in a two-dimensional particle bed. *Experimental mechanics*, 42(3):329–337, 2002.

[24] Gustavo Gioia, Alberto M Cuitiño, S Zheng, and T Uribe. Two-phase densification of cohesive granular aggregates. *Physical review letters*, 88(20):204302, 2002.

[25] Marcial Gonzalez and Alberto M Cuitiño. A nonlocal contact formulation for confined granular systems. *Journal of the Mechanics and Physics of Solids*, 60(2):333–350, 2012.

[26] Grn R Hadley. Thermal conductivity of packed metal powders. *International journal of heat and mass transfer*, 29(6):909–920, 1986.

[27] Heinrich Hertz. On the contact of elastic solids. *J. reine angew. Math*, 92(156-171):110, 1881.

[28] Daniel Howell, RP Behringer, and Christian Veje. Stress fluctuations in a 2d granular couette experiment: a continuous transition. *Physical Review Letters*, 82(26):5241, 1999.

[29] Heinrich M Jaeger, Sidney R Nagel, and Robert P Behringer. Granular solids, liquids, and gases. *Reviews of Modern Physics*, 68(4):1259–1273, 1996.

[30] D. J. Jeffrey. Conduction through a random suspension of spheres. *Proceedings of the Royal Society of London. A. Mathematical and Physical Sciences*, 335(1602):355–367, 1973.

[31] Kenneth Langstreth Johnson. *Contact mechanics*. Cambridge university press, 1987.

[32] MG Kaganer. Contact heat transfer in granular material under vacuum. *Journal of engineering physics*, 11(1):19–22, 1966.

[33] M. Kaviany. *Principles of Heat Transfer in Porous Media*. Mechanical Engineering Series. Springer, 1995.

[34] Luigi Preziosi Konstantin Markov. Micromechanics modeling methods and simulations. In *Heterogeneous Media*. Springer, 2000.

[35] A Koynov, I Akseli, and AM Cuitiño. Modeling and simulation of compact strength due to particle bonding using a hybrid discrete-continuum approach. *International journal of pharmaceutics*, 418(2):273–285, 2011.

[36] Watson L Vargas and JJ McCarthy. Stress effects on the conductivity of particulate beds. *Chemical engineering science*, 57(15):3119–3131, 2002.

[37] LD Landau and EM Lifshitz. *Theory of Elasticity*. Pergamon Press, 1959.

[38] CH Liu, Sydney R Nagel, DA Schecter, SN Coppersmith, Satya Majumdar, Onuttom Narayan, and TA Witten. Force fluctuations in bead packs. *SCIENCE-NEW YORK THEN WASHINGTON-*, pages 513–513, 1995.

[39] Chu-heng Liu and Sidney R Nagel. Sound in sand. *Physical review letters*, 68(15):2301, 1992.

[40] MD Liu and JP Carter. A structured cam clay model. *Canadian Geotechnical Journal*, 39(6):1313–1332, 2002.

[41] Jonathan Loh, William Ketterhagen, and James Elliott. Multiscale modelling of pharmaceutical powders: Macroscopic behaviour prediction. In *POWDERS AND GRAINS 2013: Proceedings of the 7th International Conference on Micromechanics of Granular Media*, volume 1542, pages 161–164. AIP Publishing, 2013.

[42] Grunde Løvoll, Knut Jørgen Måløy, and Eirik G Flekkøy. Force measurements on static granular materials. *Physical Review E*, 60(5):5872, 1999.

[43] Trushant S Majmudar and Robert P Behringer. Contact force measurements and stress-induced anisotropy in granular materials. *Nature*, 435(7045):1079–1082, 2005.

[44] HA Makse, N Gland, DL Johnson, and L Schwartz. The apparent failure of effective medium theory in granular materials. *Physics and Chemistry of the Earth, Part A: Solid Earth and Geodesy*, 26(1):107–111, 2001.

[45] Hernán A Makse, Nicolas Gland, David L Johnson, and Lawrence M Schwartz. Why effective medium theory fails in granular materials. *Physical Review Letters*, 83(24):5070–5073, 1999.

[46] James Clerk Maxwell. Electricity and magnetism, 1873. *also in*, 2:322.

[47] RD Mindlin. Compliance of elastic bodies in contact. *J. of Appl. Mech.*, 16, 1949.

[48] RD Mindlin. Compliance of elastic bodies in contact. *Journal of applied mechanics*, 16, 2012.

[49] RD Mindlin and H Deresiewicz. Elastic spheres in contact under varying oblique forces. *J. of Appl. Mech.*, 20, 1953.

[50] Daniel M Mueth, Heinrich M Jaeger, and Sidney R Nagel. Force distribution in a granular medium. *Physical Review E*, 57(3):3164, 1998.

[51] AN Norris and DL Johnson. Nonlinear elasticity of granular media. *TRANSACTIONS-AMERICAN SOCIETY OF MECHANICAL ENGINEERS JOURNAL OF APPLIED MECHANICS*, 64:39–49, 1997.

[52] I Nozad, RG Carbonell, and S Whitaker. Heat conduction in multiphase systems—ii: Experimental method and results for three-phase systems. *Chemical engineering science*, 40(5):857–863, 1985.

[53] Srdjan Ostojic, Ellák Somfai, and Bernard Nienhuis. Scale invariance and universality of force networks in static granular matter. *Nature*, 439(7078):828–830, 2006.

[54] Farhang Radjai, Michel Jean, Jean-Jacques Moreau, and Stéphane Roux. Force distributions in dense two-dimensional granular systems. *Physical review letters*, 77(2):274, 1996.

[55] Farhang Radjai and Stéphane Roux. Friction-induced self-organization of a one-dimensional array of particles. *Physical Review E*, 51(6):6177, 1995.

[56] Leo Rothenburg and RJ Bathurst. Analytical study of induced anisotropy in idealized granular materials. *Geotechnique*, 39(4):601–614, 1989.

[57] Andrew Schofield and Peter Wroth. Critical state soil mechanics. 1968.

[58] DR Shonnard and S Whitaker. The effective thermal conductivity for a pointcontact porous medium: an experimental study. *International journal of heat and mass transfer*, 32(3):503–512, 1989.

[59] WWM Siu and SH-K Lee. Effective conductivity computation of a packed bed using constriction resistance and contact angle effects. *International journal of heat and mass transfer*, 43(21):3917–3924, 2000.

[60] WWM Siu and SH-K Lee. Transient temperature computation of spheres in three-dimensional random packings. *International journal of heat and mass transfer*, 47(5):887–898, 2004.

[61] Jacco H Snoeijer, Thijs JH Vlugt, Martin van Hecke, and Wim van Saarloos. Force network ensemble: a new approach to static granular matter. *Physical review letters*, 92(5):054302, 2004.

[62] MR Sridhar and M Yovanovich. Review of elastic and plastic contact conductance models-comparison with experiment. *Journal of Thermophysics and Heat Transfer*, 8(4):633–640, 1994.

[63] MR Sridhar and MM Yovanovich. Elastoplastic contact conductance model for isotropic conforming rough surfaces and comparison with experiments. *TRANSACTIONS-AMERICAN SOCIETY OF MECHANICAL ENGINEERS JOURNAL OF HEAT TRANSFER*, 118:3–9, 1996.

[64] L Stainier, AM Cuitino, and M Ortiz. Multiscale modelling of hardening in bcc crystal plasticity. In *Journal de Physique IV (Proceedings)*, volume 105, pages 157–164. EDP sciences, 2003.

[65] S Timoshenko and JN Goodier. Theory of elasticity, 1951. *New York*, 412.

[66] S Torquato. Thermal conductivity of disordered heterogeneous media from the microstructure. *Reviews in Chemical Engineering*, 4(3-4):151–204, 1987.

[67] Olivier Tsoungui, Denis Vallet, and Jean-Claude Charmet. Use of contact area trace to study the force distributions inside 2d granular systems. *Granular Matter*, 1(2):65–69, 1998.

[68] Watson L Vargas and JJ McCarthy. Heat conduction in granular materials. *AIChE Journal*, 47(5):1052–1059, 2001.

[69] Watson L Vargas and JJ McCarthy. Conductivity of granular media with stagnant interstitial fluids via thermal particle dynamics simulation. *International journal of heat and mass transfer*, 45(24):4847–4856, 2002.

[70] Watson L Vargas and JJ McCarthy. Thermal expansion effects and heat conduction in granular materials. *Physical Review E*, 76(4):041301, 2007.

[71] Watson L Vargas-Escobar. *Discrete modeling of heat conduction in granular media*. PhD thesis, University of Pittsburgh, 2002.

[72] K Walton. The effective elastic moduli of model sediments. *Geophysical Journal of the Royal Astronomical Society*, 43(2):293–306, 1975.

[73] K Walton. The effective elastic moduli of a random packing of spheres. *Journal of the Mechanics and Physics of Solids*, 35(2):213–226, 1987.

[74] S Zheng and AM Cuitino. Consolidation behavior of inhomogeneous granular beds of ductile particles using a mixed discrete-continuum approach. *Kona*, 20:168–177, 2002.

[75] HP Zhu, ZY Zhou, RY Yang, and AB Yu. Discrete particle simulation of particulate systems: theoretical developments. *Chemical Engineering Science*, 62(13):3378–3396, 2007.

[76] Alexander Z Zinchenko. Effective conductivity of loaded granular materials by numerical simulation. *Philosophical Transactions of the Royal Society of London. Series A: Mathematical, Physical and Engineering Sciences*, 356(1749):2953–2998, 1998.